

Preliminary Design of the Guidance, Navigation, and Control System of The Altair Lunar Lander

Allan Y. Lee,^{1,*} Todd Ely,¹ Ronald Sostaric,² Alan Strahan,² Joseph E. Riedel,¹ Mitch Ingham,¹ James Wincentsen,¹
and Siamak Sarani¹

¹*Jet Propulsion Laboratory
4800 Oak Grove Drive, Pasadena, CA 91109-8099
California Institute of Technology*

²*Johnson Space Center
NASA Johnson Space Center, 2101 NASA Parkway, Houston, Texas 77058*

Guidance, Navigation, and Control (GN&C) is the measurement and control of spacecraft position, velocity, and attitude in support of mission objectives. This paper provides an overview of a preliminary design of the GN&C system of the Lunar Lander Altair. Key functions performed by the GN&C system in various mission phases will first be described. A set of placeholder GN&C sensors that is needed to support these functions is next described. To meet Crew safety requirements, there must be high degrees of redundancy in the selected sensor configuration. Two sets of thrusters, one on the Ascent Module (AM) and the other on the Descent Module (DM), will be used by the GN&C system. The DM thrusters will be used, among other purposes, to perform course correction burns during the Trans-lunar Coast. The AM thrusters will be used, among other purposes, to perform precise angular and translational controls of the ascent module in order to dock the ascent module with Orion. Navigation is the process of measurement and control of the spacecraft's "state" (both the position and velocity vectors of the spacecraft). Tracking data from the Earth-Based Ground System (tracking antennas) as well as data from onboard optical sensors will be used to estimate the vehicle state. A driving navigation requirement is to land Altair on the Moon with a landing accuracy that is better than 1 km (radial 95%). Preliminary performance of the Altair GN&C design, relative to this and other navigation requirements, will be given. Guidance is the onboard process that uses the estimated state vector, crew inputs, and pre-computed reference trajectories to guide both the rotational and the translational motions of the spacecraft during powered flight phases. Design objectives of reference trajectories for various mission phases vary. For example, the reference trajectory for the descent "approach" phase (the last 3-4 minutes before touchdown) will sacrifice fuel utilization efficiency in order to provide landing site visibility for both the crew and the terrain hazard detection sensor system. One output of Guidance is the steering angle commands sent to the 2 degree-of-freedom (dof) gimbal actuation system of the descent engine. The engine gimbal actuation system is controlled by a Thrust Vector Control algorithm that is designed taking into account the large quantities of sloshing liquids in tanks mounted on Altair. In this early design phase of Altair, the GN&C system is described only briefly in this paper and the emphasis is on the GN&C architecture (that is still evolving). Multiple companion papers will provide details that are related to navigation, optical navigation, guidance, fuel sloshing, rendezvous and docking, machine-pilot interactions, and others. The similarities and differences of GN&C designs for Lunar and Mars landers are briefly compared.

*Manager, Guidance, Navigation, and Control System, Altair Lunar Lander. Mail Stop 230-104, Jet Propulsion Laboratory, 4800 Oak Grove Drive, Pasadena, California 91109-8099, USA. Allan.Y.Lee@jpl.nasa.gov

Acronyms

ACC	Accelerometer	GPS	Global Positioning System
AGS	Abort Guidance System	GRAIL	Gravity Recovery and Interior Laboratory
AL	Air Lock		
ALHAT	Autonomous Landing Hazard Avoidance Technology	IMU	Inertial Measurement Unit
Altair	Lunar Lander Vehicle	JPL	Jet Propulsion Laboratory
AM	Ascent Module	LCROSS	Lunar Crater Observation and Sensing Satellite
ARS	Ames Research Center	LEM	Lunar Excursion Module
ATP	Authority to Proceed	LEO	low-Earth orbit
ARES-I	Launch vehicle for Orion	LH2	Liquid Hydrogen
ARES-V	Launch vehicle for Altair	Lidar	Light Intensification, Detection, and Ranging
BOB	Bang Off Bang (an attitude control algorithm)	LIDS	Low Impact Docking System
B/U	Backup	LLRV	Lunar Lander Research Vehicle
BW	Bandwidth (of a controller)	LLO	Low Lunar Orbit
Canb	Canberra DSN Complex, Australia	LLV	Lunar Lander Vehicle
CARD	Constellation Architecture Requirement Documents	LOC	Loss of Crew
CCD	Charge Coupled Device	LOI	Lunar Orbit Insertion
CEV	Crew Exploration Vehicle	LOM	Loss of Mission
c.m.	center of mass	LOX	Liquid Oxygen
CSI	Control Structure Interactions	LRO	Lunar Reconnaissance Orbiter
DCO	Data Cut Off	LV	Launch Vehicle
DM	Descent Module	Mad	Madrid DSN complex, Spain
DOI	De-orbit Injection (burn)	MCC	Mission Control Center
DRM	Design Reference Mission		Mid-course Correction (Apollo terminology. Same as TCM)
DSN	Deep Space Network	MER	Mars Exploration Rover
EBGS	Earth Based Ground System (DSN tracking complexes plus three other receive-only stations)	MET	Mission Elapsed Time
EDS	Earth Departure Stage	MIB	Minimum Impulse Bit (of a thruster)
ETDP	Exploration Technology Development Program	MMH	Monomethylhydrazine
EVA	Extra-vehicular Activity	mrads	milli-radians (about 0.057296°)
FDIR	Fault Protection, Isolation, and Recovery System	MRO	Mars Reconnaissance Orbiter
FITH	Fire-In-The-Hole	MSL	Mars Science Laboratory
FLAK	Unfortunate Lack of Acceleration Knowledge	NAC	Narrow Angle Camera
FPA	Flight Path Angle	NCC	Number, Corrective Combination (Apollo terminology)
FOM	Figure of Merit	NF	Navigation Filter
FOV	field of view (of an optical sensor or radar)	NTO	Nitrogen Tetroxide
FSFO	Failed Safe and Failed Operational	ONSS	Optical Navigation Sensor System
FSW	Flight Software	OpNav	Optical Navigation
GN&C	Guidance, Navigation, and Control subsystem	Orion	Crew Exploration Vehicle
GNC	guidance, navigation, and control	PDI	Powered Descent Initiation
Gold	Goldstone DSN Complex, US	PEG	Power Explicit Guidance
		PGS	Primary Guidance System
		PRA	Probabilistic Risk Assessment
		RCAH	Rate Command Attitude Hold
		RCS	Reaction Control System
		RDM	Radiation Design Margin
		R/F	Radio Frequency

RHESE	Radiation-Hardened Electronics for Space Exploration		(same as MCC)
RPODU	Rendezvous Proximity Operations Docking and Undocking	TD	Touchdown
RSS	Root Sum (of) Squares	TDRS	Tracking Data Relay Satellite
SAR	Single Axis Rotation		Terminal Descent Radar System
S/C	Spacecraft	THDSS	Terrain Hazard Detection Sensor System
SEU	Single Event Upset	TLC	Trans-Lunar Coast
SMAA	Semi-major Axis	TLI	Trans Lunar Injection (burn)
SPS	Service Propulsion System (Apollo terminology)	TPBVP	Two Point Boundary Value Problem
SRU	Stellar Reference Unit (usually called a Star Tracker)	TPI	Terminal Phase Initiation
TBD	To Be Determined	TOF	Time Of Flight
TBR	To Be Resolved	TRL	Technology Readiness Level
TBS	To Be Supplied	TVC	Thrust Vector Control (a ΔV burn performed by a gimbal engine)
TCM	Trajectory Correction Maneuver	USO	Ultra-Stable Oscillator
		VDI	Vertical Descent Initiation
		VMS	Vertical Motion Simulator
		VNS	Video Navigation Sensor

Table of Contents

<u>Section</u>	<u>Page</u>
Acronyms.....	2
1. Introduction.....	4
2. Design Reference Mission.....	5
3. Altair Guidance, Navigation, and Control Requirements and Functionalities.....	7
4. A Preliminary Altair GN&C System Design.....	9
4.1. GN&C Sensor Suite.....	11
4.1.1. Impacts of Lunar Radiation Environment on GN&C Sensors.....	19
4.1.2. Power On/Off Plan of GN&C Sensors and Equipment.....	19
4.2. Estimations of Altair’s Inertial Attitude and State Vector.....	20
4.2.1. Functionality Checked out and Calibration Plan of GN&C Sensors.....	22
4.3. RCS Thruster Configuration Designs.....	23
4.4. Attitude Control System Design.....	26
4.5. Propulsive Maneuver Control System Designs.....	28
5. Navigation.....	31
5.1. Navigation Via Radiometric Tracking.....	32
5.2. Optical Navigation.....	33
5.3. Flight Path Control.....	34
5.4. Preliminary Altair Navigation Performance.....	35
6. Guidance.....	41
6.1. Descent and Landing Guidance.....	41
6.2. Ascent Insertion Burn Guidance.....	43
6.3. Rendezvous, Proximity Operations, and Docking Guidance.....	44
7. Special Altair GN&C Design Challenges.....	46
7.1. Unstable Interactions between Thrust Vector Control and Sloshing Fuel.....	46
7.2. Protection Against the Dusty Environment.....	50
7.3. Docking Operations: Constraints and LIDS Docking Requirements.....	52
7.4. GN&C Considerations for Piloted Lunar Landings.....	56
8. Summary and Conclusions.....	58
Acknowledgements.....	60
References.....	60

1. Introduction

“... The final ten minutes are especially tense. The tape-guided automatic pilots are now in full control. We fall more and more slowly, floating over the landing area like descending helicopters as we approach, ... The whirring of machinery dies away. There is absolute silence. We have reached the Moon. Now we shall explore it.” These are words used by Dr. Werner von Braun in 1952 to describe the powered descent phase of an imagined lunar landing.¹ The call for action was made by President John F. Kennedy in 1961 when he said “... I believe that this nation should commit itself to achieving the goal, before this decade is out, of landing a man on the moon and returning him safely to Earth. ...”² His vision became a reality in 1969 with the first lunar landing by two astronauts of the Apollo-11 mission. That event represented one of the greatest technological accomplishments of mankind, by NASA, in the 20th Century.

The Constellation Program⁺ is NASA’s response to the human exploration goals set by former President George W. Bush for returning humans to the Moon by 2020. In January 2004, former President Bush announced the new Vision for Space Exploration for NASA. The fundamental goal of this vision is to advance U.S. scientific, security, and economic interests through a robust space exploration program. To this end, the NASA Constellation Program is working on two spacecraft (the Crew Exploration Vehicle named Orion and the Lunar Lander Vehicle named Altair), two launch vehicles (ARES-I will launch Orion and ARES-V will launch Altair), and surface support systems to establish a lunar outpost. This work will provide experience needed to expand human exploration farther into the Solar System. The first crewed flight of the Orion spacecraft is scheduled for no later than 2015, when it will fly to the International Space Station. Altair’s first landing on the Moon with an astronaut crew is planned for no later than 2020.

The Lunar Lander Altair is the linchpin in the Constellation Program for human return to the Moon. In the spring of 2007, a small group of engineers from multiple NASA centers were assembled in Houston, Texas to kickoff the lunar lander project. The “home” of the Altairians was Building 51 of the Johnson Space Center (JSC). In the first design cycle, the team focused on the establishment of a “minimal functionality” vehicle design for a polar sortie mission. After six months of work, with many collocations of team members at JSC, the team created a viable but “single string” design. This “minimal functionality” design provides no redundancy and has no provision for most contingencies. One failure and you lose the mission. NASA does not intend to fly anything like this stripped-down Altair, but the concept enabled the team to produce a design that copes with the immutable physics of executing a lunar landing. Managers can then consciously add safety and reliability features with full knowledge of how much risk reduction those enhancements are buying.

In early March 2008, many Altair team members attended a “Go for Lunar Landing: From Terminal Descent to Touchdown” conference in Tempe, Arizona. The purpose of this conference was to allow Constellation personnel and management (such as the Altair team) to leverage the experiences and lessons learned from the six Apollo lunar landings. The project manager of Altair at that time, Lauri Hansen, was one of the keynote speakers of the conference. In mid-March 2008, five 210-day study contracts were awarded to contract teams to do independent feasibility studies. The contract teams supplemented the experience base of the Altair team especially on the “manufacturability” of the Altair design. Two design cycles (cycles 2 and 3) were also performed in 2008 to improve the resiliency of the minimal-functionality design relative to, first the “Loss of Crew” (LOC) and then the “Loss of Mission” (LOM) risks. This was achieved via selective addition of vehicle functionality, new sensors, and redundancy of selected equipment. The risk-driven design methodology that was adopted for this project has been previously presented,³⁸ and will not be discussed in detail in this paper; rather, only the result of these design iterations is presented here. Beside the sortie lander (which was the focus in 2007), the Altair team also studied two other lander variants: an outpost lander and a cargo lander. The outpost Altair will execute seven-month missions to a future lunar base, and it does not carry an air lock. The unpiloted cargo Altair will have neither an ascent module nor an airlock. The Altair team nicknamed it a “pickup truck.”

The focus of the team in 2009 was on the development of vehicle system requirements. The team also examined how compliancy with these system requirements impacts the vehicle design. Time was also spent to re-examine selected architecture choices made in prior years, to re-examine selected subsystem solutions, and to increase the maturity level of vehicle and subsystem designs. A three-day Vehicle Performance Review was conducted in early

⁺The future of the human space flight program, and thus the Constellation program, is currently being discussed at the highest levels of the U.S. government. For the purposes of documenting the Altair design, this paper is written without consideration of any forthcoming changes in the direction (or even existence) of the program.

March 2010 to establish a common understanding of the vehicle performance. The review also helped to identify areas in the design (or integration) that have not been sufficiently addressed. This paper is written to capture the status of the GN&C design in early April of 2010.

The Guidance, Navigation, and Control (GN&C) system must perform many functions that are critical to the Altair mission. The purpose of this paper is to provide an overview of the Altair GN&C systems design. To this end, the overall mission profile will first be reviewed. Key requirements the GN&C system must satisfy, and functions it must perform, in various mission phases will then be described. The GN&C system, (including its sensor suite and thruster configurations) that is configured to support these requirements and functions will then be described. The Reaction Control System (RCS) thruster systems were designed by the GN&C team, in collaboration with the Propulsion design team. The emphasis of this paper is on the overall GN&C system architecture. Details that are related to specific GN&C functions, including navigation, optical navigation, guidance, interactions between thrust vector control and sloshing liquids, etc., are given in seven companion papers.⁴⁻¹⁰ The GN&C team also provided support for the design teams of various subsystems including Thermal, Power, Avionics, Flight Software, Structures, Commands and Data Handling, Comm. and Tracking, and others. Details on these sub-system designs will not be described in this paper.

2. Design Reference (Polar Sortie) Mission

Similar to that of the Apollo Lunar Module, Altair is envisioned to be a two-stage vehicle, comprising a Descent Module (DM) and an Ascent Module (AM). Using propulsion elements carried by the unmanned DM, the mated DM/AM will descend from a lunar parking orbit and land on the Moon. Altair will be capable of landing four astronauts on the Moon and of providing life support and a base for weeklong initial surface exploration missions. Using propulsion elements carried by the manned AM, only the AM will ascend from the lunar surface, returning the crew to the Orion spacecraft that will bring them back to Earth. A representative Altair mission profile consists of the following sub-phases:

- Pre-launch ground operations and launch vehicle (LV) boost phases
- LEO operations and mating of Altair/EDS with Orion
- Trans-lunar injection of the mated EDS/Altair/Orion
- Separation of the mated Orion/Altair from EDS
- Trans-lunar coast
- Lunar orbit insertion of the mated Orion/Altair vehicle into a low lunar orbit (LLO)
- Undocking of Altair with Orion in LLO
- Plane change (ΔV) burn
- De-orbit ΔV burn
- Descent and landing
- Lunar surface operations
- Ascent, rendezvous, and proximity operations
- Docking of the ascent module with Orion in LLO
- Control of the mated Orion/AM by Orion GN&C system
- Separation of Altair from Orion
- Disposal of Altair

The mission starts with the use of the ARES-I launch vehicle to insert Orion into a 100-km low Earth Orbit (LEO). Next, the ARES-V heavy-lift launch vehicle will insert Altair, which is mated with the Earth Departure Stage (EDS), into the same orbit. At liftoff, Altair has a mass of 45 metric tons. During docking operations with Orion in LEO, the passive Altair/EDS stack will be controlled by EDS. After spending 2–3 days in LEO, the EDS will be fired to impart 3.1–3.2 km/s ΔV on the mated Orion/Altair vehicle and send it on its way to the Moon. The duration of the trans-lunar injection (TLI) burn is about 6 min. Within 0.5–1 hour after the completion of the TLI burn, EDS will be separated from the mated Altair/Orion. Post-separation, the Altair GN&C system will begin to execute all guidance, navigation, and control functions of the mated Orion/Altair vehicle.

The Trans-lunar Coast (TLC) will last 90–100 hours. During the TLC phase, Altair GN&C will perform four (or more) trajectory correction maneuvers (TCM) in order to keep the spacecraft on a pre-computed reference trajectory. Typically, these are small burns (<30 m/s) that will be executed using RCS thrusters of the Descent Module. The long coast time offers opportunities to perform many checked out and calibrations of GN&C sensors and equipment. Upon arrival at the Moon, the powerful gimbaled engine of the Altair descent module will be fired for 10–11 minutes in order to slow down the velocity of the stack by 891 m/s. At the end of the lunar orbit insertion (LOI) burn, the gravity field of the Moon will capture the mated vehicle into a 100-km low lunar orbit (LLO). This LLO will be a polar orbit for landing targets that are located near the south pole of the Moon.

After spending about one day in the LLO, Altair will undock with Orion. Orion will execute both the undocking and the separation maneuvers. About 1.5 hours after the separation event, Altair will use the DM engine to perform a small (28.3–28.5 m/s) Plane Change (PC) ΔV burn in order to target the Shackleton landing site near the South Pole. The duration of the PC burn is about 19 s. Another 1.5 hours after the PC burn, Altair will use the DM RCS thrusters to perform a small (19.2–19.4 m/s) de-orbit insertion (DOI) ΔV burn. The DOI burn will last about 5.7 min., and Altair has a mass of about 32 metric tons at the end of the DOI burn. The DOI burn will place Altair on an orbit that has a perilune of 15.24 km. At the perilune, the gimbaled engine of the DM will be ignited to initiate the powered descent burn.

Initially, the powered descent burn (2074 m/s) will focus on braking the orbital speed of the vehicle. To do this efficiently, the engine thrust will be closely aligned with the velocity vector of Altair. At an altitude of about 2 km, nearly 3 minutes before touchdown, the Altair will make a large change in its attitude via a “pitch-up” maneuver. In so doing, the guidance algorithm will sacrifice fuel utilization efficiency in order to provide landing-site visibility for both the crew and the terrain hazard detection sensor system. With this attitude change, hazardous terrain features (craters, rocks, and surface slopes with angles too great for the Altair landing gear design) could be identified by both crew members and sensors, and a landing site “re-designation” made, if necessary, to avoid the hazardous landing site. During the final vertical descent of the vehicle, GN&C will focus on achieving a vehicle’s touchdown state that is consistent with the landing gear design. Nominally, it will take Altair about twelve minutes, from the initiation of the powered descent burn, to land on the Moon. At the time of touch down, Altair will have a mass of 19-20 metric tons.

After a stay of 5–7 days on the Moon, a series of burns will be executed to bring the Ascent Module (AM), housing the Crew, back to a 100-km LLO where it will dock with the orbiting un-crewed Orion. At liftoff, the Altair AM has a mass of about 7 metric tons. The first burn, named ascent insertion burn, will be executed using the un-gimbaled engine of the AM in three sub-phases. After a vertical rise to achieve an altitude of 100 m, thrusters will be fired to execute a single-axis rotation (SAR) and orient the vehicle attitude to a desirable flight path angle for the next sub-phase. The AM GN&C will then use the Powered Explicit Guidance (PEG) algorithm to complete the insertion burn until engine cutoff. The time of this insertion burn is about 7 min. Nominally, the ascent insertion burn will place AM in a 15.24 km \times 75 km orbit. Rendezvous, Proximity Operations, and Docking (RPOD) maneuvers are initiated 10–15 min. after the completion of the ascent insertion burn. These are discrete maneuvers with coasting in between discrete burns. They are relatively small and therefore will be executed using the AM RCS thrusters. The first discrete burn, about 1–2 m/s, will be used to “clean up” any undesirable trajectory dispersions generated by the ascent insertion burn. Next, the larger Terminal Phase Initiation (TPI) burn, about 19-20 m/s, will place Altair on a coasting trajectory to acquire the R-bar (see Section 7.3 for details) at a distance of 2 km from the orbiting Orion with a radial relative velocity. Between TPI and the R-bar acquisition, small maneuvers will be used to shape the trajectory and correct any dispersion.

The proximity operations phase consists of many small maneuvers to be executed by Altair, to close the gap between Altair and Orion, in “steps”. During proximity operations, the uncrewed Orion will be the passive vehicle, and its thrusters will be used to maintain the spacecraft in a quiescent state. To achieve a soft docking, Altair will measure the relative angular and translational displacements and rates between vehicles via its docking sensor. The AM thrusters with small minimum impulse bit will then be used to generate the needed small translational and angular rate changes. To achieve a safe docking, the contact conditions between the vehicles must be controlled to levels that are acceptable to the Low Impact Docking System (LIDS). Key contact conditions include the relative translational and angular rates between the mating vehicles as well as the relative translational and angular attitudes, about all spacecraft axes. Altair has a mass of 3.3 metric tons at the time of docking. Measuring from the time of lunar liftoff, the AM will be able to complete the entire process in just less than 3 hours.

After a successful transfer of Crew from the AM to Orion, the crewed Orion will perform the undocking and separation maneuvers to achieve a safe separation distance the vehicle. Before the Crew start their preparations for the Trans-Earth Injection (TEI) burn, they will send commands for Altair GN&C system to execute a second deorbit insertion to “dispose” the AM near a pre-selected site on the Moon. Henceforth, the Orion GN&C system will assume all GN&C responsibilities.

3. Key Altair GN&C-related Requirements

The Constellation Architecture Requirements Document (CARD) defines requirements controlled by the Constellation Program for hardware, software, facilities, personnel and services needed to perform the design reference missions.¹⁶ The CARD is structured to provide top-level design guidance, architecture wide requirements, and allocations to the systems. A survey of the CARD document produces a list of key GN&C-related requirements that are summarized in Table 1.

Table 1 Key Altair GN&C-related Requirements

Requirement Number	GN&C-Related Requirements
CA0135	Altair shall function as the maneuvering vehicle during RPOD operations with the Orion in LLO prior to crew transfer back to the Orion.
CA0136	Altair shall perform GN&C functions of the integrated Altair/Orion mated configuration, post-EDS separation through Altair/Orion separation in LLO.
CA0284	Altair shall land within 1 (TBR-001-044) km of a designated landing site on the lunar surface independent of lunar vicinity landing aids.
CA0286	Altair shall be capable of landing site re-designation in order to perform a controlled soft landing at any point in the landing area.
CA0418	Altair shall land within 100 (TBR-001-012) m of a designated landing site on the lunar surface using lunar vicinity landing aids.
CA0461	Altair shall perform the Lunar orbit insertion into the Lunar destination orbit.
CA0840	Altair shall compute translational maneuver targets.
CA0891	Altair shall be a minimum of one- failure tolerant for controlling catastrophic hazards, except for areas approved to use “Design for Minimum Risk” criteria. ... The failure tolerance requirement cannot be satisfied by use of EVA during flight, emergency operations or emergency systems.
CA3144	Altair shall perform navigation and attitude determination beginning with Earth orbital operations through Altair disposal.
CA3145	Altair shall compute maneuvers associated with lunar descent and landing beginning with DOI after the completion of LOI.
CA3205	Altair shall perform trajectory correction maneuvers during the trans-lunar coast and Lunar orbital operations.
CA3206	Altair shall deliver the crew and cargo from Lunar destination orbit to the lunar surface for Lunar sortie and Lunar outpost crew missions.
CA3251	Altair shall compute rendezvous maneuvers for lunar orbit operations for Lunar sortie crew and Lunar outpost crew missions.
CA3286	Altair shall perform Lunar sortie missions without the aid of pre-deployed lunar surface infrastructure.
CA5193	Altair shall perform the functions necessary to return to LLO within 3 (TBR-001-171) hours with an unpressurized cabin for Lunar sortie and Lunar outpost crew missions.
CA5236	Altair shall perform aborts from post TLI until lunar landing for Lunar sortie and Lunar outpost crew missions.

Requirement Number	GN&C-Related Requirements
CA5238	Altair shall return the crew from the surface of the moon to docking with Orion in the Lunar rendezvous orbit in 12 (TBR-001-179) hours or less for Lunar sortie and Lunar outpost crew missions.
CA5273	Altair shall perform Rendezvous Proximity Operations Docking and Undocking (RPODU) independent of lighting conditions.
CA5275	Altair shall be capable of functioning as the target vehicle while performing RPOD with Orion in LLO for Lunar sortie and Lunar outpost crew missions.
CA5278	Altair shall provide onboard, manual control of flight path, attitude, and attitude rates when the human can operate the system within vehicle margins for Lunar sortie crew and Lunar outpost crew missions.
CA5284	Altair shall function as the target vehicle during undocking and departure proximity operations from Orion after the crew transfer to Orion.
CA5285	Altair shall be capable of performing as the maneuvering vehicle functions during undocking and departure proximity operations from Orion prior to lunar descent for Lunar sortie crew and Lunar outpost crew missions.
CA5290	Altair shall perform attitude control of the Orion/Altair mated configuration after separating from the ARES-V EDS for Lunar sortie and Lunar outpost crew missions.
CA5293	Altair shall provide target vehicle interfaces in the Altair/ARES-V EDS mated configuration, during RPODU operations with Orion in LEO, for Lunar sortie and Lunar outpost crew missions.
CA5303	Altair shall land on the lunar surface only under the lighting conditions specified in Table (TBD-001-460) for Lunar sortie crew and Lunar outpost crew missions.
CA5316	Altair shall return the crew to Orion independent of communications with the mission systems.
CA5440	Altair shall automatically perform abort for Lunar sortie and Lunar outpost crew missions.
CA5469	Altair shall detect system faults that could result in loss of vehicle, loss of life, and loss of mission.
EA0028	The Constellation Architecture shall return the crew to the Earth surface independent of communications with mission systems during all mission phases.
EA0216	The Constellation architecture shall provide fault detection, isolation and recovery.

Based on the current interpretations of these requirements, the following set of GN&C functions is identified:

- Estimate the three-axis attitude and attitude rate of Altair (with respect to an inertial frame), at all times, satisfying a set of attitude determination accuracy requirements.
 - Perform inflight calibrations of GN&C sensors and equipment. Flight software shall have the ability to update selected sensor parameters using results from these calibrations.
 - Provide a capability to (temporarily) propagate the estimated three-axis attitude and attitude rate of Altair analytically without the use of gyroscope data.
- Control both the three-axis attitude and attitude rate of Altair relative to their commanded state, at all times, satisfying a set of attitude control pointing accuracy requirements.
 - Provide a capability to (temporarily) suspend the three-axis attitude control of Altair for a commandable time duration.
 - Provide onboard manual control of flight path, attitude, and attitude rates when crew can operate the vehicle safely.
 - Respond to a crew command to terminate a turn in progress.
 - Function as either the maneuvering (active) or target (passive) vehicle during undocking and departure proximity operations from Orion prior to lunar descent.

- Function as either the maneuvering or target vehicle during undocking and departure proximity operations from Orion after the crew transfer to Orion in LLO.
- Pointing selected axes of Altair to celestial objects (e.g., the Sun) will cause irreversible damage to Altair sensors or equipment. GN&C will track potential violation of any of these pointing control constraints. Both crew and flight system will be alerted to an imminent constraint violation.
- Determine the “state” of Altair (both the three-axis position and velocity vectors) with respect to a reference frame, at all times, satisfying a set of position and velocity determination accuracy requirements.
 - Determine the “state” of Altair without the use of Earth-Based Ground System (EBGS) tracking data, satisfying a set of position- and velocity-determination accuracy requirements.
- Compute maneuvers associated with lunar descent and landing beginning with DOI after the completion of LOI.
- Compute rendezvous maneuvers associated with lunar ascent and RPOD after the completion of the ascent insertion burn.
- Execute fixed or time-varying commanded ΔV burns:
 - Using either the AM or DM RCS thrusters, satisfying a set of RCS maneuver execution accuracy requirements.
 - Using the gimballed DM engine, satisfying a set of DM engine maneuver execution accuracy requirements.
 - Using the ungimballed AM engine, satisfying a set of AM engine maneuver execution accuracy requirements.
 - Response to a crew command to terminate a burn in progress.
- Land Altair near the landing site in any lighting condition and without the aid of pre-deployed lunar surface infrastructure, satisfying a pre-selected landing accuracy requirement.
 - Identify terrain hazards (craters, slopes, and rocks) with “sizes” that exceed pre-specified levels, within a given time constraint. Based on these identified hazards, GN&C will provide the crew with a prioritized list of alternative landing sites.
 - Land Altair at the selected landing site with touchdown conditions that are consistent with the capability of the landing gear design. Touchdown conditions of Altair shall include its vertical and lateral velocities, its per-axis angular rates, and the angular deviation of Altair’s axis of symmetry from the local vertical.
- Determine the landing site (longitude and latitude) with respect to a pre-selected reference frame.
- Determine the orientation of the landed Altair relative to a pre-selected reference frame.
- Function as either the maneuvering or target vehicle while performing RPOD with Orion in LLO.
 - Carry cooperative hardware (such as a docking target for Orion) to support RPOD operations with Orion.
- Accept both real-time and stored command sequences from either the mission control center or the crew.
- Collect a pre-selected set of GN&C telemetry data and then routed it either directly to the ground, or to an onboard recorder (for later transmission to the ground).
- Provide onboard manual control of flight path, attitude, and attitude rates when the crew can operate the vehicle.
 - Generate and display selected GN&C data to the crew at a pre-specified update frequency.
- Detect a GN&C system fault, isolate the root cause of the detected fault, and autonomously reconfigure the GN&C system to restore the affected GN&C functionalities.

4. A Preliminary Altair GN&C System Design

The lunar lander vehicle Altair is a three-axis stabilized spacecraft. Three-axis stabilized spacecraft are best suited to missions where a high degree of maneuverability is required. Like the Apollo lunar lander designs, Altair consists of a descent module and an ascent module.

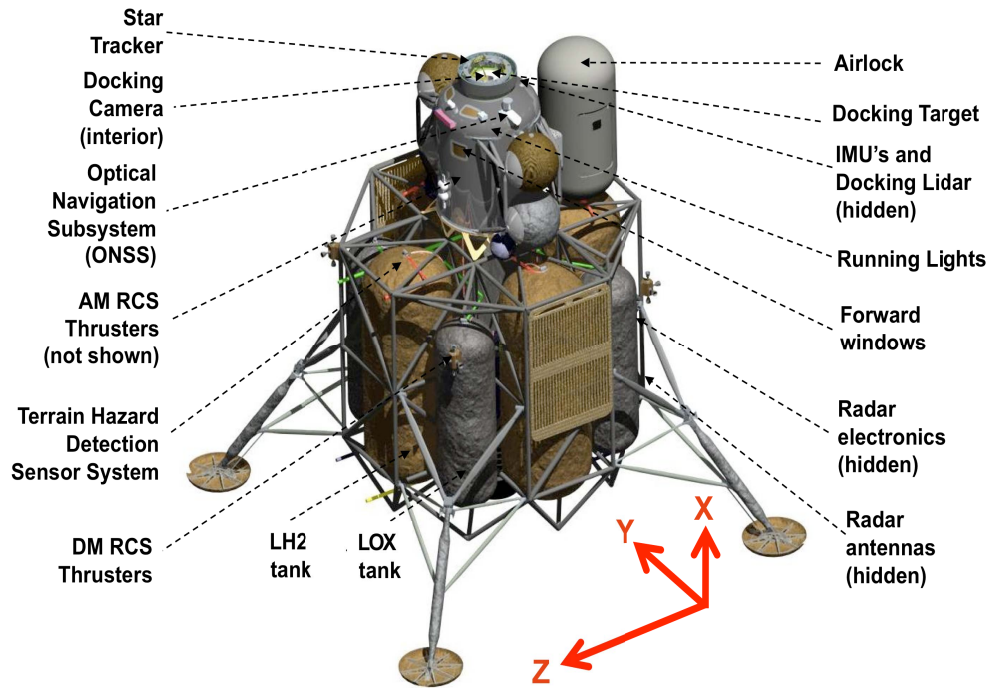


Figure 1. The Altair lunar lander vehicle (“Sortie” lander).

The descent module (DM) is the unmanned portion of Altair. It carries the large descent main propulsion engine, and eight propellant tanks. It also carries a set of RCS thrusters (four thruster pods, with four thrusters per pod). The DM also provides structural supports for both the ascent module and the landing gear. The landing gear provide the impact attenuation required to land Altair on the lunar surface, preventing vehicle tip-over at touchdown. The entire descent module will be enveloped in a thermal and micro-meteoroid shield. As depicted in Fig. 1, the radar system and the terrain hazard detection system are mounted on the descent module.

The ascent module (AM) has a crew compartment that provides a controlled environment for up to four astronauts. The sortie lander, depicted in Fig. 1, will carry an airlock for surface EVA. Crews will be in the ascent module at times of lunar landing and docking with Orion. Crew visibility of the landing site will be via the two forward windows. Visibility to Orion at time of docking will be via the two top windows. Near the top of the module is the passive side of the Low Impact Docking System (LIDS) adapter. Three Altair/Orion S-band radio antennas are also mounted near the top of the module. The ascent module carries the ascent main propulsion engine and the associated fuel tanks. It also carries a set of RCS thrusters (four thruster pods, with five thrusters per pod). As depicted in Fig. 1, many GN&C sensors are also mounted on the ascent module.

The relative “sizes” of the Apollo Eagle lander and Altair are compared in Fig. 2. Note that Altair is much larger and heavier than Eagle. This is largely because the Constellation program has directed that Altair perform the lunar orbit insertion burn. This choice leads to an Altair’s descent stage that is much larger than its Apollo counterpart. For Apollo missions, the lunar orbit insertions were executed by the service and command module. But the current ARES-I design simply cannot lift a service module that is powerful enough to handle the lunar orbit insertion. The Altair team did briefly study solutions to this challenge (e.g., Altair to carry a jettisonable orbit insertion stage). But this did not become an area of significant focus for the team.

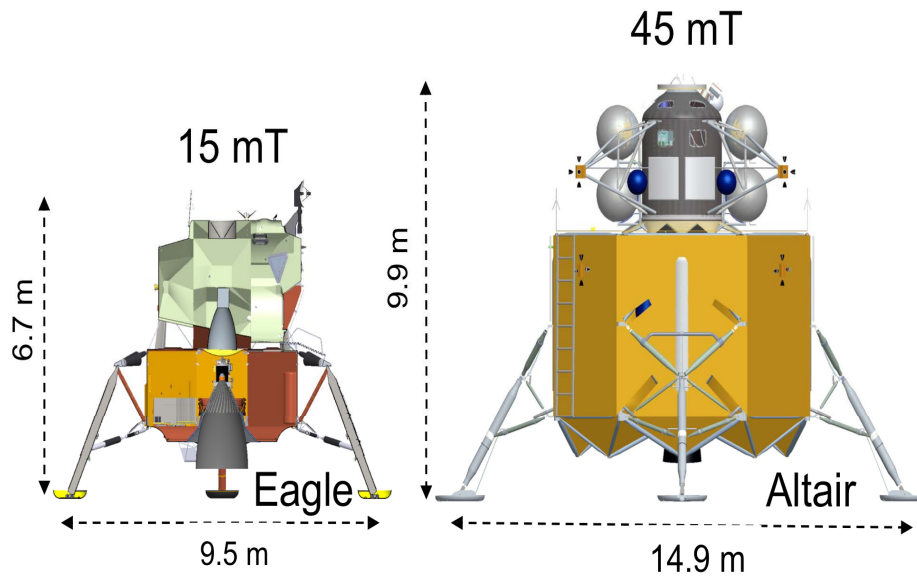


Figure 2. Relative size of Altair (“Sortie”) and Eagle.

4.1. Guidance, Navigation, and Control Sensor Suite

To perform the multitude of GN&C functions listed in Section 3, a set of GN&C sensors is selected. The intent in making this selection was not to promote any particular vendor’s sensor or rule out possible use of different sensors in the ultimate spacecraft design, but rather to specify a representative set of sensors that can provide the requisite functionality, based on currently-available technology. The mapping between these GN&C sensors and the functions they support is depicted in Fig. 3. Some GN&C functionalities, e.g., the estimation of the range between Altair and Orion (in LLO), are supported by measurements made available from other Altair’s subsystems (such as the Command and Tracking system). Hence, some non-GN&C sensors are also listed in Fig. 3. In this figure, sensors that are denoted “P” are primary sensors that are needed to perform the indicated function, and sensors that are used as backup are denoted by “S”.

GN&C (and non-GN&C) Sensors and Equipment	Inertial attitude and rate estimations	Inertial position and velocity estimations	Bring crew home with degraded ground links	Surface-relative position and velocity estimation	Terrain hazard detection	Provide crew display data	TVC guidance and control (LOI, PC, PDI)	Vertical descent and burn cutoff at touch down	Determine landing site and landing attitude	Orion-relative bearing and range estimation	Rendezvous ΔV guidance and control	Pose estimate for docking control	Disposal guidance and control
IMU gyroscopes	P	P	P	P	P	P	P	P	P	P	P	P	P
IMU accelerometers	P	P	P	P	P	P	P	P	P	P	P	P	P
Star trackers	P	P	P	P	P	P	P	P	P	P	P	P	P
Descent radar system				P		P	P	P					
Optical navigation sensor system		S	P	P	S	P	S		S	S			S
Terrain hazard detection sensor system				S	P	P	S	S	S				
DSN station state vector updates		P		S		P			P	S	S		P
Orion/Altair 2-way S-band radio link data						P				P	P		S
Docking lidar						P				P	P	P	S
Hand-held laser range finder				S				S		S		S	
Docking camera						P				S		S	S

Figure 3. Mapping of GN&C functionality with sensors.

The spacecraft’s attitude in a celestial frame is estimated using a Stellar Reference Unit (SRU, sometimes called a star tracker) and a set of three gyroscopes. The primary star tracker is mounted on the AM. The backup star tracker, together with a narrow angle camera, are mounted on a 2-dof gimbal platform. This sensor package, named Optical Navigation Sensor System (ONSS), is specifically included in the GN&C sensor suite for the purpose of performing optical navigation.⁵ All Constellation elements are required to “get the crew home” even when communications links are down or degraded. In CARD requirement CA0028, it is stated: “The Constellation architecture shall return the crew to Earth surface independent of communications with Mission System during all mission phases.” This will ensure the safety of the crew by allowing the Constellation systems to still function adequately if there were permanent or unplanned intermittent communication service outages preventing or limiting the ability of Mission Systems to interface with the vehicles used for the given mission. Without state vector

updates, optical navigation is the only way to estimate the vehicle's state vector. The ONSS, depicted in Fig. 4, is also mounted on the AM.

The ONSS as shown in Fig.4 consists of two gimbal-mounted cameras, with wide and narrow FOV optics. This concept instrument would use a narrow angle camera (NAC) similar to the Mars Reconnaissance Orbiter (MRO) Optical Navigation Camera (ONC) now flying on the MRO mission as the narrow-angle camera (NAC). The wide-angle camera (WAC) would be similar to the Inertial Stellar Compass (ISC) as flown on the TacSat2 mission. The NAC would be used for long-range observations, principally in trans-lunar cruise, in the early phase of RPOD, and in lunar orbit (in the latter case where instantaneous determinations of position can be at the 10 meter level, when availability of surface maps allow). The WAC would be used for close-range observations (principally throughout the descent and landing phase) and for the mid and terminal phases of RPOD. The gimbal is considered a necessary part of the ONSS instrument in order to alleviate Altair from having to change attitude in order to obtain navigation data, and it is required during descent to enable Altair to track the landing site. In addition, the gimbal allows the WAC component of the ONSS to serve as a back-up star tracker.

As indicated in Fig. 3, ONSS can also serve other important GN&C functions. On descent, the GN&C system plans to use ONSS to perform terrain relative navigation (TRN). This is a navigation technique that takes advantage of known locations of landmarks on the lunar surface. On ascent, the GN&C system plans to use ONSS to perform Orion-relative navigation. The range and bearing angles between the two vehicles could be estimated using measurements from ONSS cameras together with supporting onboard software. Estimated mass and power of both the star tracker and ONSS are given in Table 2.

Three Inertial Measurement Units (IMU) are included in the Altair GN&C sensor suite. The primary IMU contains four gyroscopes and four accelerometers. The two backup IMU's are identical, and each unit contains three gyroscopes and three accelerometers. If these three IMU's are not co-aligned, and if they are all powered on, independent measurements from 10 gyroscopes and accelerometers will be available. Measurements from three selected prime gyroscopes will be used to support the attitude determination function. Measurements from three selected prime accelerometers will be used to support the propagations of spacecraft's "state" vector (the position and velocity vectors of the spacecraft). Estimated mass and power of both the prime and backup IMU's are given in Table 2.

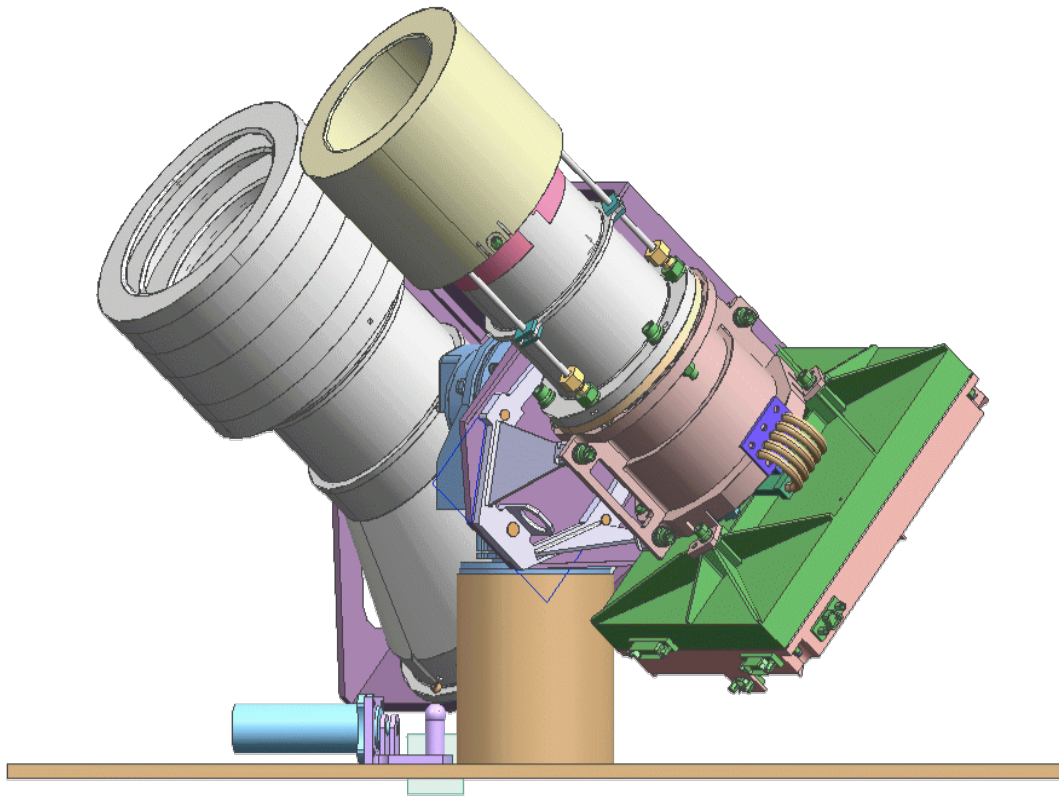


Figure 4. Optical Navigation Sensor System.

For guidance and control of Altair in the descent and landing phase, a Terminal Descent Radar System (TDRS) will be used to estimate the surface-relative Altair's altitude and velocity. Radars were used on all Mars landers, such as Phoenix.⁵¹ But the specific Altair TDRS is the radar that is being readied for the Mars Science Laboratory (MSL), which will be launched in 2011. The MSL radar uses pulse-Doppler technology to simultaneously provide estimates of altitude and velocity. The Ka-band (35.75 GHz) radar has little susceptibility to dust and engine plumes,⁴⁴ and it could operate in complete darkness. The operational slant range of the TDRS in the "altitude-only" mode is 20 km (those of Apollo-11 and Apollo-15 radar were 11 and 15 km, respectively⁶¹). The "altitude/velocity" mode is active when the rate is ≤ 210 m/s. In general, radars do not perform well when they are close to the surface (in the terminal descent phase). Range measurements from another GN&C sensor, the Terminal Hazard Detection Sensor System (THDSS) described below, will be used to fill this performance "gap."

As indicated in Fig. 5, this radar system has six radar beams that are cross-strapped to a set of two redundant radar electronics. In the current placeholder configuration, two beams are co-aligned and pointed "down" in the nadir direction. Two beams are pointed off-nadir with an elevation angle of 20° and azimuth angles of $\pm 45^\circ$. The remaining two off-nadir beams have an elevation angle of 45° and azimuth angles of $\pm 45^\circ$. The "radius" of each beam is about 20° . It is important to mount the antennas (on the DM) in such a way that the "foot print" of none of these six beams intersects the deployed landing gear of Altair. During descent and landing, some of the six beams might intersect the surface with an acceptably large incidence angle $\beta > 60^\circ$ (see Fig. 5). Assuming uniform distribution of the incidence angle over $0-90^\circ$, four of the six beams will have incidence angles that are acceptable. This is one more than a minimum set of three beams. Estimated mass and power of TDRS are given in Table 2.

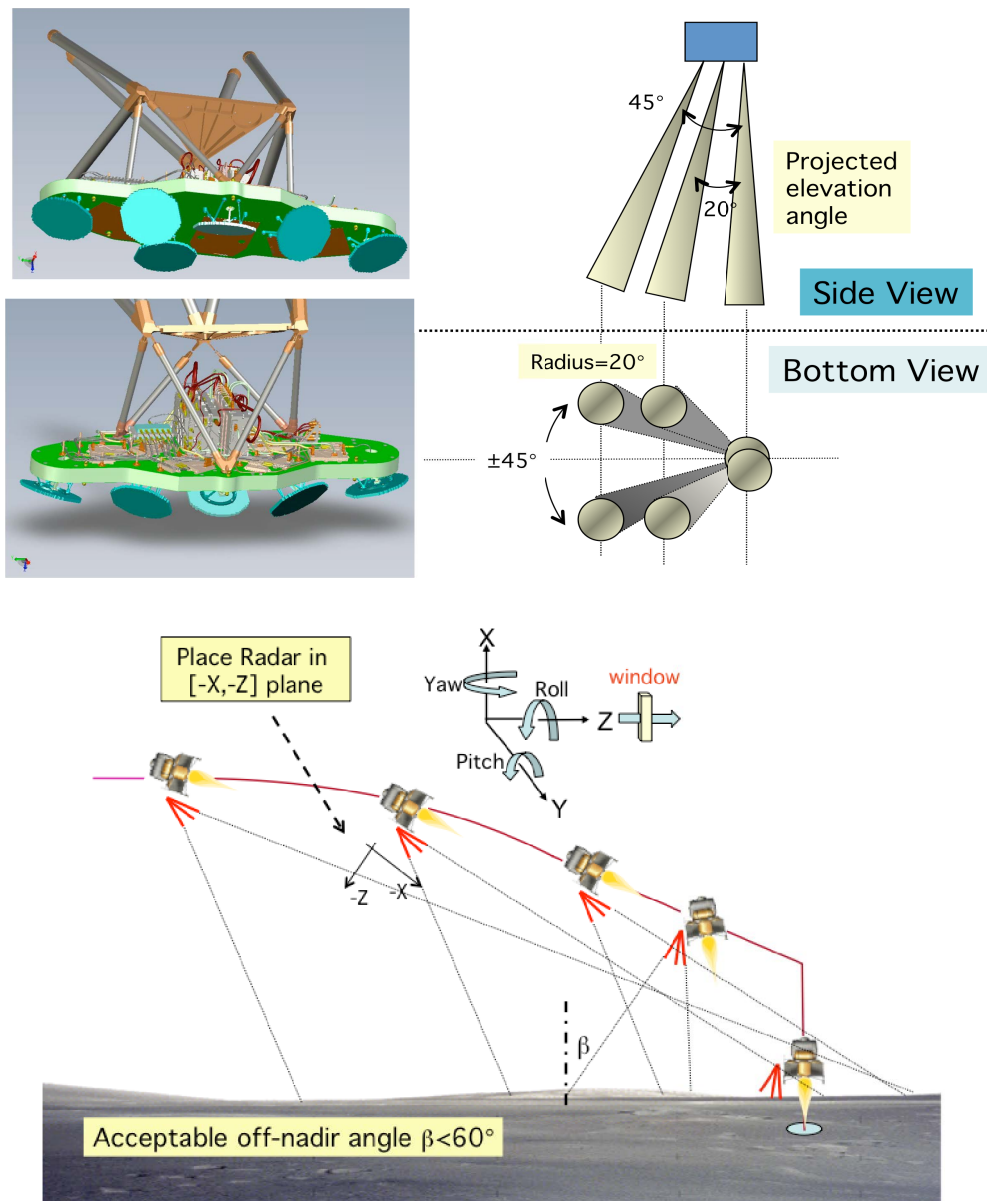


Figure 5. Terminal Descent Radar System.

In the general vicinity of the intended landing site of Altair near the South Pole, there are many terrain hazards that will be challenging to the Altair's landing gear. These hazards include craters, slopes, and rocks. The presence of these types of terrain hazards forced the Apollo-12 crew to make seven re-designations of the landing site before a safe touch down.²⁰ For the Apollo missions, the identifications of terrain hazards were all made by the crews. This is feasible for well-lighted landing sites that are located within $\pm 20^\circ$ from the Equator. But even for these missions, near the end of the approach phase of the descent trajectory, crew vision was obscured by the presence of dust clouds. Apollo-11 crews observed dust cloud at an altitude of 30 m.⁶¹ Dust cloud became so intense at 12–15 m that it impaired the visibility of the Apollo-11 crew during the terminal descent and landing phase of the mission. The detection of terrain hazards by crew alone might be risky.

The biggest challenge for safe landing is having a real-time system that can detect hazards and identify safe landing areas. For Altair, a sensor named Terrain Hazard Detection System Sensor (THDSS) will be the primary mean of terrain hazard detection.⁸ Crew visual detection will be the backup (via out-the-window viewing). THDSS will generate a prioritized list of “hazard free” landing sites and the re-designation to one of these recommended sites will be authorized by the crews. The THDSS is modeled after a sensor that is being developed under a technology program named Autonomous Landing Hazard Avoidance Technology (ALHAT).³⁵⁻³⁷ As a placeholder, THDSS will consist of a flash Light Intensification, Detection, and Ranging (lidar) that is mounted on a 2-dof gimbal. To detect terrain hazard, the relative elevation data of surface features is the most important information that is needed. It appeared that flash lidar is a best-candidate sensor for acquiring the needed real-time terrain hazard data.⁴⁹ Flash lidar could acquire the needed information in any lighting condition which is an advantage for Altair missions to the South Pole of the moon. Early analyses indicated that the performance of flash lidar is robust in the presence of lunar dust and descent engine plume.³⁴ But this placeholder sensor does not have any flight heritage. By placing the sensor on a gimbal, THDSS will be able to greatly increase its search areas while the Altair’s attitude changes continuously with time during the approach phase. The THDSS is mounted on the DM to maximize its field of regard. The operations range of THDSS is 0.8–1 km, and the objective is to be able to detect hazard sizes as small as 30–50 cm. Estimated mass and power of THDSS are given in Table 2.

The rendezvous and docking process consists of a series of orbital maneuvers and spacecraft attitude control motions that successively bring the active vehicle into the vicinity of, and eventually into contact with, the passive vehicle. In low lunar orbit, Altair will be the active vehicle and Orion will be the passive vehicle. Rendezvous and docking is a complex and challenging task, and it must be supported by a set of rendezvous and docking sensors with adequate redundancy. Fundamental to this set of sensors are the star tracker and the IMU. Feeding measurements from these sensors to the flight software will provide the GN&C system with estimates of the Altair’s position, velocity, attitude, and attitude rate. The range and bearing angles between Altair and Orion could be computed accordingly. However, it is also advantageous to acquire these relative measurements directly. In the current GN&C plan, the bearing angles from Altair to Orion will be estimated using the prime star tracker. As a backup, the cameras of ONSS will be used. The range and range-rate between the two vehicles will be estimated via the two-way S-band radiometric ranging data. Again, as a backup, they could also be estimated using the ONSS cameras. Once the vehicles are within a range of 4–5 km, estimates of the bearing angles and range with better accuracy could be provided by a scanning lidar (Laser Imaging, Detection, and Ranging). Multiple alternative means to acquire these data are available, and lidar was adopted by Altair GN&C only as a placeholder.^{13-14,40-41} Once the vehicles are within 100–150 m, lidar will also provide estimates of the relative attitude of Altair and Orion (also called “pose”). The uses of Altair RPOD and docking sensors as a function of vehicle range is depicted in Fig. 6. A list of mass and power specifications of all placeholder GN&C sensors are given in Table 2. Research and development on the miniaturizations of radar and lidar are making steady progress. The mass, power, and size of these sensors at the time of launch of Altair will likely be significantly better than those given in Table 2. All GN&C sensors are placed on the AM except the TDRS and THDSS, which are placed on the DM. See Figs. 1 and 7.

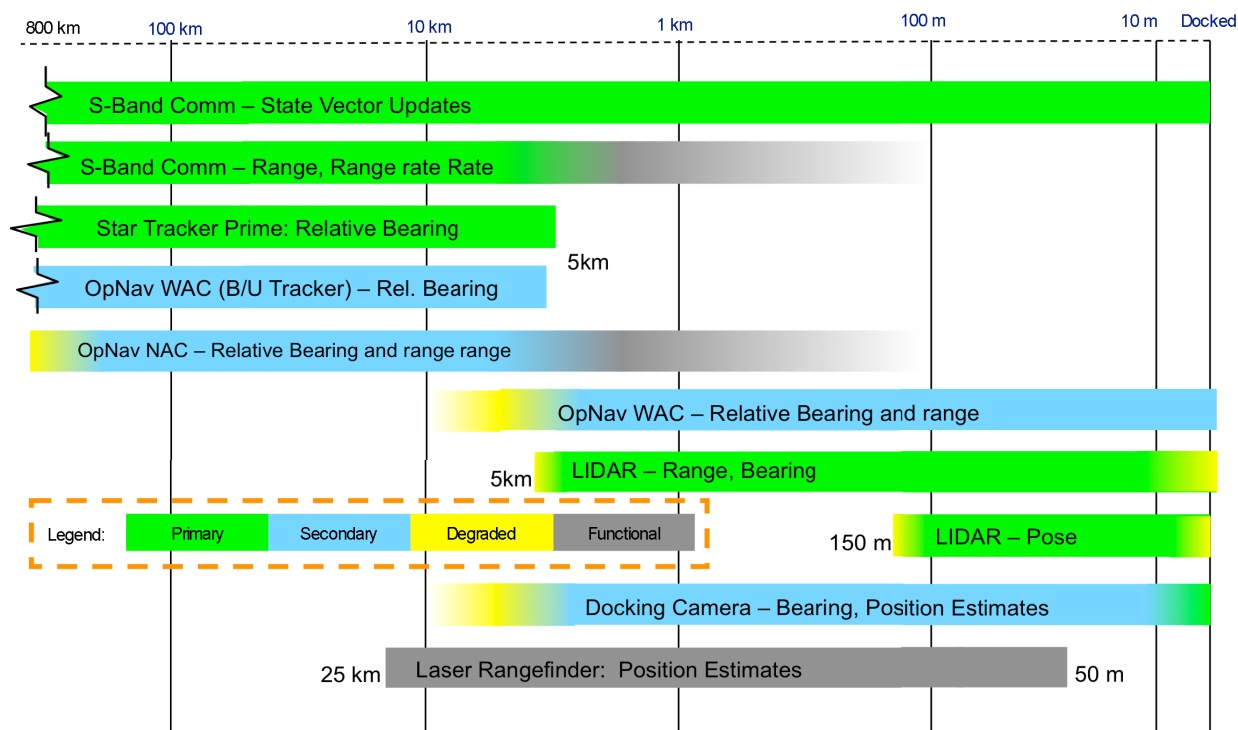


Figure 6. GN&C (and non-GN&C) Sensors Used in RPOD.

Table 2. A set of placeholder Altair sensors.

GN&C Sensors and Equipment	Mass [kg]	Power [W]	Placeholders ⁵
IMU (prime)	6.5	45	Honeywell MIMU
IMU (two identical backup's)	5.3 (each)	28.5 (each)	Northrop Grumman SIRU
Stra tracker (prime)	2.5	10	Ball Aerospace
Deployable tracker cover	1.53	10	Conceptual JPL design
Optical navigation sensor system	9.2	16.6	A gimballed platform on which is mounted a NAC and a WAC (backup tracker)
Terminal descent radar system (with 6 antennas)	26.8	115	JPL radar design (for MSL mission)
Lidar, optics and electronics	10	75	MDA/Optech scanning lidar
Docking camera	4.2	3	Boeing
Docking target	4.65	0	Orion-like design
Running light (two)	1.9	20	Orion-like design (0.95 kg and 10 W each)
Hand-held laser range finder	1.9	Battery	Newcon Optik
Terrain hazard detection sensor system	10	150	Mass and power are requirements

⁵The intent in making this selection was not to promote any particular vendor's sensor or rule out possible use of different sensors in the ultimate spacecraft design, but rather to specify a representative set of sensors that can provide the requisite functionality, based on currently-available technology.

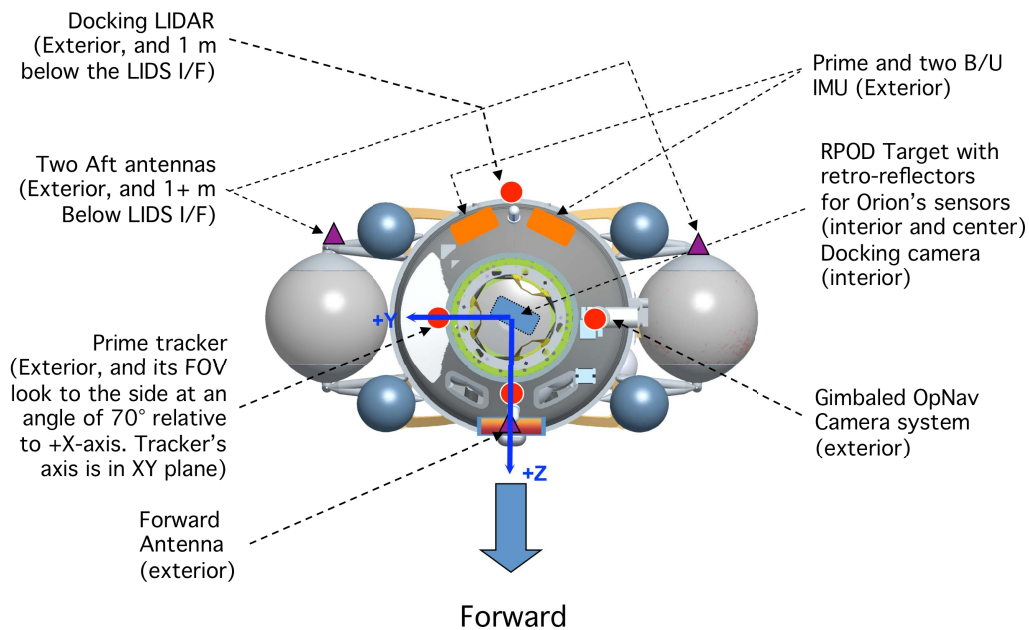


Figure 7. Notional placements of GN&C sensors and telecom antennas on ascent module (top view).

In summary, the Altair GN&C sensor suite is selected and used based on the following general principles:

- A “minimal functionality” set of GN&C sensors is selected to establish a baseline. The set was subsequently enhanced with backup unit(s) based on a risk-driven design methodology⁷² that leveraged a Probabilistic Risk Assessment (PRA).
- Both prime and backup sensor and equipment must have high technology readiness level (TRL), and have rich flight heritage.
- Dissimilar prime and backup sensors are employed whenever practical.
- Sensors must have high coverage in Built-In-Test (BIT).
- Performance of all GN&C sensors shall be monitored using sets of “error monitors” in the flight software. Decisions to make changes in the primeness of these sensors will depend on the “triggered states” of these error monitors. This approach is similar to that used by the Cassini spacecraft.⁵⁶
- All GN&C sensor and equipment shall be checked out in flight (at least once) before their flight uses.
- Both IMU gyroscopes and accelerometers shall be calibrated in flight (at least once) using established techniques. Calibrated values of sensor parameters shall be incorporated in the flight software.
- Both the prime and backup sensors shall be powered on during critical events (such as LOI).
- Altair GN&C performance shall be compared with those from either Orion or EDS whenever these performance data are available.
- Environmental threats to GN&C sensors are addressed proactively. Lunar dust and thrusters’ plume are dealt with using cover mechanisms. All GN&C sensor electronics are radiation harden.
- The current design reference mission offers opportunities for “mutual support” between Orion and Altair. For example, if the Altair’s docking lidar were to fail in LLO, Orion could become the chaser vehicle of docking operations. For this reason, Altair does not carry a backup docking sensor.
- The crew could provide another level of redundancy for several key GN&C tasks (e.g., landing and docking operations). But to make the crew effective, they must be provided with useful data displays.

4.1.1 Impacts of Lunar Radiation Environment on GN&C Sensors

Unlike Earth, the Moon has practically no magnetic field or atmosphere to protect it from the barrage of particles and rays that stream in from the Sun and beyond. As such, the space around the Moon contains many types of ionizing radiation: large fluxes of low-energy solar wind particles, small fluxes of high-energy galactic cosmic rays, and rare but occasionally intense particle fluxes emitted by solar flares (solar cosmic rays).⁶² Because electronics operate based on the principle of controlled carrier diffusion within the semiconductor material, the flood of ions produced by a localized passing of a single high energy particle easily causes the electronic device to perform unpredictably. This occurrence is generally known as a single event upset (SEU). Impacts of high-energy protons/ions on Cassini sensor electronics were observed inflight.³

A short mission to the Moon will be survivable for astronauts because exposure times will be low. Astronauts staying for longer periods will need shielding against the long-term effects of exposure. Similarly, GN&C sensor electronics must also be protected from SEU. The Radiation-Hardened Electronics for Space Exploration (RHESE) project is one of several technology projects within the NASA Exploration Technology Development Program (ETDP).⁶³ Not paying attention to this threat might lead to serious spacecraft anomalies such as the one experienced by Indian Chandrayaan-1 lunar orbiter.

The operations team of the Indian lunar orbiter abandoned its moon mission after contact with the probe was lost on August 28, 2009. The radiation environment in the lunar orbit was blamed for the sudden demise of the spacecraft. Upon insertion into a 100-km lunar orbit (November 8, 2008), the spacecraft was subjected to higher-than-expected direct and indirect solar radiation energy, causing the spacecraft to attain high temperature. In mid-May 2009, both the spacecraft's primary and backup star sensors had failed. Subsequent anomaly investigations revealed that the thermal problems were not the only cause of the spacecraft failure. Instead, it seems possible that the high temperatures had made some electronics components of the trackers more susceptible to ionizing radiation.

RHESE endeavors to advance the current state-of-the-art in radiation-hardened electronics by developing high performance devices robust enough to withstand the extreme radiation and temperature levels encountered within the lunar environment. Altair GN&C sensors will be one of the customers of technologies developed by RHESE. The other basic solution to radiation is the shielding of radiation-sensitive portions of the spacecraft with additional materials.⁶⁴ By including additional materials around the component to be protected, there will be an increased chance that the high-energy particle will be stopped via its interaction with the shielding material prior to reaching the component. But the obvious penalty of shielding is increased mass. Altair GN&C will use more radiation-tolerant electronics and more shielding to address the threat of the lunar radiation environment.

4.1.2 Power On/Off Plan of GN&C Sensors and Equipment in Mission Phases

The tentative power on/off plan of GN&C sensors and equipment is given below:

- *Prime IMU and prime star tracker:* Powered on from TLI-24 hr to touchdown+1 hr, and from ascent liftoff-4 hr to completion of the disposal burn. Powered off during surface stay except for an 1-hr period, per day, for calibrations and functionality checked out. From TLI-24 hr to TLI-4 hr, measurements of these sensors will feed the Altair navigation filter. The estimated state vector will be compared with that estimated by the EDS navigation filter.
- *Cover mechanism for prime star tracker:* Powered on from 1 hr before powered descent initiation (PDI) to touchdown. Powered on from 1 hr before ascent liftoff to the completion of the SAR. Powered off during surface stay except for an 1-hr checked out period 1 day before ascent liftoff. Powered on during four 1-hr checked out periods during TLC.
- *Backup IMU (two units) and backup star tracker:* Powered on from 4 hr before the start to 4 hr after the end of the following critical events: TLI, LOI, PC, DOI, powered descent burn, ascent insertion burn, and RPOD. Powered on during four 2-hr calibration periods during TLC. During the long TLC, only one of the two backup IMU will be powered on to serve as a “hot” backup to the prime IMU. Powered off during surface stay except for a 1-hr period, per day, for calibrations and functionality checked outs.
- *Optical navigation sensor system:* Powered on from TLI-4 hr to touchdown+1 hr. Powered on from ascent liftoff-4 hr to the completion of the disposal burn. Powered off during surface stay except for an 1-hr period, per day, for calibrations and functionality checked out. Powered on during four 2-hr gimbal exercise and functionality checked out periods during TLC.

- *Prime and backup radar electronics*: Powered on from LLO Orion/Altair undocking-4 hr to touchdown+1 hr. To complete all functionality checked out before DOI.
- *Terrain hazard detection sensor system*: Powered on from LLO Orion/Altair undocking-4 hr to touchdown+1 hr. To complete all functionality checked out before DOI. Powered on during four 1-hr gimbal checked out during TLC.
- *Docking camera*: Powered on during LEO RPOD activity. Powered on from ascent liftoff-4 hr to completion of the disposal burn. Powered off during surface stay except for an 1-hr period, per day, for calibrations and functionality checked out.
- *Running lights (two units)*: Powered on during LEO RPOD activity. Powered on from ascent liftoff to completion of LLO RPOD. But in off-nominal abort scenarios, these lights will be powered off to conserve power. Powered off during surface stay except for one 1-hr checked out period one day before ascent liftoff. Powered on during four one-hour checked out periods during TLC.
- *Docking Lidar*: Powered on from ascent liftoff-4 hr to completion of the disposal burn. Powered off during surface stay. Powered on during RPOD activities with Orion in LEO for functionality checked out. Powered off when Orion has docked with the mated EDS/Altair vehicle in LEO. In an off-nominal RPOD scenario, when Orion becomes the chaser (active) vehicle, Altair's docking lidar will be powered off.

4.2. Estimations of Altair's Inertial Attitude and State Vector

The Altair spacecraft's attitude in a celestial frame is estimated using measurements made by a star tracker and a set of gyroscopes. The front-end of the Altair attitude estimator is a pre-filter that combines multiple star updates into one "composite" star update. These composite star updates are then sent to the attitude estimator at a pre-selected star update frequency. In between star updates, the spacecraft (S/C) attitude is propagated using the gyro data. Once attitude is initialized, Altair GN&C will maintain knowledge of the spacecraft attitude in a celestial coordinate frame continuously. The estimated inertial attitude of the spacecraft will be used to point it, for example, at the commanded attitude of the ΔV vector. It could also be used to convert the IMU ΔV measurements from the IMU coordinate frame to an inertial frame in the propagation of the spacecraft's state vector. When star updates are not available (e.g., the star tracker cover is in a "closed" position due to dust threat), the inertial attitude of the spacecraft will be propagated using IMU gyroscope data alone. A notional schematic diagram of the attitude estimator is depicted in Fig. 8.

The "state" of the spacecraft includes both its position and velocity vectors measured with respect to an inertial frame. The state is estimated onboard, continuously, via a flight software module named the Navigation Filter. Altair GN&C will estimate the vehicle's state via a wide range of measurements. The most fundamental of these measurements is the Earth-Based Ground System (EBGS) radiometric tracking data (S-band 2-way range and 2/3-way Doppler). Tracking data will be processed on the ground, and ground-based state vector updates will be uplinked frequently (the frequency could be every few minutes up to an hour) and prior to critical events (e.g., LOI). The navigation filter will be initialized and activated while Altair is still in LEO and mated with both the EDS and Orion. State data of the mated EDS/Altair/Orion, from the GPS receiver of EDS, will also feed Altair's navigator filter. Other onboard GN&C sensors (such as the ONSS) could also provide measurements to enhance GN&C knowledge of the vehicle's state. An example is the optical images of lunar landmarks (with known locations). The uses of these and other measurements are described in details in Ref. 4. A notional schematic diagram of the state estimator is depicted in Fig. 9.

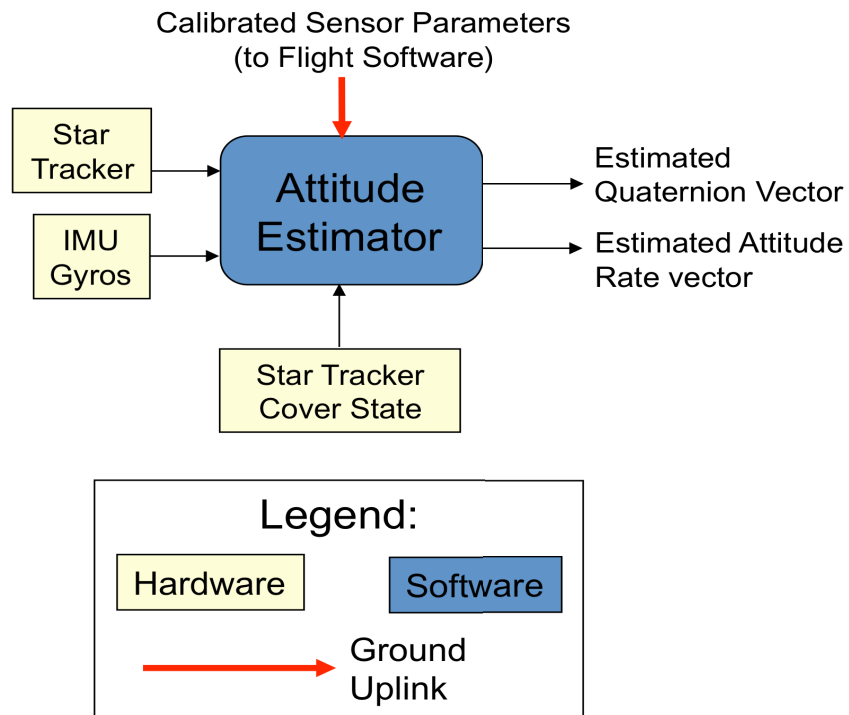


Figure 8. A notional schematic diagram of the attitude estimator.

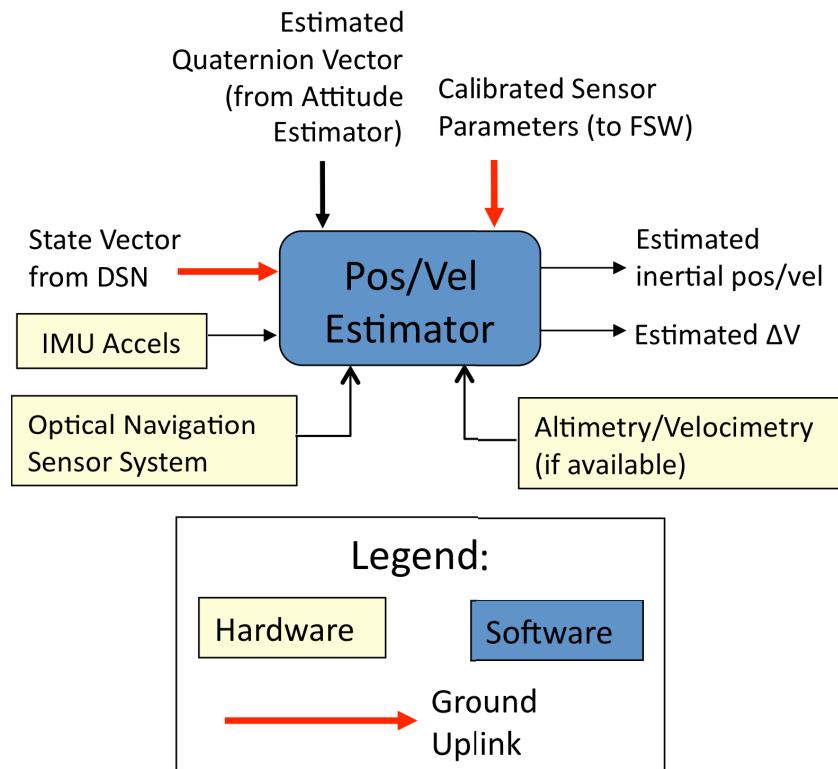


Figure 9. A notional schematic diagram of the vehicle state estimator.

4.2.1 Functionality Checked out and Calibration Plans for GN&C Sensors

All GN&C equipment should be checked out before use. The current equipment checked out plan includes:

- Prime star tracker's dust cover mechanism. The cover shall be opened and closed several times during the long TLC cruise phase. During these checked out, the backup star tracker will become the prime tracker. The cover shall also be exercised during the 7-day surface stay. These surface exercises will be conducted only when there is no threat of lunar dust and micrometeoroid.
- Gimbal system of optical navigation sensor system. The 2-dof gimbal platform of the ONSS will be checked out several times during the long TLC cruise phase. The checked out excursions shall cover the entire ranges of both the elevation and azimuth gimbal. The excursion rates of these checked out shall be comparable to predicted per-axis peak rates that the ONSS will be subjected to during all mission phases.
- Gimbal system of terrain hazard detection sensor system. The 2-dof gimbal platform of the THDSS will be checked out several times during the long TLC cruise phase. The checked out excursions shall cover the entire ranges of both the elevation and azimuth gimbal. The excursion rates of these checked out shall be comparable to predicted per-axis peak rates that the THDSS will be subjected to during the landing phase.
- Docking lidar. The functionality of the docking lidar shall be checked out during the LEO RPOD phase. In this docking operation, Orion will be the active vehicle, and the mated EDS/Altair vehicle will be passive. When the distance between the mating vehicles is within the operational range of Altair's lidar (4–5 km), and Orion is inside the lidar's FOV, the Altair's lidar could start to collect inter-vehicle measurements such as range. Comparisons of these measurements with their Orion-measured counterparts shall be made. Pointing the lidar beam to Orion (with crew onboard) would not be a safety hazard to the crew because the selected lidar beam is eye safe.
- Docking camera. The functionality of the docking camera shall be checked out during the LEO RPOD phase.
- Radar system. To land Altair on the Moon, it must first undock from Orion in LLO. Thereafter, Orion will execute a separation maneuver while Altair will perform both a plane change and a DOI ΔV maneuvers. The time duration between the separation and the PC burns is about 1.5 hr. Altair GN&C will perform end-to-end functionality checked out of the radar's short-range performance using Orion as a "target. The time duration between the PC and the DOI burns is another 1.5 hr. Another end-to-end functionality checked out of the radar's long-range performance will be performed between these burns. These checked out will use either the prime or backup radar electronics.

The Altair's IMU's (one prime and two backup units) is the "backbone" of all GN&C measurements. The accuracy of IMU measurements has direct impacts on the execution accuracy of propulsive maneuvers, landing dispersion, docking performance, and many other GN&C tasks. As such, these IMU's will be calibrated inflight so that pre-launch calibrated values of sensors' parameters (in the flight software) can be updated. The current inflight calibration plan includes:

- IMU-gyroscopes. Gyros' parameters to be calibrated include their scale factors, biases, and misalignments. These parameters could be estimated simultaneously in a well-designed calibration sequence. Typically, such a calibration sequence involves the execution of a series of slews about the spacecraft's axes, one axis at a time, and in both the clockwise and counterclockwise directions. Celestial attitude estimated by the prime star tracker is used in conjunction with the attitude estimator to estimate the gyro parameters. See Ref. 45 for a description of the slew sequence that is being used by the Cassini spacecraft to determine the IMU gyroscopes' parameters. Expected post calibration error bounds are: Scale factors $\leq 0.02\%$ and misalignments ≤ 0.2 mrad.
- IMU-accelerometers. Accelerometers' parameters to be calibrated include their scale factors, biases, and misalignments. Accelerometers' biases could be determined by monitoring the accelerometers' accumulated ΔV over a known time duration, when the spacecraft is in a quiescent state. This is the approach used by Cassini.³ During a ΔV burn, the ΔV imparted on the spacecraft is measured by the IMU accelerometers onboard. Simultaneously, the Doppler shift in the frequency of tracking signal

received by ground tracking station provides a measurement of that component of ΔV that is parallel to the Spacecraft-to-Earth vector. Since Doppler shift can estimate ΔV to better than 0.5 mm/s, it could be used to calibrate the scale factors of the accelerometers. This is the approach used by the Galileo spacecraft.⁴⁶ Alternatively, while Altair is still in LEO and mated with the EDS (which is equipped with GPS sensors), the IMU accelerometers' outputs could be calibrated against the highly accurate GPS measurements. This is the approach used by the GRACE spacecraft.⁴⁷ Expected post calibration error bounds are: Scale factors $\leq 0.01\%$, misalignments ≤ 1 mrad, and biases ≤ 4 μg .

4.3. RCS Thruster Configurations

In collaboration with the Altair Propulsion design team, the GN&C design team designed the RCS thruster configurations on Altair. Altair is equipped with two sets of RCS thrusters, one mounted on the descent module and the other on the ascent module. Both thruster sets use engines that are fed bipropellant fuel monomethyl-hydrazine (MMH) and oxidizer nitrogen tetroxide (NTO). MMH and NTO are hypergolic and have rich space heritage (Galileo, Cassini, Space Shuttle, etc.). For the AM RCS thruster configuration, MMH and NTO are each stored in two tanks. Upstream of these tanks is a high-pressure helium regulation system. The design of the DM RCS thruster configuration is similar.

Basic functions performed by the DM thrusters include:

- Control the spacecraft's attitude and attitude rate about all axes during TLC and LLO loiter. Key attitude control events include:
 - Point the spacecraft at a commanded ΔV burn attitude.
 - Calibrate and checked out GN&C sensors such as gyroscopes and radar.
 - Pitch about the spacecraft's Y-axis at the start of the Approach phase.
 - Maintain the spacecraft's attitude and attitude rate within acceptable levels at touchdown.
- Execution of TCM ΔV burns during TLC.
- Execution of "fuel settling" ullage burns before the engine-based LOI and PC burns.
- Execution of the DOI ΔV burn.
- Rotational control about the spacecraft's X-axis during the engine-based LOI and PC burn.
- Re-designation of the landing site to avoid a terrain hazard.
- Abort scenarios during the Altair descent and landing phase: Maintain the attitude of the DM at commanded state during the AM/DM separation event.

Guided by the above listed functionalities, multiple alternative DM RCS thruster configurations were considered. The DM RCS thruster configuration design depicted in Fig. 10, was selected based on the following selection criteria:

- Minimize the total mass of the thruster configuration
- Minimize the total number of thruster pods
- Minimize the total number of RCS thrusters
- Minimize thruster plume impingement on Altair's sensitive equipment
- Minimize propellant consumption
- Adequate 6-dof control authority in all phases in which the DM RCS thrusters are needed
- Maintain 6-dof control functionality with one arbitrarily failed thruster
- Use thrusters with high TRL
- Use coupled thruster to perform rotational control about all spacecraft's axes

The selected DM RCS thruster configuration consists of four thruster pods, with four thrusters per pod. The plane formed by the thruster pods is located near the predicted center-of-mass (c.m.) location of Altair at the time of touchdown. This arrangement will decouple vehicle's rotational motion from translational motion that will be beneficial to re-designation maneuvers that might be needed just before touchdown. On each thruster pod, there are four 445-N R-4D thrusters. Two thrusters are pointed in the $\pm X$ -axis directions. The other two thrusters are pointed

$\pm 45^\circ$ from the $\pm Z$ -axis and $\pm Y$ -axis (see Fig. 10). Thruster pods are mounted on DM symmetrically while maximizing their moment arms and minimizing interference with the deployment of the landing gear. Rotational control about all spacecraft axes will be performed using coupled thrusters. Thrusts generated by these thruster firings will almost cancel each other, and the ΔV imparted on the spacecraft will be small (but non-zero). This arrangement is important to minimize the size of “non-gravitational” ΔV imparted on the spacecraft. In this early design phase of Altair, plume impingements due to the firings of these DM thrusters are considered acceptable. If needed, thruster “reflectors” will be used to alleviate potential plume-impingement problems.

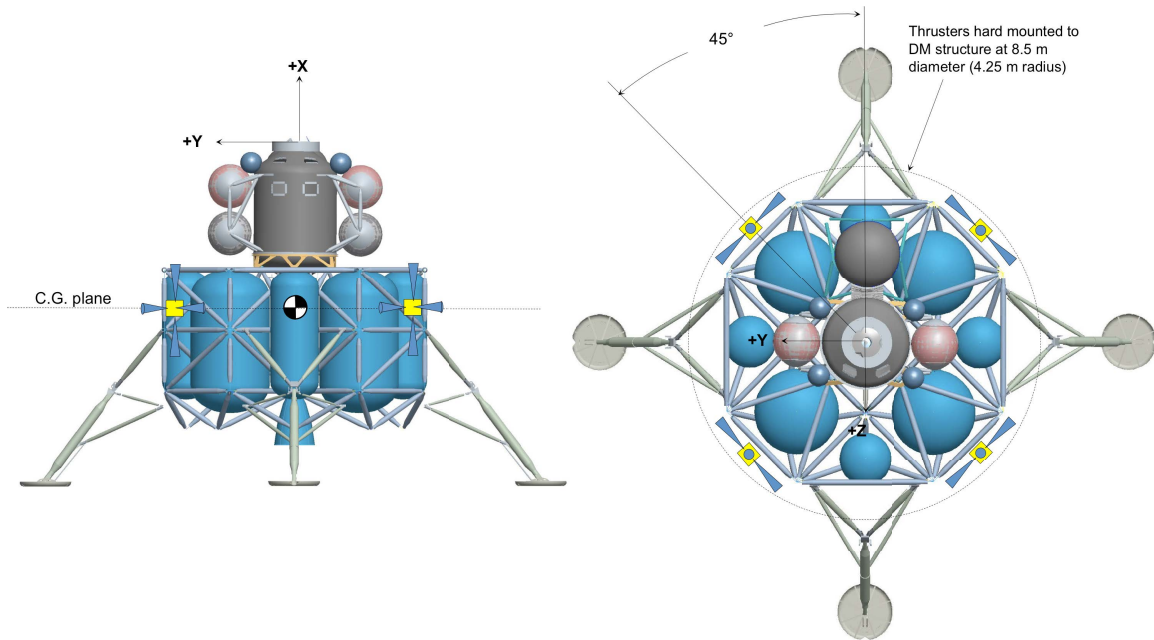


Figure 10. DM RCS thruster configurations

Basic functions performed by the AM RCS thrusters include:

- Control the spacecraft’s attitude and attitude rate about all axes during the ascent insertion burn, RPOD, and docking. Key attitude control events include:
 - Control the ascent module’s attitude at liftoff to avoid any re-contact between AM with the descent module or airlock.
 - Pitch about the spacecraft’s Y-axis at the start of the SAR phase.
 - Maintain the spacecraft’s attitude and attitude rate within acceptable levels to achieve docking with Orion.
 - Maintain a quiescent ascent module’s attitude while Orion performs the undocking maneuver (after the crew has transferred from the ascent module to Orion).
- Execution of RPOD ΔV burns in LLO.
- Execution of the disposal ΔV burn.
- Abort scenarios during the ascent insertion burn: Maintain a quiescent AM attitude during docking with the “active” Orion.

Guided by the above listed functionalities, the AM RCS thruster configuration design is depicted in Fig. 11. It consists of four thruster pods, with five thrusters per pod. The plane formed by the thruster pods is located near the predicted c.m. location of the AM at the time of docking that will be beneficial to docking controls. This arrangement will decouple vehicle’s rotational motion from translational motion. On each thruster pod, there are two

890-N R-42 thrusters (labeled “X” and pointed in the $\pm X$ direction), two 22-N *AmPac* thrusters (labeled “D” and pointed $\pm 45^\circ$ relative to the X-axis), and one 490-N *R-4D* thruster (labeled Y and pointing off the $\pm Y$ direction by 30°). Rotational control about all spacecraft axes will be performed using coupled thrusters. This will avoid imparting unwanted ΔV on the spacecraft due to attitude control thruster firing. The 22-N thrusters are needed for docking control. By pointing them 45° away from the X-axis, plume impingement on Orion due to Altair thrusters’ firing is minimized. See Fig. 12.

The AM main engine is not gimballed. Hence, there will be a need to cant the engine axis through the predicted location of the AM’s c.m. at mid-way of the 7-minute burn. The large R-42 thrusters will be used during the ascent insertion burn to counter any tumbling torque imparted on the AM due to canting error, knowledge error of c.m. location, staging torque (“fire in a hole”), etc. Conversely, the small *AmPac* thrusters will be used during docking operations. In the docking phase, the focus of the GN&C is to meet all the docking conditions dictated by the LIDS mechanism. These docking conditions include bounds on the following relative kinematics between Altair and Orion: in-line and lateral translational closure velocities, angular closure rates about all axes, lateral translational offset distance, and angular misalignments about all axes. These LIDS requirements are stringent and could only be met by the fine control provided by the small thrusters. With the AM RCS thruster configuration, all LIDS docking requirements are met with margins.⁹

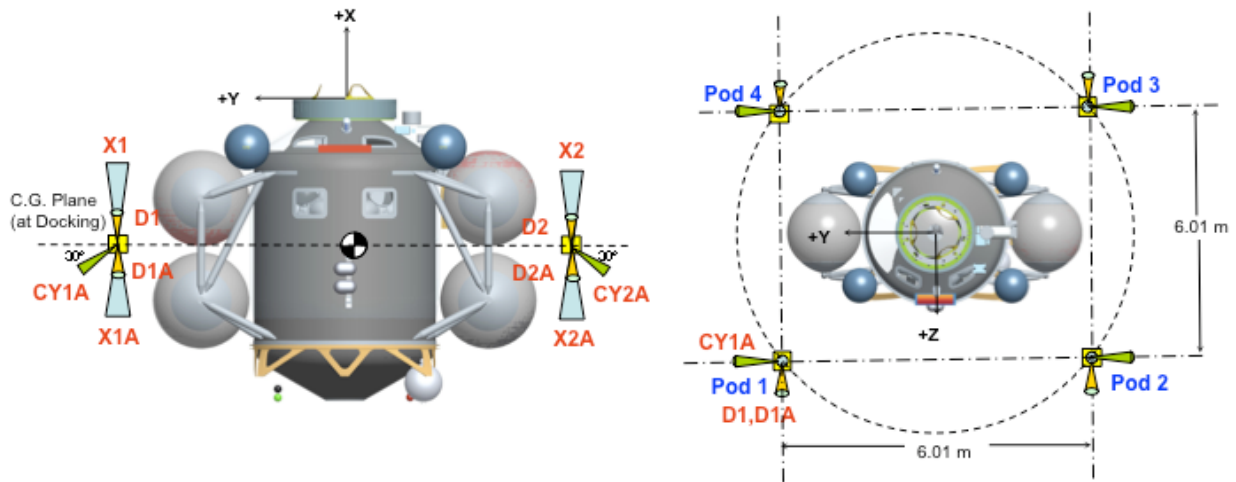


Figure 11. AM RCS thruster configuration.

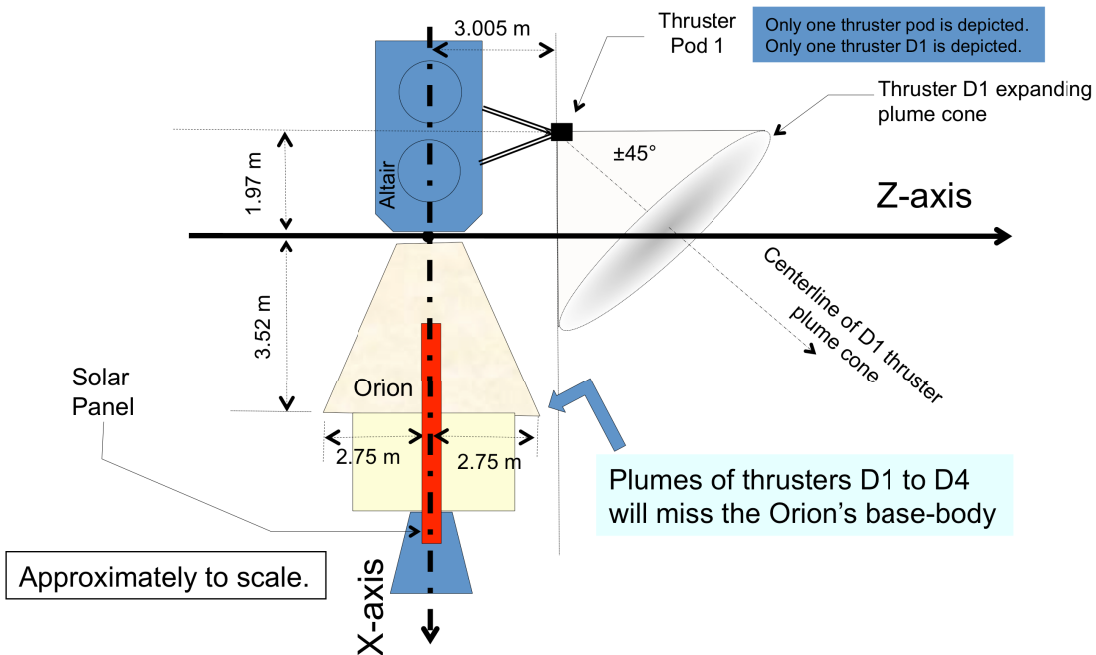


Figure 12. Minimal plume impingement on Orion due to Altair thruster firing at docking.

4.4. Attitude Control System Design

Conventional Bang-Off-Bang (BOB) thruster control algorithms will be used by Altair GN&C, one per spacecraft axis. The BOB algorithms use error signals (U) that are the weighted sums of per-axis attitude errors (e_θ) and attitude rate errors (e_ω) to control thruster firings: $U = e_\theta + K \times e_\omega$. Here, K is selected to maximize the controller damping and to minimize thruster firing activities. As depicted in Fig. 13, no thruster firing will be commanded if $|U| \leq db$, a pre-selected deadband (db). If $U > +db$, thrusters of a particular thruster couple will be fired. If $U < -db$, thrusters of another thruster couple will be fired. In the steady state, the attitude control error will ping-pong between $\pm db$ selected for that axis.

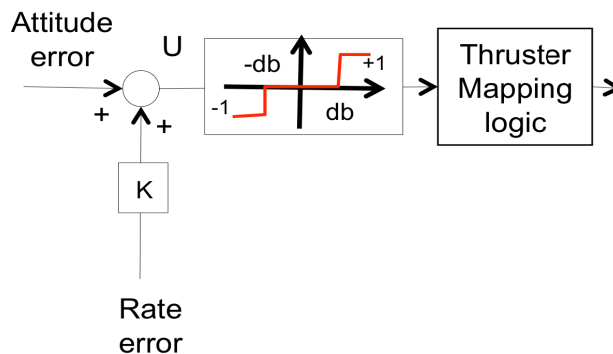


Figure 13. Altair attitude controller architecture.

Typically, BOB will produce “two-sided” limit cycles that waste both propellant and thruster on/off cycle. To overcome these drawbacks, the Altair BOB algorithms will likely incorporate a “self-learning” feature to produce, as much as possible, “one-sided” limit cycles in the presence of small non-gravitational torque (solar radiation torque,

gravity gradient torque, and others). In the “self-learning” scheme, when $U < -db$, thrusters will be fired with the a carefully selected pulse size that will cause U to get close to $+db$ but without “touching” it. The resultant “one-sided” limit cycles will save both propellant and thruster on/off cycle. This technique was successfully implemented on the Cassini robotic spacecraft.³

Another design consideration for the Altair’s attitude controller is related to the possible control-structure interactions (CSI) between thruster firings and spacecraft flexibilities. Prominent spacecraft flexibilities include the sloshing fuels in their tanks, the solar panels of Orion, the landing gear of Altair, and others. To avoid these undesirable interactions, notch filters (with appropriate notch frequencies) will be used to filter both the attitude and attitude rate control error signals before they are used by BOB. Using these filtered signals, the RCS controller will not falsely react to vehicle vibratory motions.

Per-axis deadband’s of the BOB algorithms are “command-able” by either the Mission Control Center (MCC) or the crew on board. To save fuel during the long duration coasting flight, the sizes of these deadbands are selected to be as large as possible while still meeting all the applicable pointing control requirements. During TCM burns where stringent pointing control requirements (see Section 4.5) must be met, deadbands of appropriate axes must be tighten. Table 3 is a list of placeholder deadbands that are currently envisioned for various mission scenarios.

Table 3. Placeholder RCS thruster controller per axis deadband.

Mission Phases	Per-axis RCS Thruster Controller Deadband [°]		
	X-axis	Y-axis	Z-axis
Trans-lunar coast attitude hold	±5	±2	±2
Trajectory correction maneuver burns	±1	±0.5	±0.5
LOI burn (only X-axis is controlled by thrusters)	±1	TVC gimbal control	
Low lunar orbit attitude hold	±2	±2	±2
Descent braking burn	±1	TVC gimbal control	
Descent approach phase	±0.2		
Descent terminal phase	±0.2		
Ascent insertion burn	±2	±1	±1
Rendezvous ΔV burns	±1	±0.5	±0.5
Docking control	±0.25	±0.25	±0.25

Altair will use its DM RCS thrusters to perform rest-to-rest slews of the mated Altair/Orion vehicle, and the AM RCS thrusters to slew the ascent module. The per-axis vehicle’s slew rates shall be profiled and be predictable. In general, a slew shall consist of a constant acceleration phase, a constant rate (zero-acceleration) phase, and a constant deceleration phase. To this end, a set of three per-axis acceleration limits (α_p) and another set of per-axis rate limits (ω_p) are selected. Like the deadbands, these slew profile limits shall be commandable by either the MCC or the crew. The acceleration limits should be selected consistent with the control authority of the thrusters and the moments of inertia of the vehicle. The slew rate limits should not exceed the star tracker’s operational rate limit. Representative time histories of Altair’s angular rate are depicted in Fig. 14.

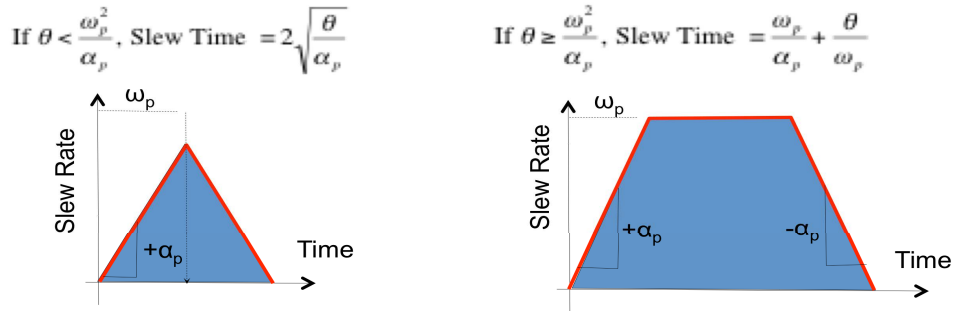


Figure 14. Profiled angular rate histories of small and large angle slews.

For slews with a small angular displacement θ , the “constant rate” sub-phase is not needed. The profiled slew rate is triangular, and the time it takes to complete the slew is $2\sqrt{(\theta/\alpha_p)}$. If the slew angle θ is large, the profiled slew rate is trapezoidal, and the time it takes to complete the slew is $(\theta/\omega_p + \omega_p/\alpha_p)$. As an example, let us compute the time it takes to slew the mated Altair/Orion vehicle during trans-lunar coast about the X and Y-axis (one axis at a time). The peak control authorities of the DM RCS thrusters about the X, and Y-axis are 7548 and 5340 Nm, respectively. The moments of inertia of the mated vehicle are 422792 and 1547242 kg-m² about the X and Y-axis, respectively. The peak acceleration limit (α_p) that is used to slew about the vehicle about its X-axis is selected to be 50% of $7548/422792 = 8.93$ mrad/s². The corresponding profiled acceleration limit that is used for slews about the Y-axis is 1.73 mrad/s². The profiled rate limit (ω_p) is selected to be 1 °/s. The time it takes to complete a rest-to-rest slew about the vehicle’s X-axis is given in Fig. 15. The slew time about the Y-axis is longer because of the larger moment of inertia and smaller control authority. The slew time about the Z-axis is almost identical to that of the Y-axis.

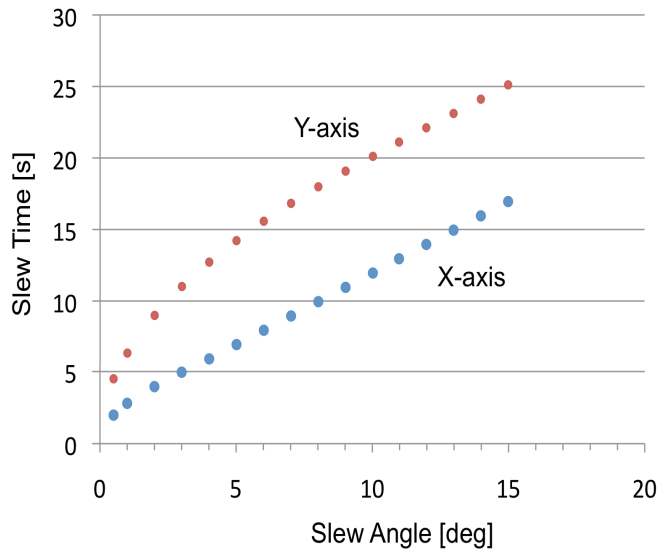


Figure 15. Slew times during Trans Lunar Coast Phase.

4.5. Propulsive Maneuver Control System Designs

Pre-launch, based on the established design reference mission (DRM), navigation analysis and design tools will be used to generate a reference trajectory for the Altair mission. Besides the obvious need to be fuel efficient, the reference trajectory must also meet other requirements such as a capability to execute the undocking maneuver of Altair and Orion (in LLO) in Earth view. The approved reference trajectory will involve the execution of both large and small ΔV burns. Large burns such as LOI (891 m/s) and the powered descent burn (2074 m/s) will obviously be

executed using the DM engine. Small burns, such as the trajectory correction maneuvers, will be executed using RCS thrusters. Intermediate size ΔV burns such as the DOI (19.2–19.4 m/s) and PC (28.3–28.5 m/s) could be executed using either engine or thrusters. The merits and demerits of using either engine or thrusters must be established, and decisions made. At times, decisions are made due to other hardware considerations. For example, there might be an upper bound on the number of times the DM engine could start and restart. In the current Altair mission design, we plan to perform DOI using DM RCS thrusters and PC using the DM engine. See Refs. 4 and 7 for details.

Three-axis stabilized spacecraft such as the Viking Mars orbiter and Cassini Saturn orbiter³ had used a two-axis gimbaled engine to successfully and accurately execute their orbit-insertion burns. Altair has adopted this proven approach. In a gimbaled engine burn, Altair’s motions about two axes are controlled by engine gimbal actuators. Thrusters will be used to control the Altair’s X-axis motion. The ΔV imparted on the spacecraft will be measured by the IMU (accelerometer). The burn is terminated once the commanded ΔV is achieved. To this end, flight software will use values of both the scale factor and the bias of the accelerometer that are estimated pre-launch. For better burn accuracy, values of these parameters in the flight software should be updated using values calibrated inflight. Before the start of an engine burn, a small RCS ullage burn will be executed to settle the fuel near the bottom of the tanks, and the vehicle will assume a predicted configuration. Engine gimbal actuators will then aim the engine axis through the predicted c.m. location of the vehicle. This practice will minimize the ignition transient motion of the vehicle, leading to better burn accuracy. At the end of the engine burn, the engine thrust vector should have passed through the spacecraft’s c.m. This should be quite close to the c.m. location of the vehicle at the start of the next engine burn (unless a vehicle reconfiguration such as undocking occurred between the two burns). As such, the telemetry of the engine gimbal angles recorded at the end of plane change ΔV (which will be an engine burn) will be used to pre-aim the engine for the critical powered descent burn. A notional schematic diagram of the engine ΔV burn is depicted in Fig. 16. This engine ΔV control architecture has successfully executed >100 ΔV burns for robotic spacecraft such as Cassini.³

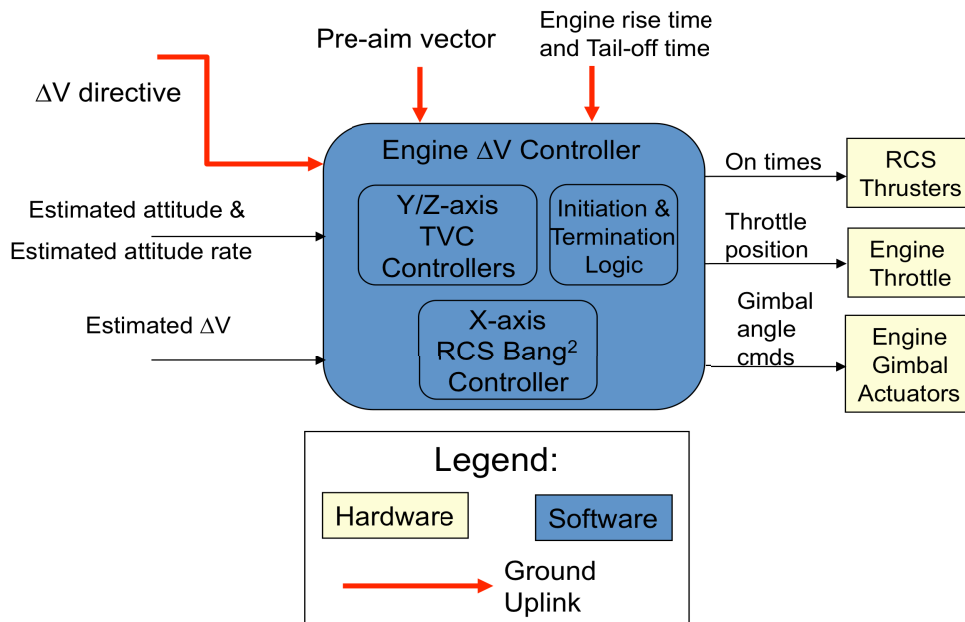


Figure 16. A notional schematic diagram of engine ΔV burn.

Small ΔV 's such as the trajectory correction maneuvers will be executed using the X-facing RCS thrusters of either the DM or AM. These burns are called RCS burns. During an RCS burn, the X-facing thrusters are fired to achieve the commanded ΔV . Again, IMU will be used to terminate the burn once the commanded ΔV has been achieved. During an RCS burn, since the vehicle’s c.m. is near but not at the exact center of the thruster pods, some

thruster off-pulsing will be needed. That is, during an RCS burn, thrusters with (slightly) larger moment arms must sometimes be off-pulsed in order to maintain the Y- and Z-axis motion of the spacecraft within their commanded deadband's. Another set of thrusters will be used to control the X-axis motion of the spacecraft within the commanded deadbands. Telemetry of the four X-facing thrusters' on-time (from the start to end of the burn) could be used to estimate the [Y, Z] coordinates of the vehicle's c.m. location. As such, the c.m. location estimated using telemetry from the last TCM burn (performed before LOI) could be used to aim the engine axis for the critical LOI burn. Placeholder deadbands selected for RCS burns are given in Table 3. A notional schematic diagram of the engine ΔV burn is depicted in Fig. 17. This RCS ΔV control architecture has successfully executed a large number of ΔV burns for robotic spacecraft such as Cassini.³

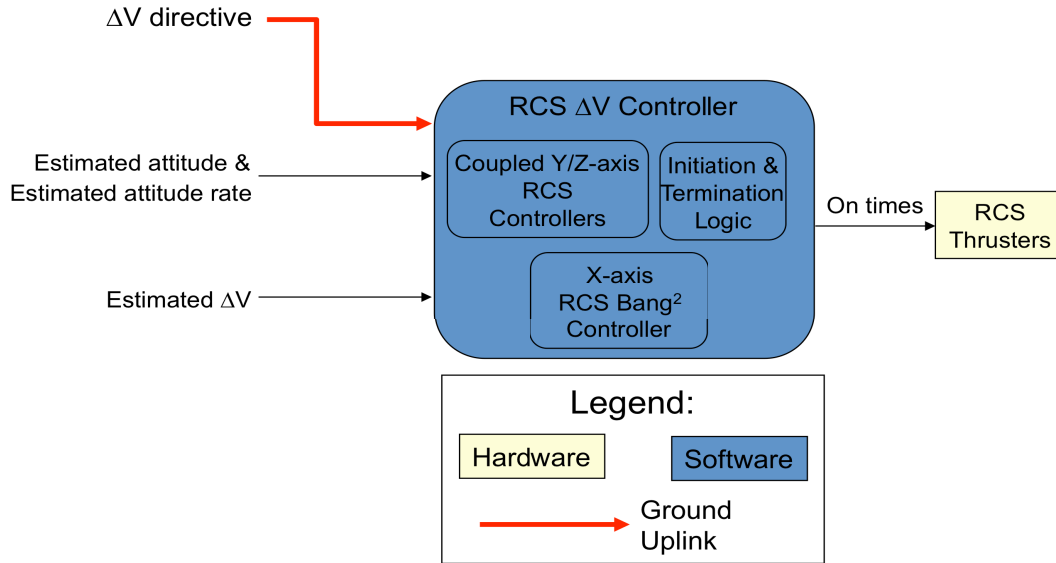


Figure 17. A notional schematic diagram of RCS ΔV burn.

Navigation typically uses a “linear” Gates model¹⁷ to represent propulsive maneuver execution errors. In this model, the ΔV magnitude error $\Delta V_{\text{Error}}^{\text{Mag}}$ is expressed as the sum of a fixed magnitude error $e_{\text{Fixed}}^{\text{Mag}}$ that is independent of the ΔV magnitude, and a proportional magnitude error $e_{\text{Prop}}^{\text{Mag}}$ that is proportional to the ΔV magnitude. The fixed magnitude error is typically specified in units of velocity, while the proportional magnitude error is specified in percent. The ΔV pointing error $\Delta V_{\text{Error}}^{\text{Pointing}}$ is modeled similarly as the sum of a fixed pointing error $e_{\text{Fixed}}^{\text{Pointing}}$ and a proportional pointing error $e_{\text{Prop}}^{\text{Pointing}}$. Again, the fixed pointing error is specified in units of velocity while the proportional pointing error is specified in units of angle. The ΔV errors along and perpendicular to the commanded ΔV vector become:

$$\begin{aligned} \Delta V_{\text{Error}}^{\text{Mag}} &= e_{\text{Fixed}}^{\text{Mag}} + e_{\text{Prop}}^{\text{Mag}} \times |\Delta V| \\ \Delta V_{\text{Error}}^{\text{Pointing}} &= e_{\text{Fixed}}^{\text{Pointing}} + e_{\text{Prop}}^{\text{Pointing}} \times |\Delta V| \end{aligned} \quad (1)$$

In these expressions, $|\Delta V|$ represents the magnitude of the ΔV burn.

To control the accuracy of the ΔV burns, Altair GN&C will impose two sets of requirements on [$e_{\text{Fixed}}^{\text{Mag}}$, $e_{\text{Prop}}^{\text{Mag}}$, $e_{\text{Fixed}}^{\text{Pointing}}$, $e_{\text{Prop}}^{\text{Pointing}}$]. One set for all engine burns (e.g., the LOI burn) and another set for burns performed by either DM or AM RCS thrusters. Placeholder Gates requirements are given in Table 4.

Table 4. Placeholder Gates requirements of Engine and RCS ΔV burns.

ΔV Burns	Maneuver Execution Error Requirements (1σ)			
	Fixed Magnitude [mm/s]	Prop. Magnitude [%]	Fixed Pointing [mm/s]	Prop. Pointing [mrad]
Engine	30	0.1	10	3
Thrusters	10	0.1	6	3

5. Navigation

The navigation process consists of two components. The first component is orbit determination, and the second is flight path control. Orbit determination is the process of measurement and computation to determine the present position and probable future position of the spacecraft. The term “state vector” is commonly used to represent both the vehicle’s velocity vector and the vehicle’s position vector, at a given time. Altair GN&C will estimate the vehicle’s state via a wide range of measurement types (cf. Section 5.1). With knowledge of the vehicle’s state, Navigation next determines trajectory maneuver corrections that might have to be performed to keep the spacecraft on a pre-designated reference trajectory. This process is named flight path control (cf. Section 5.3).

Several types of measurements will be used by GN&C for the purpose of orbit determination. The most fundamental of these measurements is the Earth-Based Ground System (EBGS) radiometric tracking data (S-band 2-way range and 2/3-way Doppler). Tracking data will be processed on the ground and ground-based state vector updates will be uplinked to the spacecraft. The uplink frequency could be once every few minutes (up to an hour) and prior to critical events (e.g., LOI). Onboard the spacecraft, the navigation filter, one component of the GN&C flight software, will be used to estimate and propagate the vehicle’s state vector using onboard navigation sensor data (i.e., from the ONSS, the IMU, etc) and the uplinked ground-based state estimates. The navigation filter will be initialized while Altair is still in LEO and mated with both the EDS and Orion. The state of the mated EDS/Altair/Orion, as estimated by EDS using GPS data, will be fed to the Altair’s navigator filter.

Onboard optical navigation data will be used to supplement the radiometric tracking measurements. Details on optical navigation will be described in Section 5.2. Proximity links will be used for relative navigation between Altair and Orion, and between Altair and radio beacons that might have been pre-planted on the lunar surface. To achieve good landing accuracy on the Moon, landmark tracking must be performed (terrain relative navigation) via the ONSS equipment (cf. Section 4.1). For the same reason, the GN&C is also equipped with radar that will return surface-relative altitude and velocity data. Navigation performance that could be achieved using this suite of measurement data is given in Section 5.4. Details are given in Ref. 4.

A question typically asked is why is there a need to use so many different types of measurements. Every individual navigation method has its strength, but all are inadequate at some level in some mission phases, or have some risks. For example, the EBGs radiometric link data is not as capable as in Apollo days, and there will be poor observability between EBGs and the spacecraft in many landing locations. Optical navigation is much more useful at this point. Navigational uses of optical images of lunar landmarks assumed that these landmarks were well surveyed and there were no lighting issues. The use of multiple navigation data types will provide improved solution accuracy (relative to single data type solutions), robustness, and availability, an approach adopted by the Altair GN&C team.

One might also wonder why so much data are required to navigate a spacecraft since it generally travels along conic sections that are well defined by state data at three points. This is because spacecraft orbit is perturbed continuously by solar pressure, un-balanced thruster firings, “waste water” dumping, etc. These perturbations are typically at the micro-g level and could not be accurately measured onboard. For this reason, these events have been nicknamed “unFortunate Lack of Acceleration Knowledge” or FLAK. These events only generate small accelerations, but over long time durations, they could lead to significant dispersion in the mission trajectory. For Apollo missions, FLAK events were at levels $<10 \mu\text{g}$ but they caused some 0.5-1.2 km trajectory dispersion per hour while the spacecraft was in a low lunar orbit.

5.1. Navigation Via Radiometric Tracking

Radio communication links between Earth and spacecraft have been used for navigation of interplanetary spacecraft since the beginning of the Space Age. An example is the navigation of the robotic Cassini spacecraft, a Saturn orbiter.⁵³ Measured properties of a radio signal convey information about the relative position and velocity between the transmitter and the receiver. When measurements of a spacecraft radio signal are made at a tracking station with known coordinates, information about the spacecraft position and velocity may be inferred. Measurements of the shift between transmitted and received frequency (Doppler shift) determine the line-of-sight velocity of the spacecraft. Two-way data (signal transmitted by station; coherently transponded by spacecraft; received at the same station) provide the best accuracy because of the high stability of the station frequency standard. One-way data (signal transmitted by spacecraft; received at a station) are strongly affected by the offset between spacecraft and station clocks. Measurements of the elapsed time between transmission of a pulse and reception of the same pulse determine line-of-sight distance (range). Finally, 3-way Doppler measurements that originate at a ground station, then are coherently transponded by the spacecraft, and finally are received by another ground station that is separated from the original station (typically by intercontinental distances) provide geometrically enhanced (via the station separation) measurements that provide a strong observable for mitigating the impact of FLAK.

The Deep Space Network (DSN), with three tracking complexes spaced around the globe (Goldstone, USA; Canberra, Australia; and Madrid, Spain) provides communication links with most NASA interplanetary spacecraft as well as spacecraft from other space agencies. The DSN has developed systems for making precise measurements of radio signals and forming observables that are used for spacecraft navigation. Measurement noise and modeling errors such as those associated with the DSN station location error, instability of the ultra stable oscillator (USO, for one-way radiometric measurements), Earth orientation errors, antenna phase center errors, etc., have been minimized. State-of-the-art accuracies for DSN observables are 0.06 mm/s for line-of-sight velocity, 75 cm for line-of-sight distance, and 2.5 nrad for angular position.⁵²

The adequacy of the DSN network relative to the navigation need of Altair has been assessed. The Apollo missions used the DSN network (for two-way range and Doppler) plus nine other receive-only stations providing three-way Doppler. Preliminary analysis has shown that the following placeholder navigation network, named the Earth-Based Ground System (EBGS), and consisting of the DSN stations (for two-way range and Doppler) plus three other receive-only stations (at Santiago, Chile; Hartebhestoek, South Africa; and Usuda, Japan), for three-way Doppler, provide sufficient tracking coverage to Altair in most flight phases. These EBGS stations are labeled IDAC4B in Fig. 18.⁴

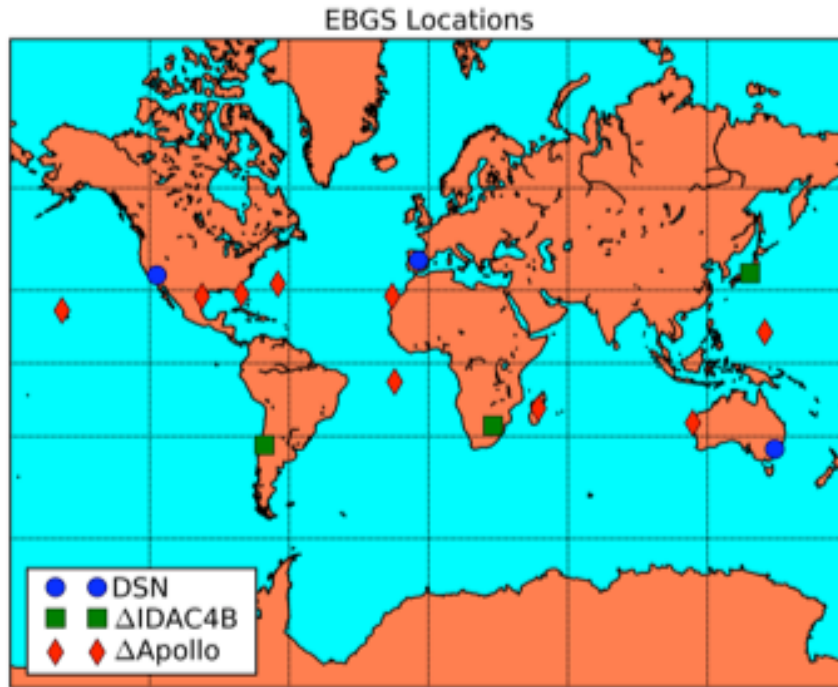


Figure 18. Locations of Earth based ground stations.

The following is a set of general assumption made regarding the use of radiometric tracking data.

- There is a set of EBGs stations that is designated as primary and another set that is designated as secondary. Primary EBGs stations collect two-way data. However, only one station is primary at a time. When there is an overlap between primary stations, the new station that comes in view will collect three-way Doppler data until handover from the originating station. The backup EBGs station is “receive” only and collects only three-way Doppler that originates from the primary complex and is received at the in-view backup complex.
- Three-way data include effects of independent frequency source at the receive-only station. The assumed 1σ a-priori USO Allan deviation is 10^{-12} on a 10-second count.
- Ground-based orbit determination shall combine EBGs tracking data, and via telemetry, optical navigation data and IMU data, to obtain the state vector solution. IMU shall be calibrated inflight with accuracies that are given in Section 4.2.1.
- It is assumed that the EBGs tracks Altair and produces ground updates to the navigation state that are to be periodically uploaded to the onboard GN&C navigation filter. State vector update frequency is assumed to be once per hour.
- Assumptions on data cut-off: Maneuver designs include a 1-hr cut off prior to the start times of maneuver executions, and knowledge cut-off for PDI is 10 min. prior to PDI (if there is a line-of-sight to the EBGs).
- Assumed a-priori uncertainties of EBGs tracking errors are given in Table 5.

Table 5. Placeholder EBGs tracking errors (1σ).

S-band 2/3-way Doppler noise	S-band 3-way Doppler bias	S-band 2-way range noise	S-band 2-way range bias
0.35 mm/s at 60 s	0.3 mm/s	2.1 m	2.1 m

5.2. Optical Navigation

All Constellation elements are required to “get the crew home” even when communications links are down or degraded. The CARD requirement CA0028 stated: “The Constellation architecture shall return the crew to Earth surface independent of communications with Mission System during all mission phases.” The rationale for this requirement is “... Ensure the safety of the crew by allowing the Constellation systems to protect for the possibility of permanent or unplanned intermittent communication service outages that prevent or limit the ability of Mission Systems to interface with the vehicles used for the given mission. Communication services include uplink and downlink services, Earth-based navigation equipment, and ground operations centers, ...” To meet this requirement, the Optical Navigation Sensor System (ONSS) is included in the Altair GN&C sensor suite (see Section 4.1). Onboard optical navigation can satisfy CA0028 because measurements of astronomical objects (in this case the Moon and possibly stars) taken and processed onboard will lead to a determination of Altair’s position independent of any radio link. Though a complete loss of the radio link from Altair to Earth is virtually impossible because of the multiple redundancy in communications equipment, corruption of the radio link to the point that radio-based navigation is jeopardized is a distinct possibility. Numerous solar storms have occurred with interplanetary and Earth atmospheric effects that can corrupt radiometric tracking severely, and is the possibility of such a storm that is the principal concern.⁶⁶

Optical navigation is not a new navigation method, and it has been used as a ground-based data type by NASA’s robotic interplanetary missions for the past 40 years. Onboard autonomous optical navigation is not as old of a method and was first used by NASA’s Deep Space 1 in 1998, where it was one of that mission’s 12 technology demonstrations.⁶⁷ Onboard autonomous optical navigation was subsequently also used on the Stardust and Deep Impact probes, where in the latter case it was the means of guiding one portion of the vehicle on an impact course with the comet Tempel-1.⁶⁸ Optical navigation is a method that measures the position of a (relatively) nearby object with respect to an inertial pointing reference. A pointing reference can be provided by an onboard star tracker for measurements limited in accuracy to the precision of the tracker (typically one or two hundred micro-radians), or alternatively, the pointing can be measured directly in the optical navigation frame by imaging stars for a precision that will be better than 1/10 pixel (picture element) – and for the case of the proposed ONSS narrow-angle camera that would be approximately 2 micro-radians. A third method exists and will be used by Altair. That method is to use images of foreground objects to estimate the pointing. In this case, in order to separate the effects of translational errors from pointing errors, it is necessary to use a camera of sufficiently wide field of view for there to be parallax effects in the scene that reveal the range to the targets – the parallax being proportional to the target separation and inversely proportional to range. Optical navigation was even used by the ground navigation team during the lunar orbital phase of the Apollo missions, but it required manual data taking – measuring locations (at predetermined times) of landmarks crossing behind reticles ground in the Command Module and Lunar Excursion Module viewports. This manual method was laborious, though highly accurate.

Optical navigation can be invoked during all phases of the Altair mission, and indeed, may be required during all phases of the mission to meet the CA0028 requirement, including landing where safe return of the crew will require a landing before ascent is possible during the terminal landing phase. The targets to be used for optical navigation aboard Altair include landmarks on the surface of the Moon, the limbs of the Moon, manmade satellites, stars, and the Orion. Landmarks will be modeled onboard Altair both in terms of terrain maps and positions of those maps. The method of locating landmarks entails a recreation of the appearance of the terrain within the landmark using luminosity/reflection laws and known illumination and view geometries. This synthetic view is then convolved with the actual image, and the location is determined by the peak-convolution response. Limb measurements are generally less accurate than landmark measurements due to the longer range to the limb, but this measurement offers the advantage of being a simpler measurement, requiring only a crude terrain model of the Moon and a simple reflection/luminosity model. In the vicinity of the Earth, images of artificial satellites (e.g., TDRSS, GPS, and communication satellites) may be used. These are very accurate measurements involving measuring the positions of the star-like spacecraft-images against a star background. Measurement techniques for these star-like images are simple forms of brightness centroiding. Orion images will also be used, and this image processing will entail either simple star-like centroiding when at a great distance, or complex landmark tracking using surface features of the Orion hull, precisely as done for the lunar surface landmarks. For navigation relative to Orion, the position of Orion as well as Altair becomes an estimable parameter. Landmark tracking of the Earth is not likely to be a good optical navigation target for Altair due to the difficulty of modeling the very complex atmosphere, and the unpredictability of landmark visibility.

Optical navigation measurements are to a large extent immune to many of the sensitivities of radio-metric measurements, especially non-gravitational accelerations (FLAK), being a direct measurement of position, and not velocity. However, optical navigation is subject to many new unique error sources, including landmark modeling errors, camera distortions, ephemeris errors, terrain-map errors, camera-pointing (or tracker-pointing) errors, image smear, and others. Generally, most of these errors can be calibrated prior to the mission, with the exception of the pointing errors that, if they are not extracted directly from the image itself (as discussed above) will have to be modeled in the navigation filter with gyro bias and drift parameters. Otherwise, the navigation filter treatment of optical navigation data can be relatively simple, with a fairly short estimation list comprised of spacecraft position and velocity, gyro parameters, accelerometer parameters, and engine thrust error models. Either a batch-sequential epoch-state or current-state filter is applicable if in the latter case provision is made for data comparison and editing.

There are certain requirements that OpNav places on the Altair system. These include carrying accurate Solar System ephemeris data (e.g., for the Moon, the Sun and the Earth), landmark models for both location and appearance (e.g., digital elevation maps), ability to point the gimballed camera and a mounting location on the vehicle that is appropriate for OpNav needs, star catalogs, instrument calibrations and mission opportunities to verify these calibrations in flight, current spacecraft ephemeris information for Orion and a priori state information for Altair, and (of course) the presence of the substantial OpNav software necessary for processing. Current estimates of the processing needs for the Altair OpNav system are approximately 10% of the power of a RAD-750 processor, assuming OpNav images are taken no more frequently than every 10 seconds – which is appropriate for all phases of the mission. Optical navigation also imposes certain geometric restrictions upon the mission using it – the most fundamental being that sufficient light is present. However, most imaginable missions landing on the Moon, including all of Altair’s prospective mission, will land with Sun illumination present. Even at the lunar South Pole, one of the most desirable areas for exploration because of the possibility of water-ice caches, there is sufficient light for optical navigation – even in the dead of lunar winter. There is a recent precedent for lunar optical navigation based on landmark tracking as Altair will perform, and that is the Lunar Crater Observation and Sensing Satellite (LCROSS) mission. As part of the impact trajectory reconstruction of the “nurse” vehicle, descent images were analyzed with landmarks created from a synthesis of the Apollo, Lunar orbiter, Clementine, and current Lunar Reconnaissance Orbiter (LRO) missions’ visual surveys. The optical navigation analysis agreed with the radio-metric data to about the 50-m level, which is believed to be the approximate residual frame-tie error associated with the LRO data from the wide-angle imager when processed with high-precision stereophotoclinometric methods.⁶⁹ For the Altair landing sites, narrow-angle imaging will be available with resolutions of better than 1 m, leading to the anticipation of excellent landing performance for Altair using optical navigation. A complete treatment of the Altair optical navigation methodology is given in Ref. 5.

5.3. Flight Path Control

Maneuver execution errors and FLAK effects disperse the trajectory of the spacecraft away from the nominal and will require ΔV to correct the dispersion. The process is named flight path control, and the ΔV 's are called Trajectory Correction Maneuvers (TCM's). Flight path control involves the determination and execution of TCM (cf. Section 4.5). These small TCM burns will be executed using RCS thrusters. The actual ΔV executed will be tracked by both the onboard IMU and the ground-based Doppler, and it will be compared with the commanded ΔV vector. One important goal of the Altair GN&C design is to minimize these maneuver-execution errors. The penalty of having large maneuver-execution error is the need to execute “clean up” burn(s) that waste fuel and stress the mission timeline. Upper bounds of RCS-based maneuver-execution errors are listed in Table 4. A preliminary linear statistical maneuver analysis has been conducted that accounts for orbit-determination error, anticipated-trajectory disturbances, and maneuver-execution error to arrive at estimates for the upper bound of each planned TCM. These are given in Table 6 for the cruise phase of the mission.

Table 6. Trans Lunar Cruise TCM Budget

TCM	ΔV [m/s]	Location	Motivation to execute this burns
1	21.6	TLI+6 h	To correct for execution errors of TLI and mapped orbit determination errors and trajectory dispersions
2	2.0	TLI+23 h	To correct for mapped orbit determination errors and trajectory dispersions
3	3.6	LOI- 20 h	To correct for mapped orbit determination errors and trajectory dispersions
4	2.7	LOI-6 h	Final maneuver to prepare for LOI

Note that the first TCM (TCM1) is relatively large; this is due to the large trajectory dispersions induced by the execution error of EDS performing the TLI burn. TCM1 magnitudes can be minimized by improving the burn performance of the EDS; the Altair project will work with the EDS project to ensure the best possible performance from the EDS engine. For the other TCMs, the primary contributor to their magnitude is the FLAK. Finally, after LOI there is a LOI clean-up burn, that like TCM1, is larger due to the dispersion of a large burn's execution error. Preliminary estimates of this burn are on the order of 6.9 m/s.

5.4. Navigation Performance

The navigation performance of Altair GN&C, from trans-lunar cruise to landing on the Moon, is described in detail in Ref. 4. Some key results from that reference are summarized in this section. To obtain these navigation results, the EBS tracking performance given in Table 5 was assumed. Assumptions made for the uses of other navigation measurements are given in the following paragraphs. Assumptions made with respect to key navigation error sources are also described.

Altair GN&C assumed the use of the current best lunar gravity field model, LP150Q, that was derived from all available data from past United States missions to the Moon including the Lunar Orbiter missions (1-5), the Apollo 15 and Apollo 16 sub-satellites, Clementine, and many other lunar missions. Data from a planned future mission, Gravity Recovery and Interior Laboratory (GRAIL), will likely improve our knowledge of the lunar gravity field for the far side of the Moon by an order of magnitude. Errors associated the modeling of the Earth/Moon spherical and non-spherical gravity effects were included in our assessment of Altair navigation performance.

Maneuver execution errors for TCM's, LOI, PC, DOI, and the powered descent burns are consistent with the Gates error model outlined in Section 4.5 (see Table 4). Note that both the TCM's and the DOI will be executed using RCS thrusters, and all other burns will be executed by the descent module main engine. The FLAK errors (due to venting, fluid dumps, and attitude misalignments) are by far the largest error source contributing to knowledge errors. Initial estimates from the Orion GN&C team indicate that these errors introduce approximately $\frac{1}{2}$ km uncertainty every 1 hr. The Altair GN&C team made the same assumption. Accordingly, the computed 1σ a-priori uncertainty of non-gravitational acceleration is 1.72×10^{-7} km/s² (which has been derived assuming the acceleration is modeled as discrete white noise process) during periods when crew is active (16 hr of a 24-hr period). The acceleration level is an order of magnitude lower when the crew is inactive.

Passive optical data of lunar landmarks will be captured via the ONSS equipment. Landmarks will be identified and compared to data given in an onboard digital map. At least ten landmarks will be identified in each image. During TLC and LLO operations, NAC images will be acquired every 10 min. until the spacecraft's altitude is <20 km (several minutes before PDI). Also, in LLO operations, WAC images are acquired every 10 min. until DOI. Thereafter, images will be acquired every 20 s until PDI-5 min. During the powered descent phase, WAC image-acquisition frequency will be once every 5 s until landing. Details of map-tie errors, camera-image noise, and other error sources are given in Ref. 4.

Based on these assumptions, the position and velocity knowledge errors of Altair in the LLO and DOI phases are given by Figs. 19 and 20, respectively. Position knowledge ranges between 50 to 400 m (3σ). Velocity knowledge error ranges between 0.05 to 0.7 m/s (3σ). Larger uncertainties occurred when Earth-based tracking is sparse (cf. period with only a two-way station and a single three-way station). Position and velocity errors at landing are given by Figs. 21 and 22, respectively. The errors reported here are solely due to navigation, and contributions due to both

the guidance and control functions were not factored in. Horizontal and vertical landing errors are 2.9 and 2.0 m, respectively (3σ). Additional Monte Carlo dispersion analysis of the guidance system (not shown) produced results that indicate the guidance error contributions will have a similar magnitude (several meters), so, to first order, the combined effect of navigation and guidance error dispersions should easily yield landing errors of less than 10 m (3σ).

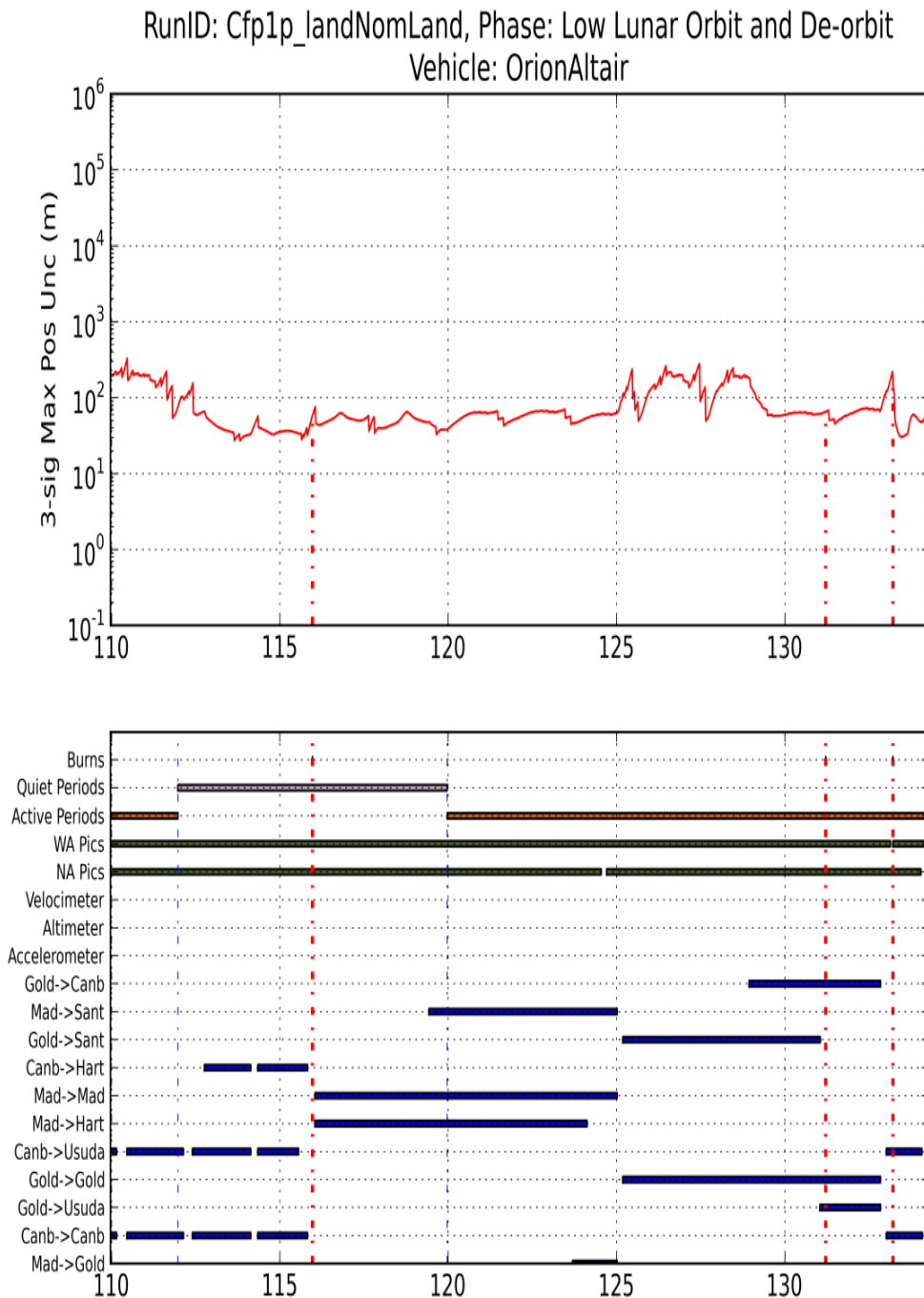


Figure 19. Position-knowledge error (Worst-axis, 3σ) in LLO and DOI phases (horizontal axis is mission elapsed time, MET).

RunID: Cfp1p_landNomLand, Phase: Low Lunar Orbit and De-orbit
 Vehicle: OrionAltair

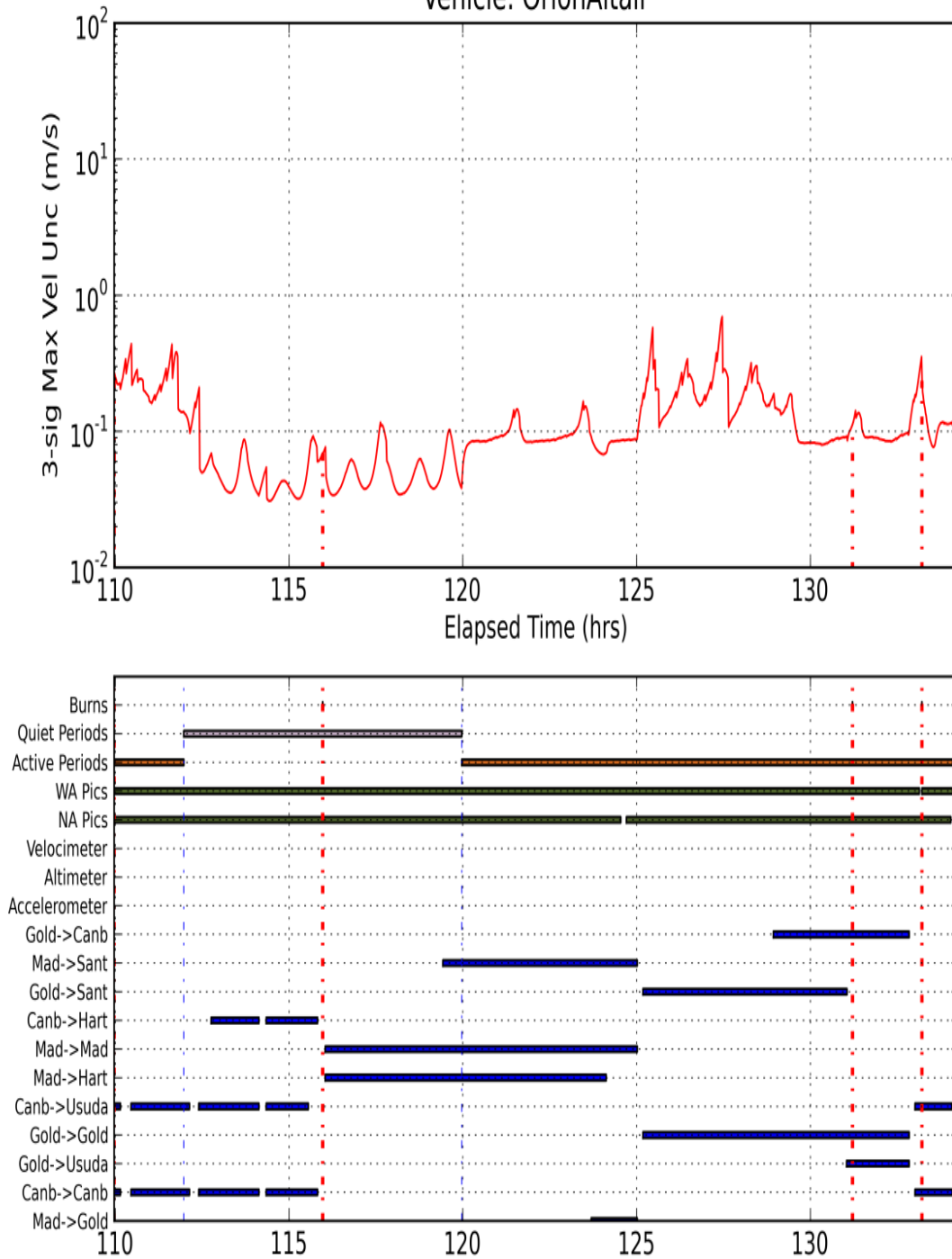


Figure 20. Velocity-knowledge error (worst-axis, 3σ) in LLO and DOI phases (horizontal axis is mission elapsed time, MET).

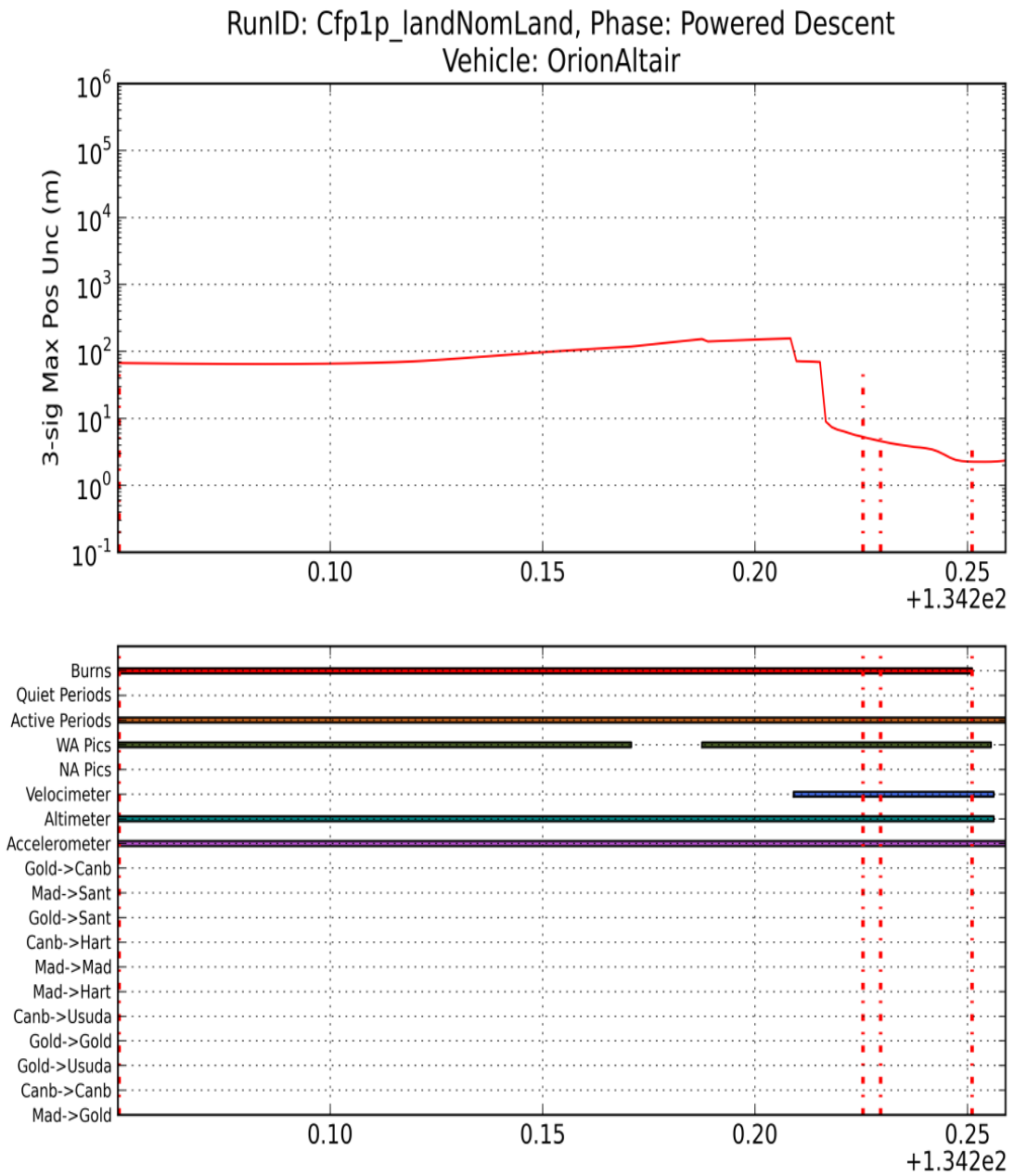


Figure 21. Position landing error (worst-axis, 3σ) in the powered Descent Phase (horizontal axis is mission elapsed time, MET).

RunID: Cfp1p_landNomLand, Phase: Powered Descent
 Vehicle: OrionAltair

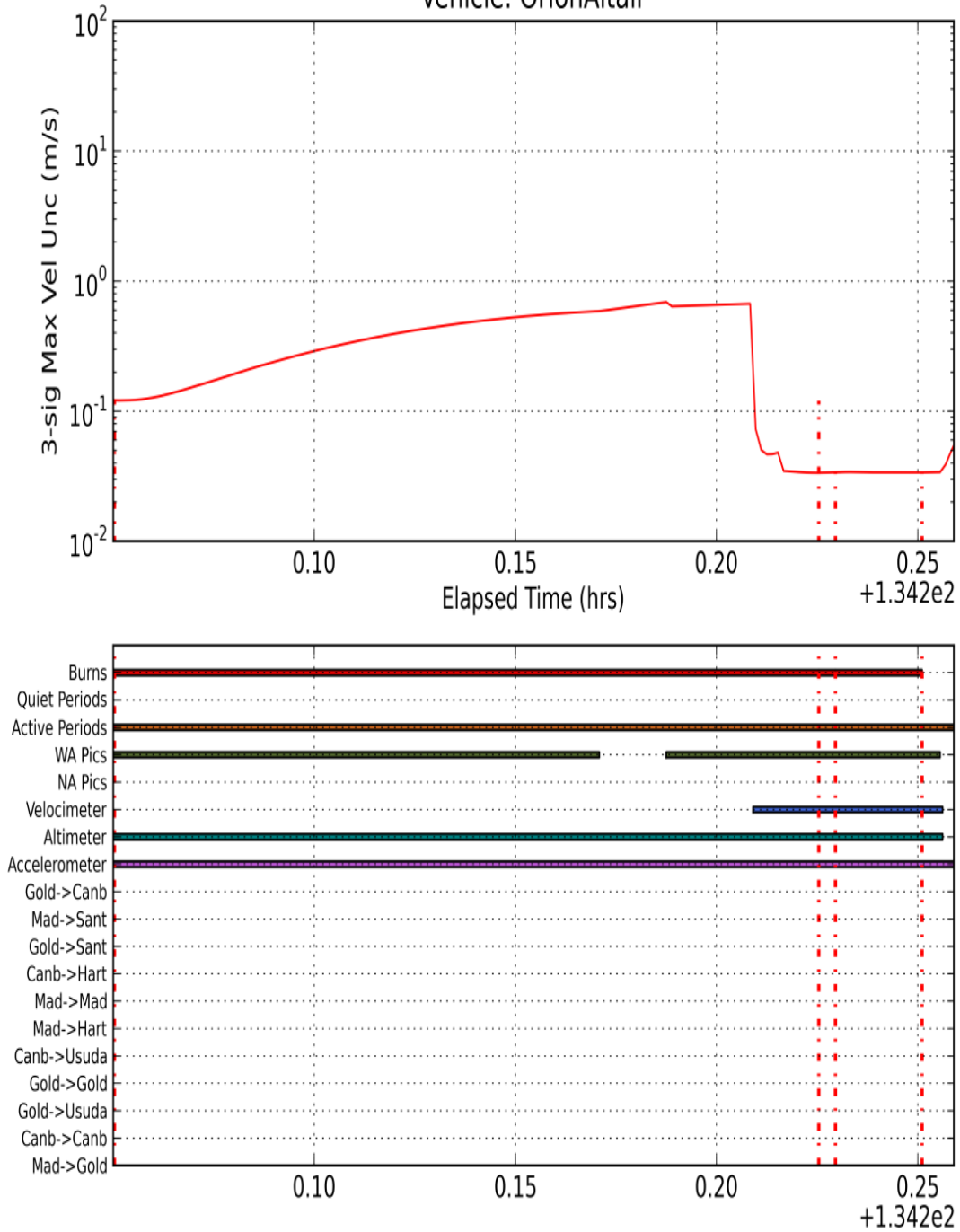


Figure 22. Velocity landing error (worst-axis, 3σ) in the powered Descent Phase (horizontal axis is mission elapsed time, MET).

6. Guidance

Guidance is the onboard flight software that uses the state-vector estimates, the crew inputs, and the pre-computed targets to guide both the angular attitude and the translational motion of the spacecraft during powered flight phases. Using the powered descent and landing phase as an example, the outputs of the guidance algorithm includes three sets of commands: [i] Steering signals to the Thrust Vector Control (TVC) gimbal system, [ii] signals to modulate descent engine thrust level in order to achieve the vehicle acceleration for a desired trajectory, and [iii] the desired vehicle's attitude (e.g., to provide the crew line of sight to the landing target). The commanded acceleration vector (the first two commands) will produce convergence to the specified target point even though the target point may be re-designated in flight and the commanded acceleration isn't precisely achieved because of controller errors. A notional schematic of the relations between navigation, guidance, TVC and attitude controls, for the descent and landing phase, is depicted in Fig. 23.

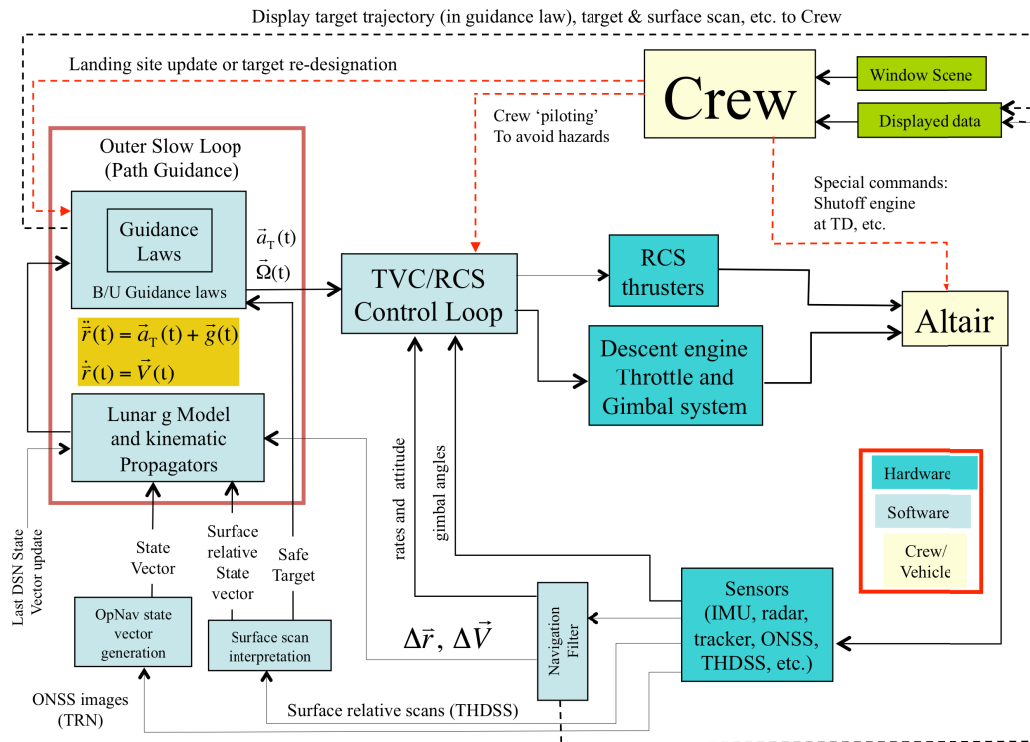


Figure 23. Integrated navigation, guidance, and control configuration (Descent and Landing Phase)

Currently, Altair GN&C assumes that the primary guidance mode for the lunar descent is automated. Both the acceleration vector and the attitude of the vehicle are generated and executed automatically. But the crew can, temporarily or permanently, select the non-automatic guidance mode if the pilot wishes to manually control, the attitude vector, the acceleration vector, or both (see also Section 7.4). Overviews of guidance designs for three mission phases, descent and landing, ascent insertion burn, and docking, are given in this section. Details of these guidance designs are given in Ref. 7.

6.1. Descent and Landing Phase^{7,15,60}

Lunar descent guidance begins with Altair at about 15-km altitude in a slightly elliptical coasting lunar orbit, and ends with Altair on the lunar surface. The objective of the guidance is to reduce both the velocity and altitude of Altair for a soft touchdown at the selected landing site. Guidance in this phase is designed based on the following considerations:

- Minimize propellant usage
- Maximize landing accuracy

- Must provide “out-the-window” line-of-sight to the landing site for the crew several minutes before touchdown
- Must provide line-of-sight to the general landing area for the gimbaled THDSS carried onboard Altair
- Must allow for re-designation of the landing site several minutes before touch down

These considerations are almost identical to those faced by the GN&C engineers of Apollo missions. Hence, not surprisingly, the descent guidance trajectory of Altair is very similar to those used by the Apollo missions.^{7,15,60} The Altair descent guidance design consists of three sub-phases: the braking phase, the approach phase, and the terminal descent and touchdown phase. These descent sub-phases are depicted in Fig. 24.

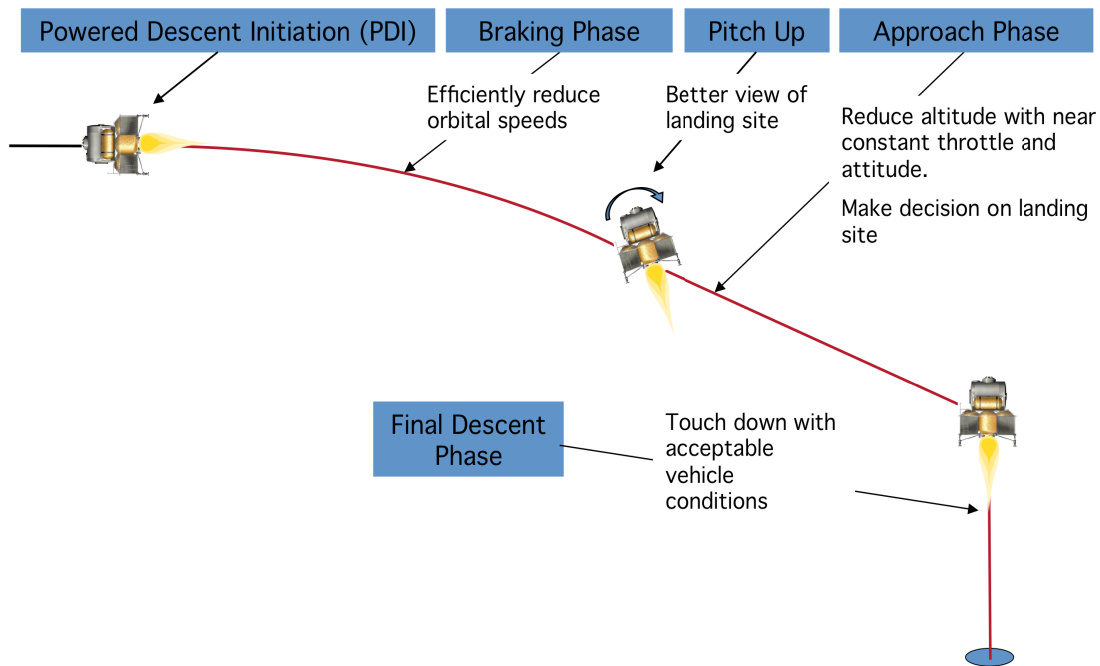


Figure 24. Sub-phases in Descent and Landing

The basic guidance law assumes a 4th-order polynomial function (of time) that describes the desired trajectory in position. The guidance equations are solved by posing a Two-Point Boundary-Value-Problem (TPBVP).^{15,60} Different target sets are used for different sub-phases of the descent and landing phase. For example, the Approach phase will use a target point that sacrifices fuel utilization efficiency in order to provide landing site visibility and landing site re-designation. Also, hazardous terrain features (such as unacceptable craters, rocks, and slopes) are to be identified during the Approach phase, and the landing site re-designated (if necessary). The guidance algorithm will “drive” the vehicle to achieve the target state in the presence of controller errors, navigation state estimation errors, and other vehicle dispersions. The algorithm also allows for target changes such as pilot-initiated re-designation of the desired landing location.

The braking phase is initiated by the crew about 10 min. before the nominal ignition of the descent engine. The braking burn is named Powered Descent Initiation (PDI), and it will start at the descent orbit perilune at an altitude of 15.24 km. The objective of the braking burn is to efficiently reduce the orbital speed of Altair.⁵⁹ Before the time of powered descent initiation (PDI), a small RCS thruster-based ullage burn has already been executed to “settle” the fuel to the tank bottom. Thereafter, the null axis of the gimbaled engine is aimed at the predicted c.m. of Altair, and this vector is aligned with the commanded ΔV vector in an inertial frame. In this way, the descent engine could slow down the velocity of Altair effectively, using a constant engine throttle of, say, 92%. In this sub-phase, the vehicle’s X-axis is almost parallel to the surface of the Moon (cf. Fig. 24).

In the approach sub-phase, the throttle will be lowered to a level that is about 60% of the full engine thrust. The very first control action is to perform a pitch-up maneuver, changing the vehicle's attitude from nearly horizontal to nearly vertical. This will allow the crew to gain a better view of the targeted landing site. This is important because re-designation of the landing target, if any, must be performed in the approach phase. The crew will be assisted by the THDSS system to make a decision on whether there is a need to re-designate and on the selection of the safe landing site(s). Time to perform these hazard-identification and diversion tasks is limited, and the pitch-up maneuver must be performed as quickly as possible. Also, to facilitate the crew's observation of the landing site, the attitude of Altair should be kept as constant as possible (after the pitch-up). The objective of the approach sub-phase is to achieve an altitude of about 30 m vertically above the selected touchdown site with no horizontal velocity.

The terminal sub-phase is intended to be a quiescent, controlled, vertical descent for 30 s at a constant 1 m/s descent rate, until it is time to shut down the DM engine. The terminal descent guidance will control velocity only, there is no position control. Undesirable horizontal velocity of the vehicle at the start of the descent, if any, should be nulled out using the RCS thrusters. Alternatively, RCS thrusters could be used to tilt the vehicle's attitude slightly so that some component of the engine thrust could null the horizontal velocity. Engine shut down will occur just prior to touch down. For Apollo missions, engine shutdown was performed manually when contact probes touched the ground and a light was activated in the cockpit. The length of the probes "reflected the estimated delay of the pilot's response, the amount of time it took to close the valves in the descent engine, and the amount of time it took to actually reduce the thrust to zero". The Altair landing gear does not currently include a similar probe. Moreover, radar will not be operational at altitude <10 m. The current plan is to supplement the IMU-propagated altitude estimate with range data from the THDSS lidar. Touchdown conditions of the Apollo-11 lander were: Horizontal velocity ≈ 0.45 m/s; Vertical velocity ≈ 0.2 m/s; [pitch, yaw, roll] rates $\approx [-1.5, -6.2, -3.7]$ deg/s; and [roll, pitch] attitude $\approx [0.04, 0.25]$ deg. Acceptable touchdown conditions for the Altair's landing gear design are work-in-progress.

6.2. Ascent Insertion Burn Guidance¹¹

Lunar ascent guidance begins with Altair on the lunar surface, preparing for an "on-time" liftoff. The Altair launch window is determined by the overlay of the ascent plane window and the rendezvous phase window.¹¹ With the target vehicle Orion in a 100 km \times 100 km orbit, the launch windows open approximately every 2 hours. The objective of the ascent insertion burn is to place the ascent module in a 75 km \times 15.24 km orbit, in plane with the Orion orbital plane at the time of engine cutoff. Guidance in this phase is designed based on the following considerations:

- Minimize propellant usage.
- Minimize the risk of a collision between the ascent module and neighboring lunar terrain features.
- Must provide "out-the-window" visibility of the lunar surface for the crew throughout the insertion burn.
- Complete the insertion burn as quickly as possible (see requirement CA5193 in Table 1).

The ascent insertion burn is comprised of three sub-phases. These sub-phases are the vertical rise, the single-axis rotation (SAR), and the PEG (powered explicit-guidance) sub-phases. These sub-phases are depicted in Fig. 25.

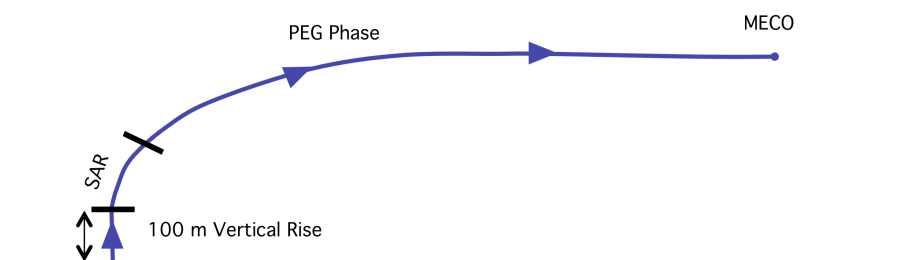


Figure 25. Ascent insertion burn guidance.¹¹

The vertical rise sub-phase is executed immediately to get the lander to a sufficient altitude to allow clearing of local terrain in the subsequent sub-phases. Although Altair is flying directly against (lunar) gravity to a height of

approximately 100 m, which is quite an inefficient way to fly, it is only for a short time: less than 10 s. The 100-m “height” was selected to be consistent with that used by Apollo missions.

The purpose of the single-axis rotation (SAR) maneuver is to align the Altair’s attitude at the end of the vertical rise with a selected [yaw, pitch, roll] attitude that is optimal for the next sub-phase (the PEG phase), as quickly as possible. At the time of landing, the X-axis of the ascent module might not be perpendicular to the local lunar “g”. Also, the lander’s Z-axis might not be in the orbital plane of the Orion at the time of liftoff. For example, when landed, the Apollo-11 lander had an off-vertical angle of 4.5° , and a yaw angle error of 13° . The SAR logic calculates a single axis time optimal rotation (an Euler rotation) from the initial attitude (including the off-vertical and yaw angle errors due to the landing) to the computed attitude command. At 50% control authority, the [X, Y, Z] angular acceleration capabilities of the ascent module are [5, 42, 17] $^\circ/\text{s}^2$, respectively. Nominally, the magnitude of the SAR rotation is about 50° about the Y-axis. If the peak angular rate limit is assumed to be $5^\circ/\text{s}$, then the time to complete the SAR rotation is about 10 s. Once the SAR is completed, the optimal flight path can begin.

The powered explicit guidance (PEG) sub-phase is executed to deliver the ascent module to the desired orbit. For a given constant ascent-engine throttle, PEG calculates the steering command to achieve the commanded radius magnitude, velocity magnitude, and flight path angle targets. The solution calculated by PEG is the minimum ΔV solution, given the targets that are provided to the algorithm. The nominal AM flight time to main-engine cutoff (MECO) is about 7 min. The terminal velocity of the AM at MECO is about 1690 m/s. Nominally, the ascent insertion burn will place AM in a 15.24×75 km orbit. Throughout the PEG sub-phase, the crews will have line-of-sight viewing of the lunar surface.

The ascent insertion burn will be executed using the un-gimbaled engine of the Altair in all three sub-phases. To this end, the ascent engine will be canted to align its thrust to the predicted c.m. of the ascent module at the mid-point of the ascent insertion burn. Throughout the ascent insertion burn, thrusters will be fired to control the ascent module’s attitude. Thrusters will also be used to perform the SAR and all other angular rotations. The control authority of the AM RCS thruster configuration has been analyzed and found to be adequate for all sub-phases of the insertion burn, with margin.

6.3. Rendezvous, Proximity Operations, and Docking Guidance⁹

As the name implies, the Rendezvous, Proximity Operations, and Docking (RPOD) phase are comprised of three sub-phases. The rendezvous phase involves infrequent, discrete maneuvers with coasting phases. The proximity operations phase consists of smaller, more frequent maneuvers, and docking initiates at docking port contact. A simplified graphic of the reference trajectory is shown in Figure 26.

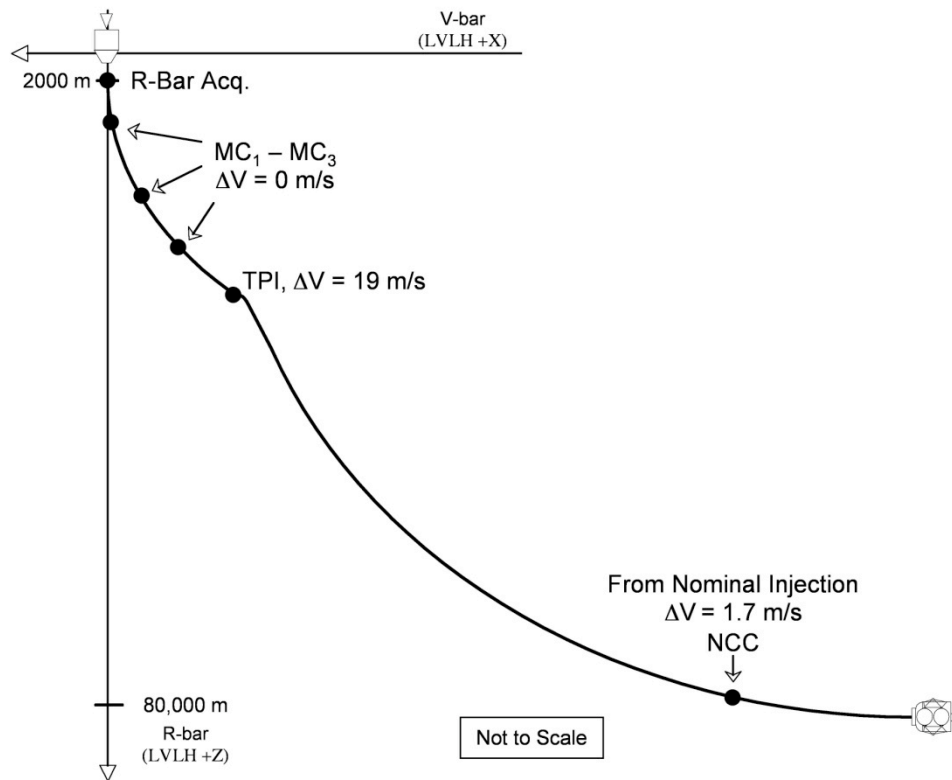


Figure 26. Rendezvous trajectory schematic.^{7,9}

To deliver the Altair back to Orion, Altair will approach Orion from “below” and will make an “R-bar acquisition” at a relative distance of about 2 km. Here, we use the “target local orbital frame” to describe Altair/Orion docking operations.⁴⁸ In this coordinate frame, the orbit direction is named V-bar after the orbital velocity vector \vec{V} . The coordinate in the direction from the spacecraft to the Moon’s c.m. is named R-bar after the radius vector \vec{R} , and the third coordinate completing the system is named H-bar after the orbital angular momentum vector \vec{H} . The R-bar approach enables use of natural braking from orbital mechanics to slow Altair during its approach to Orion. This strategy has the advantages of a shorter approach time and lower propellant consumption.

The rendezvous phase begins at insertion (see Section 6.2) and continues until Altair acquires the R-bar. During this time, there are five maneuvers. The Number, Corrective Combination (NCC) burn occurs 10 min. after insertion to clean up any ascent dispersions and target the proper Terminal Phase Initiation (TPI) point. The nominal value of the NCC ΔV is 1.7 m/s and will be executed using the AM RCS thrusters. The TPI burn places Altair on a natural coasting trajectory to acquire the R-bar at a point 2 km from Orion with a purely radial relative velocity. This burn is about 19 m/s. The 2-km acquisition range was chosen based on a trade study. It must be noted that since the trajectory from TPI to the R-bar is a “coasting” trajectory, the R-bar acquisition distance uniquely determines the location of the TPI point in space. This, in turn, defines the required apolune achieved during ascent. Between TPI and the R-bar, three midcourse maneuvers shape the trajectory and correct any dispersions due to the NCC and TPI burns. These three small ΔV ’s are all probabilistic in nature. One or more of these ΔV ’s might be cancelled if determined to be unnecessary. The heritage of this design is from the Apollo missions.

The Proximity Operations phase begins at R-bar acquisition and concludes at docking-port soft contact. To close the distance between the vehicles, Altair performs a series of “glide slope” maneuvers, along with two braking gates that serve to reduce the total profile time. At the conclusion of the glide slope maneuvers, Altair is delivered to a docking port-to-docking port range of 10 m with the proper range-rate for docking, thanks to natural braking from orbital mechanics. This velocity is held constant for the final 10 m until docking-port contact. Placeholder values of deadbands for attitude and translational controllers from R-bar acquisition to docking are given in Section 7.3.

Nominally, docking operations in LLO shall be executed with Altair assuming the role of active vehicle. The passive Orion shall assume a gravity gradient stabilized attitude with its X-axis pointed at the Moon's c.m. The active side of the Low Impact Docking System (LIDS) adapter, carried by Orion, will face down. Altair will approach Orion from "below". At the top of the Altair ascent module is the passive side of LIDS, and it will face "up" during docking. Also facing "up" are the GN&C docking camera and the docking lidar. Details of these sensors were described in Section 4.1. Via the two docking windows, crews can monitor the progress of the docking operations to better prepare for manual takeover if there is a need.

7. Special Design Challenges for Altair GN&C Subsystem

Besides the basic GN&C functionalities described in Section 4, a number of special Altair GN&C challenges must also be addressed to ensure mission success. Many of these challenges are related to landing Altair on the Moon. For example, the performance of landing-specific GN&C sensors must be robust relative to dust clouds that will be fanned by the descent engine plume during the last 50–100 m of the descent (visibility of Apollo-11 crew was degraded at an altitude of 30 m⁶¹). The GN&C design must also avoid any potential unstable interactions between the engine thrust vector control system design and the sloshing fuels in partially filled tanks. These and other special GN&C design challenges are addressed in the following sections. See also references 4–10. Other equally important GN&C issues, such as the need for detecting terrain hazards in the landing zone was discussed in Section 4.1 and in several references;³⁴⁻³⁷ thus, it will not be repeated here.

7.1. Unstable Interactions between Thrust Vector Control and Sloshing Liquids in Tanks⁶

Thrust vector stabilization and control is the closed-loop process that keeps the vehicle attitude from tumbling under the high thrust of engine firing and that accepts guidance steering commands to change the direction of the engine-caused acceleration vector. Vehicle motions about the two axes that are perpendicular to the thrust vector are controlled by the gimbal actuators. RCS thrusters are used to control vehicle motion about the remaining axis. Engine throttle is varied to change the magnitude of the acceleration vector. The TVC algorithm will be used to execute three critical ΔV burns of the Altair mission: LOI, PC, and the powered descent burn. A schematic diagram of the TVC is depicted in Fig. 16.

The Altair DM carries eight fuel tanks, four for liquid oxygen (LOX) and four for liquid hydrogen (LH2). During thrusting maneuvers, the sloshing of liquid fuels in partially filled tanks can interact with the controlled system in such a way as to cause the overall system to be unstable. In the post-flight guidance, navigation, and control (GNC) report of the Apollo-11 mission,¹⁹ there were numerous mentions of the impacts of sloshing fuels on vehicle control. For example, during the powered descent phase, the vehicle pitch rate started to diverge near PDI (at 102:36:57 MET). At that time, the peak-to-peak pitch rate was 0.6 °/s. It became 3.0 °/s when MET was 102:39:00. At MET = 102:39:30, the pitch-up maneuver was executed at the start of the approach phase, together with a throttle down and a tightening of deadband (from $\pm 1^\circ$ to $\pm 0.3^\circ$). These control actions arrested the divergence of pitch rate. The peak-to-peak pitch rate dropped from 3.0 to 2.2 deg/s.¹⁹ Experience from the Apollo-11 and other Apollo missions¹⁸⁻²¹ testified to the need to carefully consider the threat of unstable interactions between the TVC and sloshing fuels. To address this threat, the Altair GN&C team studied the following issues in greater depth:

- Tanks with sloshing fuels should be placed "underneath" the vehicle's c.m. to create a stable interaction between TVC and the sloshing fuel.
- TVC bandwidth should not be selected too close to the sloshing frequencies.
- Use of baffles to increase the damping of the sloshing fuels.
- Fuel sloshing modes should always be included in the dynamics model of the spacecraft used for control design synthesis.

To give some insight into the importance of tank placement, we shall consider a simplified rigid spacecraft with a spherical fuel tank, and include the lowest-frequency sloshing mode in the dynamic model (cf. Fig. 27).

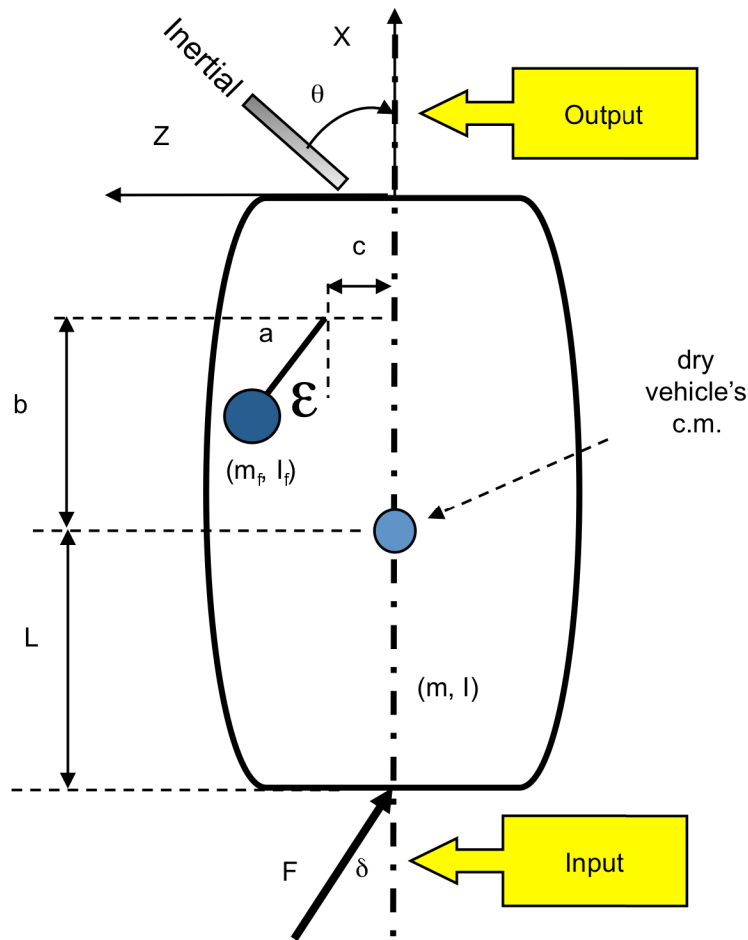


Figure 27. A spacecraft with a fuel pendulum.

In this figure, the motion of the sloshing propellant is modeled by an equivalent mechanical pendulum. This approach is similar to those used for the Voyager and Cassini robotic spacecraft.²⁵⁻²⁶ The symbols m and m_f denote the masses of the dry spacecraft and the fuel lump, respectively. Here, the word “dry” is used to represent all spacecraft masses that aren’t “sloshing”. The moments of inertia of the dry spacecraft and fuel are denoted by I and I_f , respectively. The symbols ω and ω_f denote the inertial rates of the dry spacecraft and the fuel, respectively. θ is the attitude of the spacecraft relative to an inertial frame, “ a ” is the length of pendulum, “ b ” is the distance between the pendulum pivot point and the S/C’s dry c.m., along X -axis, and “ c ” is the distance between the pendulum pivot point and the S/C’s dry c.m., along the Z -axis. Using D’Alembert’s principle, equations of motion of the spacecraft and the pendulum bob, as well as relevant kinematics relations are written. Invoking small angle motions of the spacecraft and fuel bob relative to their trimmed states, the transfer function of the system, from the gimbal angle input (δ) to the spacecraft’s attitude (θ) is written below.

$$\frac{\theta(s)}{\delta(s)} = -\frac{K}{s^2} \frac{\{1 + \frac{s^2}{\Omega_Z^2}\}}{\{1 + \frac{s^2}{\Omega_p^2}\}}$$

$$K (\text{sec}^{-2}) = \frac{F(L + \frac{m_f}{M} b)}{1 + \frac{mm_f}{M} (b^2 + c^2 - ab)}$$

$$\Omega_Z^2 (\text{sec}^{-2}) = \frac{aF(L + \frac{m_f}{M} b) \frac{m_f}{M}}{(L + \frac{m_f}{M} b)I_f + \frac{La^2 mm_f}{M}} \quad (2)$$

$$\Omega_p^2 (\text{sec}^{-2}) = \frac{aF \frac{m_f}{M} \{1 + \frac{mm_f}{M} (b^2 + c^2 - ab)\}}{I_f + \frac{mm_f}{M} (I_f (b^2 + c^2) + Ia^2) + \frac{m^2 m_f^2 a^2 c^2}{M^2}}$$

$$M = m + m_f$$

To avoid unstable interactions between the TVC and the sloshing fuel, the open-loop “pole” (Ω_p) must be larger than the open-loop “zero” (Ω_Z): $\Omega_p - \Omega_Z > 0$. This is the case if $b < 0^{6,22}$, that is, if the slosh pendulum pivot is located *below* the dry S/C’s c.m. Performing a similar analysis for a spacecraft with multiple sloshing fuels, one will arrive at the same conclusion. The placements of all fuel tanks on the current Altair DM satisfy this vehicle stability requirement, in all phases of the mission.

Basic pendulum modeling techniques exist in the literature to define slosh parameters for both spherical and cylindrical tanks. Key slosh parameters include the slosh frequency, participating slosh mass, equivalent pendulum length, and the attachment point of the pendulum. The literature includes 1960’s era NASA and more recent Southwest Research Institute (SwRI) publications.²⁷⁻²⁹ Like Altair, Apollo Lunar Excursion Module (LEM) tanks were cylindrical with hemispherical end caps. As such, the Apollo GN&C team adopted a hybrid slosh modeling approach, combining spherical and cylindrical modeling techniques. The Altair GN&C team repeated this hybrid tank model approach for both the LOX and LH2 tanks. Slosh parameters for three mission phases are of particular interest: LOI, PC, and the powered descent and landing. To estimate slosh parameters for these phases, we used, beside the tank geometry, baseline values of the LOX and LH2 tank fill fractions, thrust levels, and vehicle masses, for these mission phases. The resultant fuel sloshing frequencies are depicted in Fig. 28.

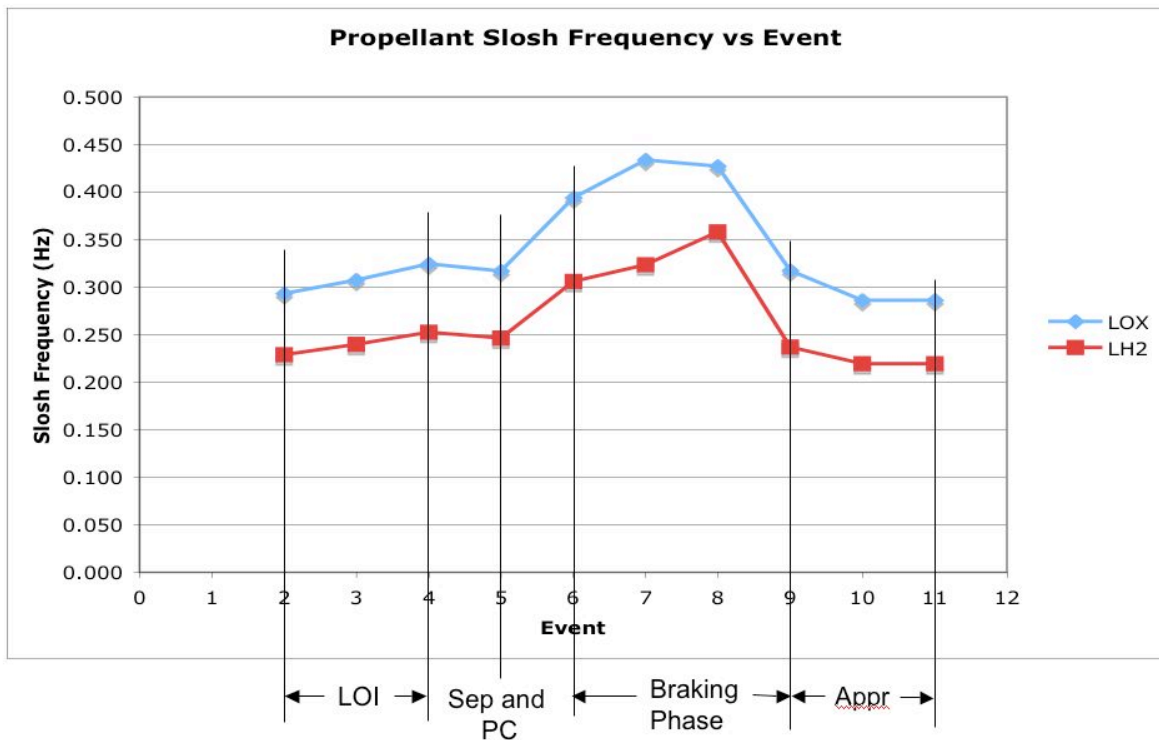


Figure 28. Estimated LOX and LH2 sloshing frequencies as functions of mission phases.

Thrust vector control of a spacecraft in a powered flight is in general quite challenging. This is because the TVC controller must compensate for a broad range of system dynamics (e.g., fuel slosh) some of which are poorly damped and others might have frequencies that are relatively close to the natural frequency of the total system. There are two obvious issues associated with controlling a spacecraft in a powered burn with propellant sloshing. First, the TVC control engineer must consider the amount of mechanical passive damping that might be needed. The second issue is related to the separation between the TVC controller bandwidth (BW) and the slosh mode frequency.

Damping ratio of fuel slosh is a function of fuel tank geometry, longitudinal acceleration, and kinematic viscosity of the liquid fuel. Estimated values of damping ratios of Apollo fuel slosh modes are on the order of 0.1–0.16%.⁷² Using available empirical formulae,²⁷ Altair GN&C team made estimates of the damping ratios of fuel slosh modes in various powered flight phases. These estimates indicate that Altair fuel slosh damping ratio is even lower than those of Apollo's. Baffles for the Altair's fuel tanks on both the ascent and descent modules will be needed. Baffles of various configurations add passive damping to the sloshing fuel. Damping ratios of 1–5% are achievable via baffles. The obvious penalties of baffles are the weight increase and the manufacturability of tanks with baffles. Compartmentation of a tank will, in general, increase the slosh mode frequency. This is the case because, in general, slosh mode frequency is inversely proportional to the square-root of the tank characteristic dimension. Again, there will be a weight penalty.

The type of slosh controller that is needed to stabilize fuel sloshing during a powered burn depends on the degree of passive damping afforded by baffles.²² Also, if the slosh mode frequency is significantly larger than the TVC controller BW, a gain stabilization of the slosh mode could be achieved via a roll-off filter. Else, the control engineer will have to use phase-lead filter to stabilize the slosh mode dynamics. To this end, the sloshing modes must be characterized with accuracy and the phase-lead filter carefully designed taking into consideration the dynamics of the gyroscope, gimbal actuator, etc.

There is a general desire to select the TVC bandwidth as large as possible, not only to minimize maneuver errors (cf. Section 4.5), but also to keep spacecraft and engine gimbal rates to acceptable levels during ignition transients. Large bandwidth will also help to bound the magnitudes of the gimbal angles to levels that are within

available gimballed excursion range (say, $\pm 6^\circ$), during ignition transients. The ratios of slosh mode frequency to BW of the Apollo TVC systems were ≈ 2 , and that for the space shuttle TVC system was 1.94.²³⁻²⁴ Also, as depicted in Fig. 28, slosh mode frequencies vary over a range of 0.2–0.44 Hz from LOI to touchdown. Based on the general guideline of maintaining a 2:1 ratio between fundamental slosh mode frequency and the TVC BW, the Altair GN&C team picks a placeholder TVC bandwidth of 0.12–0.15 Hz. This selection is comparable with the bandwidths used by Apollo, which was 0.13–0.18 Hz.²³ The TVC bandwidth of the space shuttle was 0.13 Hz.²⁴ Note that the selected TVC BW is also more than an order of magnitude lower than all other system dynamics and “flexibilities” including sampling frequency, engine gimbal actuator bandwidth, sensor bandwidth, structural frequency, and the “tail-wags-dog” spacecraft-engine interaction frequency^{71,72} (see also Fig. 29).

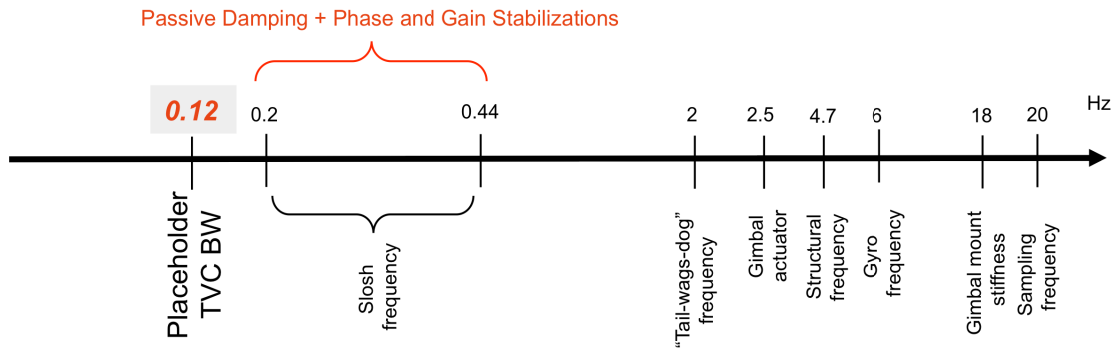


Figure 29. Placeholder TVC BW relative to slosh and other system dynamics.

The placeholder TVC controller bandwidth wasn’t selected based solely on the slosh mode frequency. The TVC control engineer must also consider sets of performance and stability requirements in his selection of the bandwidth. A representative performance requirement is the time it takes the control system to respond and settle to within $\pm 5\%$ of a commanded attitude command. Representative stability requirements are the commonly-used gain and phase margins of control system. Details are given in Ref. 6.

The AM engine is not gimballed, so large AM RCS thrusters will be used to control the spacecraft attitude during the ascent insertion burn. Like the descent module, the ascent module carries multiple tanks with sloshing fuels. Again, preliminary analyses indicated that it is desirable to ascertain that the fuel slosh pendulum pivots are placed below the dry S/C’s c.m. Details are also given in Ref. 6.

7.2. Dusty Environment of the Moon

The lunar surface is covered by granular materials with an average size of about 20 microns distributed in layers as much as several tens of meters thick.³⁰ The upper few centimeters of these dust deposits can be easily disturbed by human activities on the Moon. During the last few minutes of the landing phase, the descent engine exhaust plume, with exit velocity that is $>4,000$ m/s, can also generate huge dust clouds. These dust clouds represent a source of possible contamination to optical instruments. The visibility observed by the Apollo-11 crew was degraded at an altitude of 30 m.⁶¹ The dust cloud became so intense at 10–15 m that it impaired the visibility for the Apollo-11 crew during the terminal descent and landing phase of the mission. For Altair, with a larger DM engine, it is estimated that dust clouds will begin to threaten the functionality of GN&C optical sensors when the vehicle’s altitude is lower than 100 m. Dislodged dust particles drifting in space, when illuminated by the Sun, can look very much like stars to a star tracker.³¹ Altair GN&C optical sensors that must be protected from the dust particles include the prime star tracker and the optical navigation sensor system. The docking camera is placed in the interior of the ascent module and is free from this threat.

The prime star tracker will be protected by a deployable cover mechanism. The cover will be deployed during landing and liftoff, and it will shield the optics completely from both the engine exhaust plume and the lunar dust particles. A conceptual design of the star tracker cover mechanism is depicted in Fig. 30. This cover mechanism is

designed with the following set of placeholder requirements. Lessons learned from the designs of other cover deployment and latch mechanism of past missions has been incorporated in the current design.³²

- Fault Tolerance: Single fault tolerant
- Cover is in the “open” position in any “loss of power” scenario
- Mass: Lower than 1.5 kg
- Power: Lower than 10 W
- Operations temperature range: $-30/+65$ °C
- A minimum of 20 open/close cycles for the entire Altair mission
- Telemetry: Positive indication of the cover’s open (or closed) position
- Motion of cover is to be restrained during launch and other major propulsive maneuvers

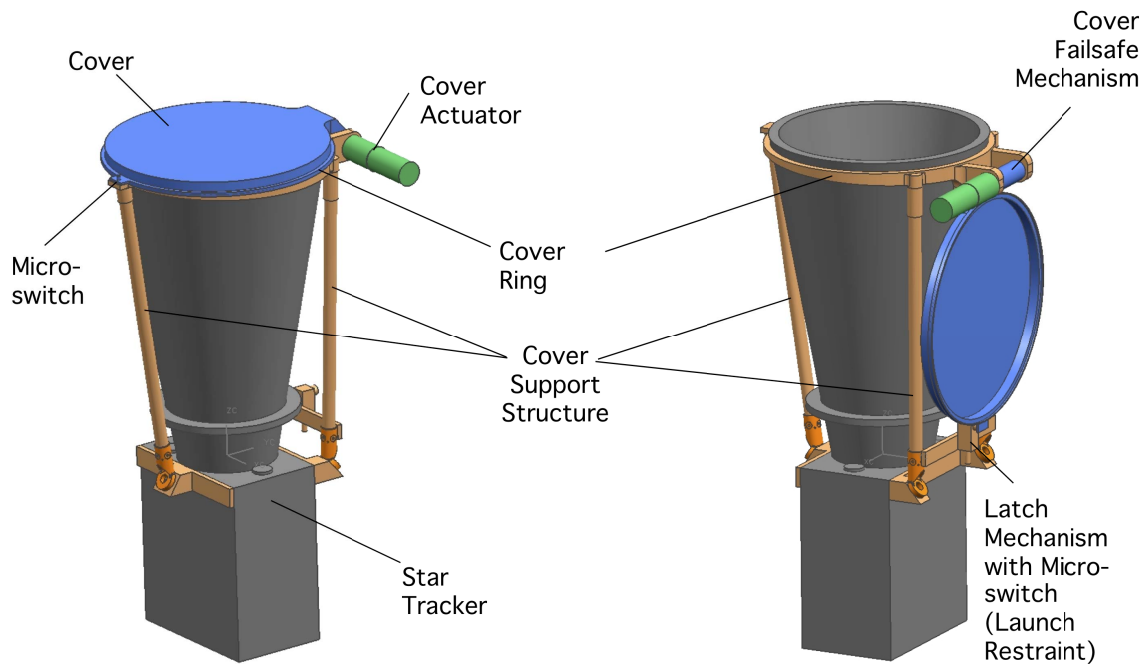


Figure 30. Deployable cover mechanism for star tracker.

As depicted in Fig. 30, the deployable cover mechanism consists of a cover ring on top of a cover support structure, a cover, a cover actuator, a latch mechanism, and two micro-switches. Both the cover structure and the cover use aluminum (7057-T7351) to match the star tracker baffle. The cover ring and hinge do not contact the star tracker baffle. This design used a labyrinth seal based on a heritage design used on the inlet cover of instruments mounted on the Mars Science Laboratory (MSL) rover. The cover is driven open (or closed) by a dual-wound stepper motor. Actuator stalls driving the cover into the cover ring to hold the cover closed. The cover mates to the cover ring to keep contamination from entering the tracker baffle. If the actuator were to fail, the failed actuator is decoupled from the hinge shaft using a low-temperature melt alloy decoupler. Torsion springs will allow the cover to rotate open once decoupled. The springs are sized to drive the cover into latch for stowing. The heritage of this fail-safe mechanism is the Mars Pathfinder rover (1997). The latch functions as a launch lock. It is reset-able using a paraffin actuator. When heat is applied to paraffin, it will convert from solid to liquid. Expanded volume pushes a rod to release the latch. When heat is removed, the paraffin will convert back from liquid to solid, and torsion springs allow the cover to rotate open once decoupled. A micro-switch mounted inside the latch mechanism provides telemetry on the latch/unlatch state. Another micro-switch provides telemetry on the cover open/closed state.

In flight, the star tracker cover will be latched during the launch of ARES-V. It will also be latched during all major propulsive maneuvers including TLI, LOC, PC, and powered descent ΔV burns. During the long TLC phase, the cover mechanism will be “exercised” several times to perform functionality checked out. Except during these brief checked out periods, the cover will be open except for the last 100 m of the powered descent and the first 100 m of the powered ascent phases. After landing, the optical sensors should continue to be protected. This is because once lunar dust is lofted from the lunar surface, there is no atmosphere to resist its motion, and thus even the smallest grains follow ballistic paths. This path can be quite extensive due to the low lunar gravity field. Together, these facts imply that lunar dust can be easily disturbed and spread to great distance and height.

The optical navigation sensor system (ONSS), depicted in Fig. 4, must also be protected from the dust particles. However, because ONSS is articulatable, the simplest way to protect it is to stow it down into a dust “shield.” This concept is depicted in Fig. 31. Using 7075-T7 aluminum materials, a light-weight dust shield panel structure could be easily manufactured.

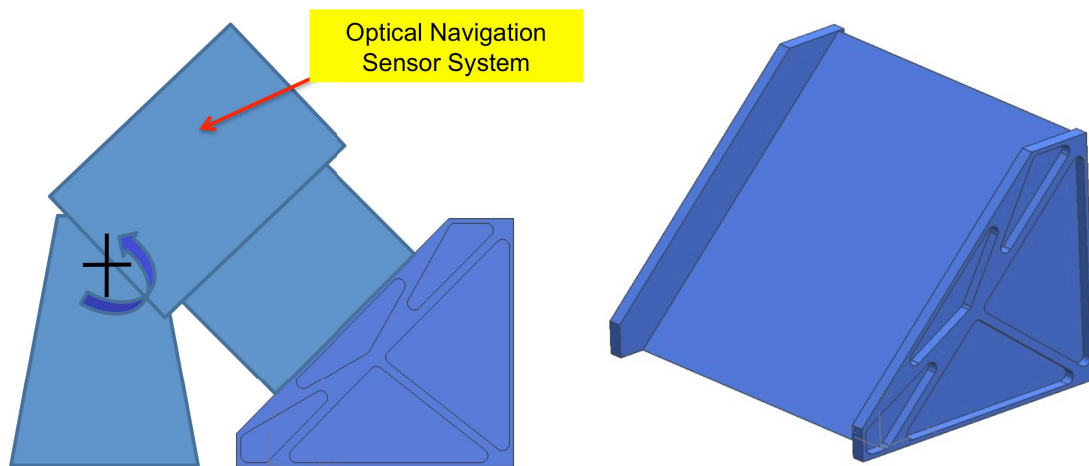


Figure 31. Altair stow dust shield concept.

7.3. Docking Operations: Constraints and LIDS Docking Requirements

Nominally, docking operations in LLO shall be performed with Altair assuming the role of active vehicle. The passive Orion shall assume a gravity-gradient-stabilized attitude with its X-axis pointed at the Moon’s c.m. The active side of the Low Impact Docking System (LIDS) adapter, carried by Orion, will face down. Altair will approach Orion from “below” and will make an “R-bar acquisition” at a relative distance of about 2 km. Here, we use the “target local orbital frame” to describe Altair/Orion docking operations.⁴⁸ In this coordinate frame, the orbit direction is named V-bar after the orbital velocity vector \vec{V} . The coordinate in the direction from the spacecraft to the Moon’s c.m. is named R-bar after the radius vector \vec{R} , and the third coordinate completing the system is named H-bar after the orbital angular momentum vector \vec{H} . The R-bar approach enables use of natural braking from orbital mechanics to slow Altair during its approach to Orion. This strategy has the advantages of a shorter approach time and lower propellant consumption. At the top of the Altair ascent module is the passive side of LIDS, and it will face “up” during docking. Also facing “up” are the GN&C docking camera and the docking lidar. Via the two docking windows, crews can monitor the progress of the docking operations to better prepare themselves for manual takeover if there is a need.

The common focus of the GN&C systems of both Altair and Orion in the docking phase is to meet all the docking requirements dictated by the LIDS. The LIDS-related docking conditions are listed in Table 7. Note that since LIDS is an impact docking system (with passive capture latches), there must be an axial contact velocity (requirement listed in Table 7 is 1.525–4.575 cm/s) as energy is needed to operate the capture latches. Altair GN&C will command the close-in rate to be 3 cm/s which is near the mid-point of the requirement range.

A systematic approach in designing a successful docking capability for Altair starts with building error budgets for all the LIDS contact requirements listed in Table 7. Based on the docking issues described above, error sources that degrade Altair docking performance are identified. Current estimated capabilities are listed in Table 7. All LIDS docking requirements are met with margins. See Ref. 9 for details.

Table 7. LIDS docking requirements and estimated capabilities.

Docking Criteria	Unit	Docking Requirements (3σ)	Estimated Docking Capabilities (3σ)
Close-in (Axial) Speed	cm/s	1.525 – 4.575	3.0
Lateral (Radial) Speed	cm/s	4.575 (Y and Z combined)	4.35
Angular Rate	deg/s	0.15 (X-axis) 0.15 (Y-axis) 0.15 (Z-axis)	0.12 0.109 0.109
Lateral (Radial) Offset	cm	8.128	6.77
Angular Misalignment	deg	3.0 (X axis) 3.0 (Y and Z combined)	2.42 2.38

In docking operations, the instantaneous docking axis of the target (on Orion) changes continuously with time. This could be due to the attitude control (deadbanding) motions of Orion, vibratory motions of Orion’s flexible structures, as well as Orion’s motions in response to plume (from the firings of Altair’s thrusters) that impinged on its surfaces. It is possible for the chaser to track this time-varying docking axis only if a docking sensor is able to measure, in addition to axial and lateral positions (or range and bearing angles), the relative attitude between the vehicles. The docking sensor described in Section 4.1 (see also Fig. 6) serves this function.

Two-way impacts of plume impingements between mating vehicles is an important docking-related lesson learned from Apollo missions. In addition to exerting pressure on Orion, hot plume gases from Altair’s thrusters can damage exposed equipment (e.g., solar panels) and contaminate sensitive optical surfaces on Orion. To minimize these impacts, the axes of the four AM RCS thrusters D_i ($i = 1-4$) are canted 45° away from the docking axis (X-axis). See Fig. 11. The expansion plume cones of thrusters are typically bounded by $\pm 45^\circ$. Hence, plumes from the firing of thrusters D_i ($i = 1-4$) will not impinge on Orion (see Fig. 12). However, this conclusion is made under the assumption that the Altair’s X-axis is nearly aligned with Orion’s X-axis when they are in the close proximity of one another. If that alignment has not yet been achieved, as depicted in Fig. 32, expanding plume cones of some AM RCS thrusters D_i ($i = 1-4$) might intersect Orion. Therefore, it is highly desirable to align the vehicle’s docking axes at a time when the vehicles are separated from one another by a large distance. The narrowing of the separation distance will be executed only after the alignment has been achieved.

Guided by these considerations, both the angular and translational deadbands of the AM RCS thruster controller shall be tightened gradually as functions of the separation distance between the two vehicles (cf. Fig. 33). The approach rate is also made a function of the separation distance between these vehicles. The heritage of the approach rate given in Table 8 is from Space Shuttle/ISS docking experience.

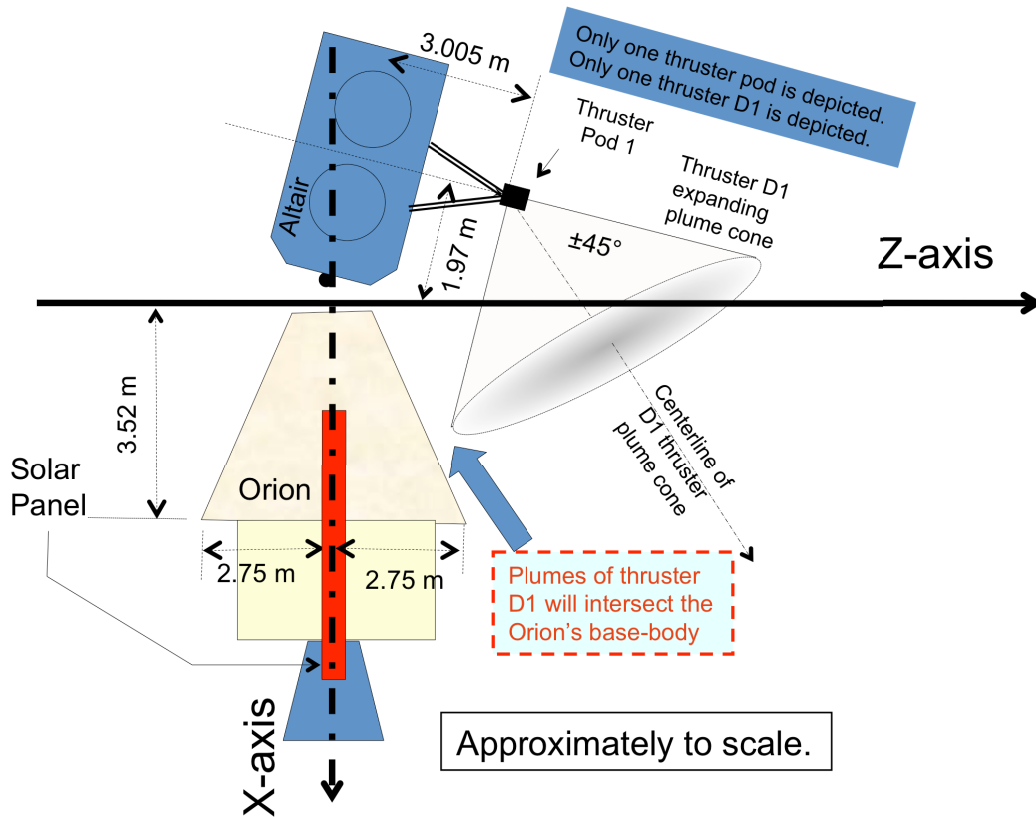
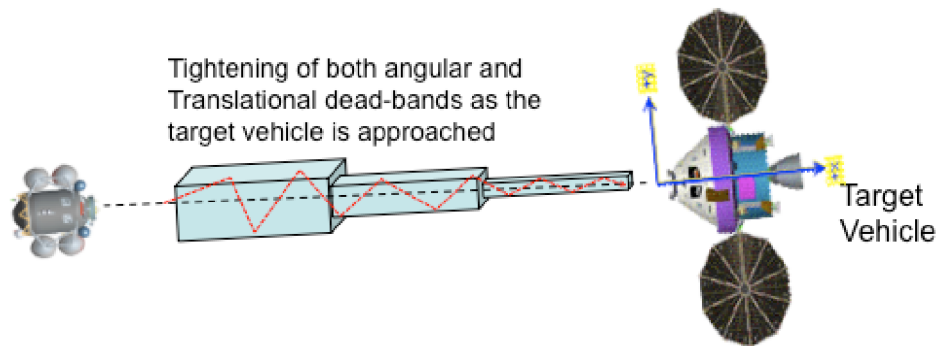


Figure 32. Plume impingement problem experienced by non-aligned mating vehicles.



¹¹This is a set of approach rate derived from Shuttle experience.

¹²This is selected to be near the mid-point of the acceptable LIDS close-in speed range of 1.525-4.575 cm/s (see also page 10).

¹³As used in Ref. 4.

Figure 33. Tightening of deadband as Altair approaches Orion.

Table 8. Docking approach rate and Altair’s dead band as functions of separation distance.

Distance between vehicles [m]	Approach Rate [cm/s]	Per-axis one-sided Angular Dead band [deg]	Per-axis one-sided Translational Dead band [cm]
150 – 30	45.8 – 5.8	1	2
30 – 10	5.8 – 3.0	0.5	1.5
10 – 0	3.048	0.25	1

The AM RCS thrusters will be used to perform both translational and rotational control of the spacecraft. As described in Section 4.3, large R-42 thrusters will be used during the ascent insertion burn (at liftoff) to counter large tumbling torque imparted on the AM due to canting error of the AM engine, staging disturbance torque (“fire in a hole”), etc. The small AmPac thrusters will be used during docking operations. This thruster configuration is necessary because the minimum impulse bit (MIB) of a thruster is generally a function of thruster’s maximum force. Large thrusters, with larger MIB, will likely generate ΔV and/or $\Delta \omega$ that are too large relative to the LIDS docking requirements (see Table 7).

In the current plan, Altair GN&C will control its position and attitude to achieve full translational and rotational alignments of the two docking adapters (on Orion and Altair) simultaneously. The three per-axis position controllers will send force commands of varying amplitudes to appropriate pairs of thrusters to zero out the displacement vector from the Altair LIDS adapter to the Orion LIDS adapter. The three per-axis attitude controllers will send torque commands of varying amplitudes to other pairs of thrusters. To avoid coupling between the translational and rotational motions of the spacecraft, the AM RCS thruster pods are placed with their X-axis coordinates that are close to the predicted X-axis coordinate of the spacecraft’s c.m. (at the time of docking). In this way, thruster firings that are commanded to generate a translational motion along the Y-axis (for example) will not generate an undesirable rotational motion about the spacecraft’s Z-axis. Similarly, to avoid translational motions from commanded rotational motions, all attitude control torque commands will be executed using thruster couples. In this way, impulses generated by the two thrusters of the couple will nearly “cancel” each other, and there will be no translational motion. Unfortunately, random variation (say, 5%) of thrusters’ MIB could still lead to small undesirable translational motion. Finally, equipment on the ascent module will be placed and distributed in such a way that the AM’s c.m. is on the X-axis, and all the products of inertias of the AM are small relative to the moments of inertia. That is, the mechanical axes of the AM are closely aligned with its principal axes. With this configuration, commanded rotational motion about one spacecraft axis will not generate unwanted rotational thruster firings about the other two axes, which wastes fuel. Note that the ratios of products of inertias to moments of inertia of the AM, listed in Table 9, are all smaller than 2.3%.

Table 9. Ratios of products of inertias to moments of inertia at docking.

	I_{XY}/I_{XX}	I_{XZ}/I_{XX}	I_{YX}/I_{YY}	I_{YZ}/I_{YY}	I_{ZX}/I_{ZZ}	I_{ZY}/I_{ZZ}
Ratios	0.16	2.3	0.12	0.63	1.8	0.60

7.4. GN&C Considerations for Piloted Lunar Landing¹⁰

The provisions to involve the crew in controlling the lander might appear as an unnecessary complication to the design of the GN&C system. Many tasks are best left to the machine. Tasks that are tedious, repetitive, or require quick response that is outside crew’s capabilities are best performed automatically. In the evolution of Apollo missions, the trend had been to rely more and more on automatic modes as systems experience had been gained. For example, computer programs for rendezvous were reworked to require for less operator input than had originally been planned. Nevertheless, the entire rendezvous sequence was designed so that the pilot could always monitor the automated system's performance and apply a backup solution if deviations were noted. The approach and landing

tasks could also take advantage of the crew's ability to make real-time decisions to avert selected unanticipated threats. Almost all participants of the "Go for Lunar Landing" conference (Tempe, Arizona, March 2008)⁴⁹ agreed that future landers should be designed with at least a backup manual landing capability. Their assessment is that the added capability will enhance mission success and crew safety. Given Apollo's six successes in six landing attempts, some conference participant even thought that the crew should perform the landing task as "prime". Whether prime or backup, these manual control tasks are challenging (e.g., Neil Armstrong evaluated the Apollo 11 landing tasks as "a 13 on a scale of 1–10") and training will be needed.

There was significant work to understand piloting performance and requirements during the Apollo Program, including the use of various fixed and motion-based simulators and also a free-flying Lunar Lander Research Vehicle (LLRV) flown at Edwards Air Force Base.⁵⁵ The LLRV was developed to identify desirable Apollo lander piloting qualities including control authority and piloting strategy. The trajectory-controlling strategy developed in ground simulators and verified with the LLRV involved using thrusters to change vehicle attitude and redirect the downward thrusting engine, to effect horizontal translation of the vehicle (diversion maneuver). Vertical descent rate was itself affected by the engine throttle, though from various simulation analyses, it was determined that pilots preferred commanding descent rate with the computer automatically adjusting throttle, rather than directly controlling throttle. It was also determined that the preferred piloting command interface was that of a Rate Command Attitude Hold (RCAH) concept, where the flight computer would command attitude rates proportionate to the deflection of the hand controller, then hold its current attitude when the controller was returned to detent.

As depicted in Fig. 2, the current Altair design is taller than the Apollo lander by about 50%, and three times as massive. Also, while the landing accuracy today is 1 km (cf. Table 1), it might be tightened to 100 m in the future. The Altair landing requirements also extend to all reaches of the moon, with particular interest in polar landings (with poor lighting condition), and including the potential to land in rough terrain. The increased vehicle size and more demanding landing requirements will have significant impact on what the piloting task is ultimately defined to be during final approach and landing, as well as how it is executed, the definition of displays, including out-the-window and its correlated requirements on local lighting, and what type of inceptor (hand controller) and pilot-vehicle interface strategy is ultimately adopted.

With the announcement of the Constellation Program, the Ames Research Center (ARC), in 2007, began to re-examine some of these piloting issues as they relate to a precision lunar landing. Since then, researchers on handling qualities have coordinated and performed three pilot-in-the-loop studies using the Vertical Motion Simulator (VMS, see Fig. 34). These studies included the buildup of a generic lunar lander cockpit with standing pilot and co-pilot, translational and rotational hand controllers (similar to those used for Apollo and Shuttle missions), a flat-panel screen to provide out-the-window scenes, and limited digital instrument displays. This cockpit was mounted "on the beam" of the VMS facility for 6-dof motion and was driven by a lunar lander simulation. The simulation was originally configured for an Apollo type lander but later adapted to the Altair lander.

The first study in 2007 investigated the impacts of RCS thruster control authority on piloted landing with only an Apollo lander configuration. The 2008 study included an Altair configuration (per the configuration adopted at the conclusion of design cycle #2), again investigating impacts of RCS thruster control authority and maximum pilot-command attitude rates on piloted landing. The most recent study in October 2009 involved the current Altair configuration, investigating control authority coupled with various pilot interface and display methodologies. Several interesting results have come from these studies, many of which have been published.⁴⁹ Some highlights from these studies are summarized here. For attitude control of Altair, the RCAH method still appears to be the one preferred by pilots. However, the current Altair vehicle and its thruster configuration is likely underpowered near touchdown to provide favorable piloting handling qualities. Also interesting was that the direct horizontal velocity command input was found acceptable by some of the pilots even with the current control authority of the Altair vehicle.

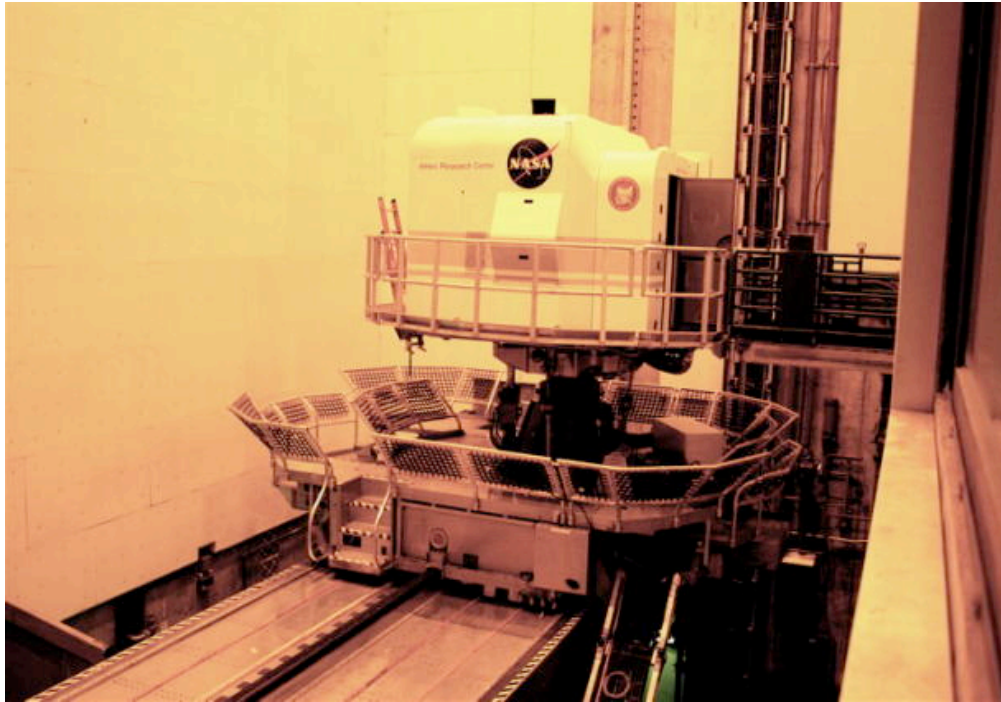


Figure 34. Vertical motion simulator (courtesy of NASA Ames Research Center).

The current plan of the Altair GN&C team is to design the system that will, for selected mission phases (e.g., descent and landing, ascent and docking, etc.), allow the pilot to select between “automatic”, “semi-automatic”, and “manual” controls. If the “semi-automatic” mode is selected by the pilot for the vertical descent phase, the vehicle’s altitude and rate of descent could be controlled automatically by the onboard guidance system while the pilot’s focus on the manual control of the vehicle’s attitude that is needed to generate horizontal divert translations. For Apollo missions, engine shutdown was performed manually when contact probes touched the ground and a light was activated in the cockpit. Pilots will be effective in performing this engine shutdown task and other manual tasks only if key GN&C data (e.g., vehicle’s altitude and attitude) are clearly displayed to them. Head-up displays of flight information for both the pilot and co-pilot is much preferred over the relatively cumbersome verbal transfer of information employed during the Apollo landings.⁴⁹

8. Summary and Conclusions

The objective of this paper is to describe the preliminary design of the Altair Guidance, Navigation, and Control subsystem. The GN&C subsystem must perform many functions that are of critical importance to the Altair mission. Guided by the DRM and a set of GN&C-related CARD requirements, a GN&C sensor suite was selected to satisfy the identified functionalities. The selected sensors and equipment are placeholders, but they were selected because of their high TRL, and most have rich flight heritage. A lesson learned from the descent and landing experience of multiple Apollo missions was the need to address the threats of terrain hazards. A placeholder sensor system is included in our GN&C design to address this threat. The radiation environment around the Moon represents another threat. In 2009, radiation caused the failure of both the prime and backup star trackers of an Indian lunar orbiter in LLO. GN&C sensor work will not be done until the radiation threat has been fully addressed, especially for long Altair missions. Via many discussions with members of the Altair Propulsion and Structure teams, we have also selected ascent and descent RCS thruster configurations that meet the control and navigation needs of the Altair mission. In particular, the RCS thruster configuration for the ascent module was designed to meet both the control needs at liftoff and the precision control needs at docking. The navigation plan and performance of Altair, from trans-lunar injection to touch down on the moon, has been described in some details. Here, we emphasized the importance of optical navigation and how optical navigation equipment could also be used to perform terrain-

relative navigation, leading to improved landing accuracy. Future work will address the navigation performance of Altair in the ascent insertion and RPOD phases of the mission. In section 6, guidance designs for the descent, ascent, and docking phases of Altair were only described qualitatively. Quantitative results are given in Refs. 7, 11, and 15. Not surprisingly, Altair guidance designs are very similar to their Apollo's counterparts. For example, in the descent and landing sub-phases of Altair, the "braking," "approach," "null the horizontal velocity," and the "terminal vertical descent" sub-phases (described in Section 6.1) correspond, one-to-one, with the Apollo's P63, P64, P65, and P66 guidance programs, respectively.⁶⁵ The Altair GN&C design described in this paper is the product of many discussions with engineers of various Altair subsystems including Thermal, Power, Avionics, Flight Software, Structures, Commands and Data Handling, Flight Mechanics, Astronauts, Safety, Comm. and Tracking, as well as the vehicle systems engineering team. We have also benefited from numerous discussions with members of the Orion GN&C team. These interactions were not only beneficial but critical to the development of a sound design for this system.

One of the interesting characteristics of the Altair lunar lander design is its traceability to past Mars lander/rover designs, and potential applicability to a future crewed Mars lander. The GN&C sensor suite selected for Altair leverages heritage from GN&C sensors from past or present robotic Mars landers/rovers, including the Viking landers (1975),⁷⁰ Mars Pathfinder (1997), Mars Exploration Rovers (2003), Phoenix (2007),⁵¹ and Mars Science Laboratory (2011).³⁹ Some similarities and differences can be summarized as follows:

- These Mars vehicles similarly carried inertial measurement units and star trackers to estimate the spacecraft's inertial attitude and attitude rate.
- Once in the Martian atmosphere, attitude propagation was performed using IMU data alone, and the "one-way" nature of all past Mars missions (no return from the Martian surface) implied that the star trackers were no longer required to achieve mission success. As such, there was no need for dust cover mechanisms for the star trackers.
- Just like Altair, the Mars vehicles' state vectors were initialized using EBGs uplink data and propagated using IMU data. For these Mars vehicles, the last EBGs uplinks were made prior to atmospheric entry.
- Because the ground-relative accuracy of the inertially-propagated state vector was generally inadequate for soft landing, the Viking landers and Phoenix also carried radars to achieve soft landing on Mars (as will MSL).
- After spending about one day in the LLO, Altair will undock with Orion. Thereafter, it will perform a PC and a DOI burns. The DOI burn will place Altair on an orbit that has a perilune of 15.24 km. At the perilune, the gimbale engine of the DM will be ignited to initiate the powered descent burn. Similarly, following separation from a Mars orbiter, the Mars lander will execute a deorbit burn. After a predetermined time had elapsed, RCS thrusters on the Mars lander will orient the lander's heat shield for the Martian atmosphere encounter. The DOI execution accuracy is of prime importance in determining subsequent trajectory parameters such as the entry velocity flight path angle. With most of the orbital speed of the Mars lander removed by the Martian atmosphere via parachutes, there will be no need for a powered braking phase in the descent guidance of Mars landers. For terminal descent guidance, the Viking's employed a gravity turn guidance algorithm,⁷⁰ but Apollo employed a vertical path guidance algorithm.¹⁹⁻²¹ Altair has adopted the vertical descent approach flight proven by Apollo missions as will MSL.³⁹
- The terminal descent radars carried by these Mars landers performed an additional function that is not required by the Altair's radar. To have a safe journey through the Martian atmosphere, the Mars landers were protected with heat shields and back-shells. In most of these missions, radar-based data were used to determine the altitudes and altitude rates at which to optimally eject these protective covers.

Given the similarities with Mars vehicle designs, and taking into account the significant differences, the work done by the Altair design team should have applicability to future crewed (and even robotic) missions to Mars, providing value and design lessons beyond the scope of the Altair project and the Constellation Program, as we expand human exploration to the Moon, Mars, other heavenly bodies, and further into the solar system.

Acknowledgments

The work described in this paper was carried out by Jet Propulsion Laboratory, California Institute of Technology, under a contract with the National Aeronautics and Space Administration. Reference to any specific commercial product, process, or service by trade name, trademark, manufacturer, or otherwise, does not constitute or imply its endorsement by the United States Government or the Jet Propulsion Laboratory, California Institute of Technology. We are grateful to Mimi Aung, Paul Bowerman, David Eisenman, Chet Everline, Melvin Flores, Martin Heynes, Erisa Hines, Andrew Johnson, Edward Konefat, Earl Maize, Wayne Lee, Scott Peer, Brian Pollard, Michael Sanders, Guru Singh, Gary Spiers, Rebekah Tanimoto, and Nick Taylor (at Jet Propulsion Laboratory), Molly Anderson, Ellen Braden, Tim Crain, Brian Derkowski, Clinton Dorris, Lauri Hansen, Brad Irlbeck, Brad Jones, Howard Law, Kathy Laurini, Jonathan Lenius, Michael Machula, James McMichael, Robert Merriam, Jacque Myrann, Michelle Rucker, Randy Rust, and Jake Sullivan (at the NASA Johnson Space Center); Kendall Brown, Jack Chapman, Larry Kos, and Tara Polsgrove (at the NASA Marshall Space Flight Center); Tim Collins and David North (at NASA Langley Research Center), as well as Alfred Menendez (at Kennedy Space Center) for much helpful assistance over the past years. Also, we would like to thank our colleagues at JPL, Glenn A. Macala and Sima Lisman, senior members of technical staff (Guidance, Navigation and Control section), for their reviews and comments on an earlier version of this paper.

References

- ¹Von Braun, W., "Man on the Moon: The Journey," *Collier's*, October 18, 1952, pp. 52–59.
- ²Kennedy, J. F., Excerpts from "Urgent National Needs," Speech to a Joint Session of the Congress, May 25, 1961.
- ³Lee, A. Y., and Hanover, G., "Cassini Spacecraft Attitude Control System Flight Performance," *Proceedings of the AIAA Guidance, Navigation, and Control Conference, and Exhibit*, San Francisco, California, August 15–18, 2005.
- ⁴Ely, T., Heyne, M., and Riedel, J. E., "Altair Navigation during Trans-Lunar Cruise, Lunar Orbit, Descent, and Landing," *Proceedings of the AIAA Guidance, Navigation, and Control Conference, and Exhibit*, Toronto, Ontario, Canada, August 2–5, 2010.
- ⁵Riedel, J. E., Ely, T., Lee, A. Y., Werner, R. A., Wang, T.-C., Vaughan, A. T., Nolet, S., Myers, D. M., Mastrodomos, N., and Grasso, C., "Optical Navigation Plan and Strategy for the Lunar Lander Altair," *Proceedings of the AIAA Guidance, Navigation, and Control Conference, and Exhibit*, Toronto, Ontario, Canada, August 2–5, 2010.
- ⁶Lee, A. Y., Strahan, A. L., Tanimoto, R., and A. Casillas, "Thrust Vector Control of the Lunar Lander Altair in the Presence of Fuel Sloshing," *Proceedings of the AIAA Guidance, Navigation, and Control Conference, and Exhibit*, Toronto, Ontario, Canada, August 2-5, 2010.
- ⁷Kos, L., Polsgrove, T., Sostaric, R., Braden, E., Sullivan, J. J., and Le, T. T., "Altair Descent and Ascent Reference Trajectory Design and Initial Dispersion Analyses," *Proceedings of the AIAA Guidance, Navigation, and Control Conference, and Exhibit*, Toronto, Ontario, Canada, August 2-5, 2010.
- ⁸Strahan, A. L., and Johnson, A., "Terrain Hazard Detection and Avoidance during the Descent and Landing Phase of the Lunar Lander Altair Mission," *Proceedings of the AIAA Guidance, Navigation, and Control Conference, and Exhibit*, Toronto, Ontario, Canada, August 2-5, 2010.
- ⁹Sullivan, J., Lee, A. Y., and Grover, R., "Rendezvous and Docking Sensor and Effector System Designs for the Lunar Lander Altair," *Proceedings of the AIAA Guidance, Navigation, and Control Conference, and Exhibit*, Toronto, Ontario, Canada, August 2-5, 2010.
- ¹⁰Strahan, A. L., Law, H. G., Bilimoria, K. D., and Mueller, E. R., "A Review of Research Into GNC Performance and Interface Design for A Piloted Lunar Landing," *Proceedings of the AIAA Guidance, Navigation, and Control Conference, and Exhibit*, Toronto, Ontario, Canada, August 2-5, 2010.
- ¹¹Sostaric, R., and Merriam, R., "Lunar Ascent and Rendezvous Trajectory Designs," *Proceedings of the 31st Annual AAS Rocky Mountain Guidance and Control Conference*, Breckenridge, Colorado, February 1-6, 2008, AAS 08-066.
- ¹²Kennedy, F. G., III, "Orbital Express: Accomplishments and Lessons Learned" *Proceedings of the 31st Annual AAS Rocky Mountain Guidance and Control Conference*, Breckenridge, Colorado, February 1-6, 2008, AAS 08-071.
- ¹³Keller, B. S., Tadikonda, S. K., and Mapar, J., "Autonomous Acquisition, Rendezvous, and Docking Using a Video Guidance Sensor: Experimental Test Bed Results," AIAA 2002-4846, *AIAA Guidance, Navigation, and Control Conference and Exhibit*, Monterey, California, August 5-8, 2002.
- ¹⁴Blarre, L., Ouaknine, J., Moussu, C., Michel, K., Moebius, B., Cunha, P. D., and Strandmoe, S., "Description and Inflight Performances of Rendezvous Sensors for the ATV," *32nd Annual AAS Guidance and Control Conference*, Breckenridge, Colorado, AAS 09-061, January 30 to February 4, 2009.
- ¹⁵Sostaric, R., "Powered Descent Trajectory Guidance and Some Considerations for Human Lunar Landing," *Proceedings of the 30th Annual AAS Guidance and Control Conference*, Breckenridge, Colorado, February 3-7, 2007, AAS 07-051.
- ¹⁶Constellation Architecture Requirements Document (CARD), CxP 70000, Release Version D, 2009, Johnson Space Center.

- ¹⁷Gates, C. R., "A Simplified Model of Midcourse Maneuver Execution Errors," JPL Technical Report 32-504, Jet Propulsion Laboratory, Pasadena, California, October 15, 1963.
- ¹⁸NASA Manned Spacecraft Center, *Apollo 10 Guidance, Navigation and Control System Performance Analysis Report*, 11176-H386-R0-00, Project Technical Report, Task E-38C, NAS 9-8166, October 31, 1969.
- ¹⁹NASA Manned Spacecraft Center, *Apollo 11 Guidance, Navigation and Control System Performance Analysis Report*, 11176-H433-R0-00, Project Technical Report, Task E-38C, NAS 9-8166, December 31, 1969.
- ²⁰NASA Manned Spacecraft Center, *Apollo 12 Guidance, Navigation and Control System Performance Analysis Report*, 11176-H524-R0-00, Project Technical Report, Task E-38C, NAS 9-8166, April 8, 1970.
- ²¹NASA Manned Spacecraft Center, *Apollo 14 Guidance, Navigation and Control System Performance Analysis Report*, MSC-04112 Supplement 1, Project Technical Report, Task E-38C, NAS 9-8166, January 1972.
- ²²Wie, B., *Space Vehicle Dynamics and Control*, AIAA Education Series, May 1998.
- ²³Smith, E. E., *Performance of Apollo Block II Thrust Vector Control Using the PGNCs (Preliminary Guidance Navigation and Control System)*, NASA Internal Note MSC-EG-69-18, Manned Spacecraft Center, April 8, 1969.
- ²⁴Penchuk, A. and Croopnick, S., "Digital Autopilot for Thrust Vector Control of the Shuttle Orbital Maneuvering System," *Journal of Guidance and Control*, Vol. 6, No. 6, November-December, 1983, pp. 436-441.
- ²⁵Lance, T. A., *Analysis of Propellant Slosh Dynamics and Generation of an Equivalent Mechanical Model for Use in Preliminary Voyager Autopilot Design Studies*, Technical Memorandum No. 33-306, Jet Propulsion Laboratory, California Institute of Technology, Pasadena, California, December 1, 1966.
- ²⁶Enright, P., and Wong, E. C., "Propellant Sloshing Models for the Cassini Spacecraft," AIAA Paper 94-3730, 1994.
- ²⁷Dodge, F. T., "The New "Dynamic Behavior of Liquids in Moving Containers," Southwest Research Institute, San Antonio, Texas, 2000 (this is an update of NASA SP-106 whose original authors are Norm Abramson, Douglas Michel, George Brooks and Helmut Bauer).
- ²⁸Helmut, F., Fluid Oscillations in the Containers of a Space Vehicle and their Influence Upon Stability, NASA TR R-187, Marshall Space Flight Center, Huntsville Alabama, February 1964.
- ²⁹Edelmann, R. and Dunn, P., *Dynamic Analysis of the LEM Flight Control System*, Grumman Aircraft Engineering Corporation. Report No. LED-500-3, re-labeled NASA-CR-117567, September 30, 1964.
- ³⁰Johnson, C. L., and Kurtis, L. D., "Effects of the Lunar Environment on Optical Telescope and Instruments," *SPIE*, Vol. 1494, *Space Astronomical Telescopes and Instruments*, 1991, pp. 208-218.
- ³¹Griffin, M. D. and French, J. R., *Space Vehicle Design*, AIAA publication, 2nd edition, 2004.
- ³²Wincentsen, J., "Heritage Adoption Lessons Learned: Cover Deployment and Latch Mechanism," *Proceedings of the 38th Aerospace Mechanisms Symposium*, Langley Research Center, May 15-17, 2006.
- ³³Difesa, A., "Four Cover Mechanisms for the Rosetta Mission," *Proceedings of the 8th European Space Mechanisms and Tribology Symposiums*, Toulouse, France, September 29 - October 1, 1999, ESA SP-438.
- ³⁴Henderson, R. L., Taylor, J. C., Goldfinger, A. D., and Torruellas, W. E., "An Investigation of Potential Performance Impacts of the Lander Descent Engine Plume on a Laser Sensing System for Precision Lunar Landing," AIAA 2009-5806, *AIAA Guidance, Navigation, and Control Conference*, August 10-13, 2009, Chicago, Illinois.
- ³⁵Johnson, A. E., Huertas, A., Werner, R. A., and Montgomery, J. F., "Analysis of On-Board Hazard Detection and Avoidance for Safe Lunar Landing," Paper 1505, *IEEE 2008 Aerospace Conference*, Big Sky, Montana, March 1-8, 2008.
- ³⁶Epp, C. D., Robertson, E. A., and Brady, T., "Autonomous Landing and Hazard Avoidance Technology (ALHAT)," Paper 1501, *IEEE 2008 Aerospace Conference*, Big Sky, Montana, March 1-8, 2008.
- ³⁷Johnson, A. E. and Montgomery, J. F., "Overview of Terrain Relative Navigation Approaches for Precise Lunar Landing," Paper 1506, *IEEE 2008 Aerospace Conference*, Big Sky, Montana, March 1-8, 2008.
- ³⁸Rust, R., "Requirements Driven Versus Risk Informed Design," *Proceedings of the 2009 NASA Project Management Challenge*, February 24-25, 2009, Daytona Beach, Florida.
- ³⁹Singh, G., San Martin, A. M., and Wong, E. C., "Guidance and Control Design for Powered Descent and Landing on Mars," *IEEE Aerospace Conference*, Big Sky, Montana, March 3-10, 2007.
- ⁴⁰Howard, R. T., Heaton, A. F., Pinson, R. M., Carrington, C. L., Lee, J. E., Bryan, T. C., Robertson, R. A., Spencer, S. H., and Johnson, J. E., "The Advanced Video Guidance Sensor: Orbital Express and the Next Generation," *AIP Conference Proceedings*, Vol. 969, January 2008, pp. 717-724.
- ⁴¹Machula, M. F. and Sandhoo, G. S., "Rendezvous and Docking for Space Exploration," 1st Space Exploration Conference Continuing the Voyage of Discovery, 30 January - 1 February, 2005, Orlando, Florida.
- ⁴²Sostaric, R. R. and Merriam, R. S., "Lunar Ascent and Rendezvous Trajectory," *Proceedings of the 31st Annual AAS Guidance and Control Conference*, Breckenridge, Colorado, February 1-6, 2008, AAS 08-066.
- ⁴³Alexander, J. and Becker, R., *Apollo Experience Report - Evolution of the Rendezvous Maneuver Plan for Lunar Landing Mission*, NASA TN D-7388, NASA, Washington D.C., August 1973.
- ⁴⁴Ho, C., Golshan, N., and Kliore, A., *Radio Wave Propagation Handbook for Communication on and Around Mars*, JPL Publication 02-5, Jet Propulsion Laboratory, California Institute of Technology, Pasadena, California, March 1, 2002.
- ⁴⁵Burrough, E. L. and Lee, A. Y., "In-flight Characterization of Cassini Inertial Reference Units" AIAA 2007-6340, *AIAA Guidance, Navigation and Control Conference and Exhibit*, 20-23 August 2007, Hilton Head, South Carolina.
- ⁴⁶Jahanshahi, M. and Lai, J., "Galileo Spacecraft Inertial Sensors In-flight Calibration Design," *IFAC Identification and System Parameter Estimation*, 1982, Washington D.C., USA.

- ⁴⁷Helleputte, T. V., Doornbos, E., and Visser, P., "CHAMP and GRACE accelerometer calibration by GPS-based orbit determination," *Advances in Space Research*, Vol. 43, 2009, 1890–1896.
- ⁴⁸Fehse, W., *Automated Rendezvous and Docking of Spacecraft*, Cambridge University Press, 2003.
- ⁴⁹Conference Report, *Go for Lunar Landing: From Terminal Descent to Touchdown*, March 4–5, 2008, Tempe, Arizona. Arizona State University, Lunar and Planetary Institute, and the University of Arizona.
- ⁵⁰Low, G. M., *What Made Apollo A Success?* NASA SP-287, NASA, Washington D.C., 1971.
- ⁵¹Skulsky, E. D., Shaffer, S., Bailey, E., Chen, C., Cichy, B., and Shafter, D., "Under the Radar: Trials and Tribulations of Landing on Mars," *Proceedings of the 31st Annual AAS Guidance and Control Conference, Breckenridge, Colorado*, February 1–6, 2008, AAS 08-033.
- ⁵²Border, J. S., Lany, G. E., and Shin, D. K., "Radiometric Tracking for Deep Space Navigation," *Proceedings of the 31st Annual AAS Guidance and Control Conference, Breckenridge, Colorado*, February 1-6, 2008, AAS 08-052.
- ⁵³Roth, D. C., Guman, M. D., Ionasescu, R., Taylor, T. H., "Cassini Orbit Determination From Launch to the First Venus Flyby," *Proceedings of the AIAA/AAS Astrodynamics Specialist Conference*, August 10–12, 1998, Boston, MA.
- ⁵⁴Burk, T., "Attitude Control Performance During Cassini Trajectory Correction Maneuvers," *Proceedings of the AIAA Guidance, Navigation, and Control Conference, and Exhibit*, San Francisco, California, August 15–18, 2005.
- ⁵⁵Hackler, C. T., Brickel, J. R., Smith, H. E., and Cheatham, D. C., *Lunar Module Pilot Control Considerations*, NASA TN D-4131, February 1968.
- ⁵⁶Brown, G. M., Bernard, D. E., and Rasmussen, R. D., "Attitude and Articulation Control for the Cassini Spacecraft: A Fault Tolerance Overview," *14th AIAA/IEEE Digital Avionics System Conference*, Cambridge, Massachusetts, November 5–9, 1995.
- ⁵⁷Jaggers, R. F., "Shuttle Powered Explicit Guidance (PEG) Algorithm", Rockwell Space Operations Company, November 1992, JSC-26122.
- ⁵⁸McHenry, R. L., Brand, T. J., Long, A. D., Cockrell, B. F., and Thibodeau, J. R., "Space Shuttle Ascent Guidance, Navigation, and Control", *The Journal of the Astronautical Sciences*, Vol. XXVII, No. 1, January–March, 1979,
- ⁵⁹Ives, D. G., *Shuttle Powered Explicit Guidance Miscellaneous Papers*, Aeroscience and Flight Mechanics Division, JSC-28774, November 1999
- ⁶⁰Klump, A. R., *Apollo Lunar Descent Guidance*, R-695, Massachusetts Institute of Technology, C.S. Draper laboratory, Boston, June 1971.
- ⁶¹Mindell, D. A., *Digital Apollo: Human and Machine in Spaceflight*, MIT Press, Boston, May 2004.
- ⁶²Heiken, G. H., Vaniman, D. T., and French, B. M., *Lunar Sourcebook: A User's Guide to the Moon*, Cambridge University Press, Boston, 1991.
- ⁶³Keys, A. S., et al, "Developments in Radiation-Hardened Electronics applicable to the Vision for Space Exploration," AIAA 2007-6269, AIAA SPACE 2007 Conference and Exposition, 18–20 September 2007, Long Beach, California.
- ⁶⁴Parnell, T.A., Watts, J.W., and Armstrong, T.W., "Radiation Effects and Protection for Moon and Mars Mission," Proceedings of the Sixth International Conference and Exposition on Engineering, Construction, and Operations in Space, Space 98.
- ⁶⁵Bennett, F.V., *Apollo Experience Report – Mission Planning for Lunar Module Descent and Ascent*, NASA TN D-6846, NASA Manned Spacecraft Center, Houston Texas, June 1972.
- ⁶⁶Morabito, D. D., et al, "The Effects of Earthward Directed Coronal Mass Ejections on Near-Earth S-band Signal Link," Submitted to *Radio Science*.
- ⁶⁷Riedel, J. E., Bhaskaran, S., Desai, S. D., Han, D., Kennedy, B., McElrath, T., Null, G. W., Ryne, M., Synnott, S. P., Wang, T. C., Werener, R. A., "Using Autonomous Navigation for Interplanetary Missions: The Validation of Deep Space 1 AutoNavigation," IAA Paper L-0807, *Fourth IAA International Conference on Low-cost Planetary Missions*, Laurel, Maryland, May 2000.
- ⁶⁸Kubischek, D. I., Kubitschek, D., Mastrodomos, N., Werner, R., Kennedy, B., Synnott, S., Null, G., Bhaskaran, S., Riedel, J., Vaughan, A., "Deep Impact Autonomous Navigation: The Trials of Targeting the Unknown," AAS 06-081, *29th Annual AAS Guidance and Control Conference, Breckenridge, Colorado*, Feb. 4–8, 2006.
- ⁶⁹Gaskell, R., O. Barnouin-Jha, D. Scheeres, T. Mukai, N. Hirata, S. Abe, J. Saito, M. Ishiguro, T. Kubota, T. Hashimoto, J. Kawaguchi, M. Yoshikawa, K. Shirakawa, and T. Kominato, "Landmark Navigation Studies and Target Characterization in the Hayabusa Encounter with Itokawa," AIAA paper 2006_6660, *AAS/AIAA Astrodynamics Specialists Conf.*, Keystone, Colorado, Aug 2006.
- ⁷⁰Ingoldby, R. N., "Guidance and Control System Design of the Viking Planetary Lander," *Journal of Guidance and Control*, Vol. 1, No. 3, May–June 1978. pp. 189–196.
- ⁷¹Enright, P. and Macala, G.A., "Attitude and Articulation Control of the CRAF/Cassini Spacecraft in the Presence of Structural Flexibilities and Propellant Slosh," *Proceedings of the 15th Annual AAS Guidance and Control Conference*, Keystone, Colorado, February 8-12, 1992.
- ⁷²Smith, E. E., "Design of a Sampled Data Control System for Attitude Control of a Spacecraft During Powered Flight in a Gravity Free Environment," NASA Internal Note MSC 68-EG-06, Manned Spacecraft Center, Houston, Texas, May 7, 1968.
- ⁷³Kopf, E.H., "A Mariner Orbiter Autopilot Design," Technical Report 32-1349, Jet Propulsion Laboratory, California Institute of Technology, January 15, 1969.